Master's degree programme in

"Conservation Science and Technology for Cultural Heritage"
(CM-60)

Final Thesis

Elucidation of the structure of Iron-gall inks by an innovative multi-analytical approach:

unexpected new insights into the chemistry of iron polyphenolic complexes revealed by NMR and EPR spectroscopy

Supervisor

Prof. Pullar Robert Carlyle

Assistant supervisors

Prof. Crestini Claudia

Dr. Cappa Federica

Graduand

Caterino Salvatore (mat. 869463)

Academic Year 2021-2022

Let us try to teach generosity and altruism, because we are born selfish. Let us understand what our own selfish genes are up to, because we may then at least have the chance to upset their designs, something that no other species has ever aspired to do.

The Selfish Gene – Richard Dawkins, 1976

Acknowledgments

I can not start without giving my warmest thanks to all the fantastic people I had the opportunity to work with and that made possible this dissertation. I would like to thank the entire PPM group of the Molecular Sciences and Nano Systems department of Ca' Foscari starting with my supervisor Prof. Crestini Claudia: her personal and technical support always guided me along the thesis project and her confidence in my potentialities spurred me on in the most difficult times. I cannot forget to thank also the two fantastic PhD students Gagliardi Valeria and Massari Daniele, with a special mention to Valeria whose help has been really important for me in the first time-consuming stages of the procedure. I want to express my gratitude also to the technical support and the effort spent by the two assistant professors of the group, Prof. Gigli and Prof. Sgarzi.

Obviously, I cannot forget to thank also all the people of INTK group of the Academy of Fine Arts of Vienna starting with my supervisor Dr. Cappa Federica. It has been a real pleasure for me to work under her supervision: her availability during and after my internship and her comprehension of the problems really had an important role in the success of the project. How can I even imagine forgetting to mention the people that made my life easier and funny in a new working environment: the PhD students Rabbachin Laura, Tichy Johannes and Derksen Katharina and Dr. Pagnin Laura. Their emotional support has been more than fundamental sometimes and their attitude inspiring.

Clearly, the overall atmosphere of both the PPM group in Venice and the INTK group in Vienna and the personal support I received from all the people I have been in contact to, have been fundamental.

I would like also to thank Prof. Pignitter Marc, from the department of Physiological Chemistry of the University of Wien, for the more than fundamental possibility he gave me to use the EPR spectrometer of the Wien University, and the practical (and crucial) support in the use of it. I want to express my gratitude also to Prof. Zoleo Alfonso, from the department of Chemical Sciences of the University of Padua, for the practical suggestions in the use of the EPR spectrometer, and the qualitative interpretation of the EPR data. The effort spent by Prof. Zoleo has been more than important and his availability and patience during the explanations a real salvation.

I want to dedicate a special thanks to one professor which has been an important figure along all my academic carrier, Prof. Benedetti Alvise. His confidence in my potentialities and his precious suggestions have been a guide in the construction of my personal career project and his interest in the personal and professional development of students inspired me.

A final mention, which I am afraid it is quite necessary, to all those people that I have always had by my side, because they were always there, the ones who left, exactly because they left, and the ones who arrived, because I have been always waiting for them.

Table of contents

Table of abbreviations

AG	Arabic gum
CT	Condensed tannins
CW	Continuous wave
DAD	Diode array detection
DMF	dimethylformamide
DMSO-d_6	Deuterated dimethyl sulfoxide
EA	Ellagic acid
EI	Electronic impact ionization
ENDOR	Electron Nuclear Double Resonance
EPR	Electron Paramagnetic Resonance
ESEEM	Electron Spin Echo Envelope Modulation
ESI	Electron spray ionization
ESR	Electron Spin Resonance
ET	Ellagitannins
Ex(n)	Aqueous gall extract (number)
FT	Fourier-transform
GA	Gallic acid
GC	Gas chromatography
GT	Gallotannins
HMBC	Heteronuclear Multiple-Bond Connectivity
HOMO	Highest occupied molecular orbital
HPLC	High performance liquid chromatography
HR	High resolution
HS	High spin
HSQC	Heteronuclear Single-Quantum Coherence
HT	Hydrolysable tannins
IGI	Iron-gall ink(s)
InS	Intermediate spin
IR	Infrared
IS	Internal standard
LS	Low spin
LUMO	Lowest unoccupied molecular orbital
MALDI	Matrix assisted laser desorption ionization
MPN	Metal polyphenols networks
MS	Mass spectrometry
NMR	Nuclear Magnetic Resonance
PC	Procyanidins
PD	Prodelphins
PGG	Pentagalloyl glucose
Q	Quadrupole
ROry	Reaction and oxidation rough yield
ROS(s)	Reactive oxygen specie(s)
RT	Room temperature
TA	Tannic acid
TMDP	2-chloro-tetramethyl-dioxaphospholane
TOF	Time of flight
ZFS	Zero Field Splitting

Introduction and state of the art

Manuscripts are documents of extreme historical, cultural and artistic value. According to the modern legislations and the current views, cultural and historical heritage includes also the archivistic heritage,[1] which is generally composed of a massive number of hand-written documents. Behind each manuscript there is an intricate socio-cultural environment, as well as a precise technological development in the use and the transformation of natural materials. The scientific study of manuscripts and their constituents is therefore important from both a conservative point of view, as well as to better understand the technological improvements or modifications in the paper, parchment, pigments, dyes and ink productions.

Ancient manuscripts actually constitute a wide set of artifacts produced through a huge variety of materials and techniques: this term therefore includes objects extremely different one another ranging from Egyptian papyrus to medieval illuminated parchment and in fact also according to European and global regulations and guidelines there is not a clear definition for "manuscript". It is important therefore to specify from the beginning that this thesis project is focused on the scientific study of a specific class of materials, inks, used in the production of a restricted class of manuscripts, typically the medieval and post-medieval ones.

Iron-gall inks (IGI) have been widely used for different centuries in almost every geographical area: there are several evidences of usage of this type of inks related to the antiquity, especially in the Middle-East,[2,3] but their success in Europe and in the Western Countries is generally more associated to the XII-XIX centuries.[4] Consequently, it is not difficult to conceive the huge variety of historical recipes for the preparation of these inks.[4,5]

1) Iron-gall inks preparation and description of the "ingredients"

Despite of this variability, in all the historical recipes at least three main components are mentioned: an extract rich in polyphenols, and in particular in hydrolysable tannins, an iron salt and an organic binder. In general, galls or other tannins sources were treated to obtain an aqueous extract rich in polyphenolic compounds.[5] The iron(II) salt was then added to the extract in order to obtain the insoluble iron-polyphenol complexes responsible for the dark bluish colour. An organic binder was therefore necessary to keep the insoluble complexes dispersed in the aqueous system. Finally, additives could be used to modulate the final properties of the ink such as colour and viscosity (Fig.1).

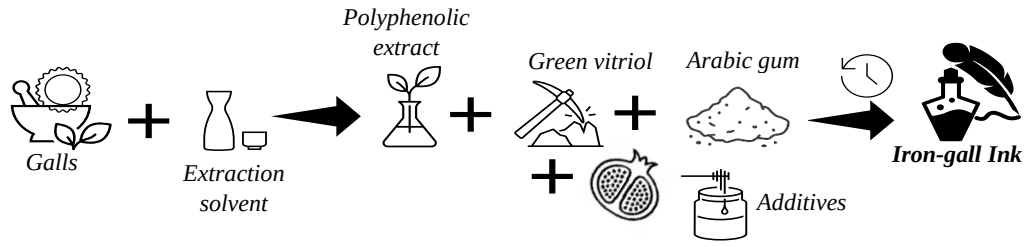

Fig. 1 Schematic representation of the most common procedure for IGI preparation

In the following paragraph a brief description of the starting materials used for the preparation of IGI is proposed.

1.1) Oak galls extracts: composition and variability

In historical recipes, polyphenols-rich extracts represent the major element of variability. Not only the vegetal matrices used for the extraction, but also the extraction methods display significant geographical variability. The most commonly used vegetal matrices in historical recipes are oak galls.[4,6] Galls, more properly called *cecids*, represent the biochemical response of the plant to the attack of a parasite. They can be found on the leaves, on the branches or on the trunk of trees; their shape and size vary according to the type of parasite that induced their formation (bacteria, fungi, insects, mites or other plant

organisms).[6] It has been also observed that galls-formers, especially in the case of arthropods, can control the levels of nutrients like sugars, amino acids, and secondary compounds like polyphenols,[7,8] which actually vary during the ripening of the galls, as demonstrated in different studies.[7,9] Aleppo gallnuts, the most mentioned in historical recipes,[4,5] are for instance produced mainly by *Quercus Infectoria* as a response to the attack of *Cynipis* hymenopters, and they are entirely beneficial to the parasite itself as they provide nourishment, shelter, and protect the cynipids larvae from fungal pathogens, hyper-parasites, leaf herbivores and some pathogenic factors.[10]
Other important types of galls used are the Morea gall, the Smyrna gall, Mar-mora, gall and Istrian gall, and other good quality galls available in France, Hungary, Italy, Senegal and Barbary. Chinese and Japanese galls are also mentioned in some recipes.[6] Other sources of tannins reported in historical recipes are: Pistacia Terebintus galls (Middle-Eastern Mediterranean area), bark or other parts rich in tannins of spruce, more properly known as *Picea Abies*, (European and Asian mountain regions), mulberry juice (Syrian area) and, probably as additive source of tannins, pomegranate peels (Mediterranean region).[2,5,11,12]
Generally, the tannin-rich matrices used to be crushed and macerated in an aqueous solution for a variable time in order to extract the polyphenolic compounds.[2,5,12] When pure water was used, the extraction generally involved a first step in which the matrix was macerated (with a variable water volume to galls' weight) at room temperature. In some cases, the system was exposed to sunlight. The second step involved heating of the extracting mixture for a given time or up to the significant reduction of the extract volume. The extracting mixtures used were not limited to water. White wine and vinegar were also used, while in most recent recipes, dated back to the end of the XIX century, ethanol is mentioned too.[2,5,12–15]
In any case, these extracts are characterized by a high content in polyphenols and in particular in tannins. The next paraph will briefly illustrate the most important characteristics of this class of organic substances as to better understand the nature of IGI.

1.1.1) Tannins: a brief overview

Tannins constitute an abundant class of polyphenols available in almost every plant, characterised by molecular weight comprised between 500 and 30000 Da and an highly hydroxylated structure.[16–18] Being secondary metabolites, as many other polyphenolic species, they have a protective role for plants against reactive oxygen and nitrogen species, UV light, plant pathogens, parasites, and predators.[16,17,19] Tannins are well known for both their beneficial effects on human heath (such as anti-inflammatory, antibacterial and anticancer properties[17,19–21]) and for their interactions with bio-macromolecules. This strong interaction, and in particular the one between tannins and collagen, has been, for instance, fundamental in leather tanning.[22,23] According to the most recent classifications, tannins can be divided at least in four main categories: condensed tannins (CT), hydrolysable tannins (HT), complex tannins and phlorotannins.[16,18,19] Gallotannins (GT), important sub-group of HT, are known to be abundant in oak gallnuts[24,25] while ellagitannins (ET), another sub-category of HT, and in particular punicalagin,[16,26] are quite concentrated in pomegranate peel, an additive mentioned in several ancient IGI preparation recipes.[5] This additive, as well as other elements of ancient historical recipes such as white wine,[5,27–29] may be seen as a source of a small amount of condensed and complex tannins.
In order to better appreciate the structural variability of the possible polyphenols actually involved in the IGI formation, in the following paragraphs a brief description of the different classes of tannins is reported.

1.1.1.1) Hydrolisable tannins

In general terms, HT can be considered as gallic acid (GA) oligomers or polymers in which GA (or its derivatives) units or are esterified around a polyol core, generally a carbohydrate such as D-glucose. All these polyphenolic compounds are bio-synthetized in plants via the shikimic acid pathway, which is synthetically described below and schematised in Fig.2. Shikimic acid is actually the precursor of different simple phenols such as hydroxycinnamic acids such as caffeic, ferulic and p-cumaric acids[17] which can be then converted to p-coumaryl, coniferyl and sinapyl alcohols, the monomers driving to the formation of lignin.[30]

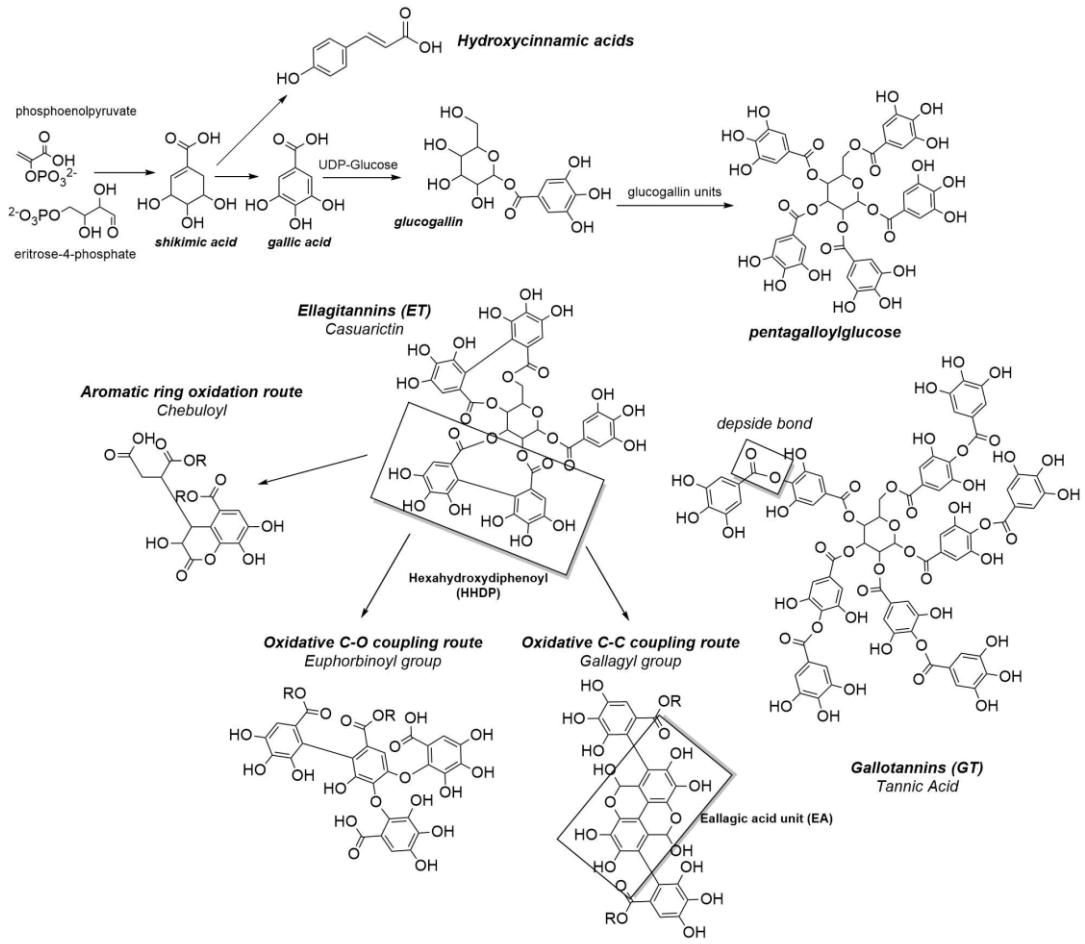

Fig. 2 Synthetic scheme of HT biosynthesis in the shikimate route.

In this bio-synthetic route, β-glucogallin is the first important intermediate and it works as galloyl-group donor. However, the key metabolite in the biosynthesis of most of the HT is the β-1,2,3,4,6-pentagalloylglucose (PGG).[19,31,32] The metabolism of this precursor, results into the two groups of HT: gallotannins (GT) and ellagitannins (ET).

On one hand, GT, such as tannic acid (TA) and its derivatives, are formed from addition of galloyl moieties on PGG free hydroxyl groups (both in meta and/or para position) through depside bonds.[17,18,31] ET, on the other hand, are formed properly via enzyme-mediated oxidative couplings of the galloyl groups of PGG.[19,31,33] ET constitute actually a relevant group of HT including more than 500 different compounds.[31] One of the reason of such variability is that hexahydroxydiphenyl, the first oxidative coupling product, and dehydro digalloyl groups, can undergo subsequent oxidative couplings reactions, both C-C and C-O, and/or aromatic ring oxidations resulting in a series of various structures.[31,32,34–37] A complete description of the HT possible structures is outside the aim of this thesis, moreover it is important to remark that other elements, such as their stereochemistry[31] and the different polyols cores,[18] should be considered to better understand the variability of this class of compounds.

1.1.1.2) Condensed tannins

This class of tannins, also known as proanthocynidins, is mostly composed of flavonoid oligomers or polymers which are generally abundant in the bark of trees.[16,38] They are formed by sequential condensation or coupling of flavan-3-ol units which can occur between the C4 of the first unit with the C8 or C6 of the second unit (B-type proanthocynidins). In some cases an additional ether bond between the C2 and the C7 is observed (A-type proanthocynidins).[16–18,39,40] The biosynthesis of flavan-3-ol units can be considered as an alternative to shikimate bio-synthetic route; in fact, malonyl-CoA units and p-cumaric acid, an hydroxycinnamic acid synthetized from shikimic acid (as reported in Fig. 2), undergo a series of enzymatically-mediated condensations resulting in the formation of naringenin, a flavanone which is one of the key intermediates in this biosynthetic route.[40,41] B-type CT represents an abundant class of molecules which can be classified according to the hydroxylation pattern of the chain-extender units. Procyanidins, prodelphins, prorobinetidins, profisetidins are the most common B-type CT classes (Fig. 3), while propelargonidins, proteracacinidins, promelacacinidins, procassinidins and probutinidins are less common sub-groups.[16,40,42] The stereochemistry of the C3 hydroxy group as well as the regiochemistry of polymerization, are additional variability elements of these compounds. Finally, certain positions of proanthocyanidins may sometimes be esterified with gallic acid or, exceptionally, with sugars (glucosides).[16,42]

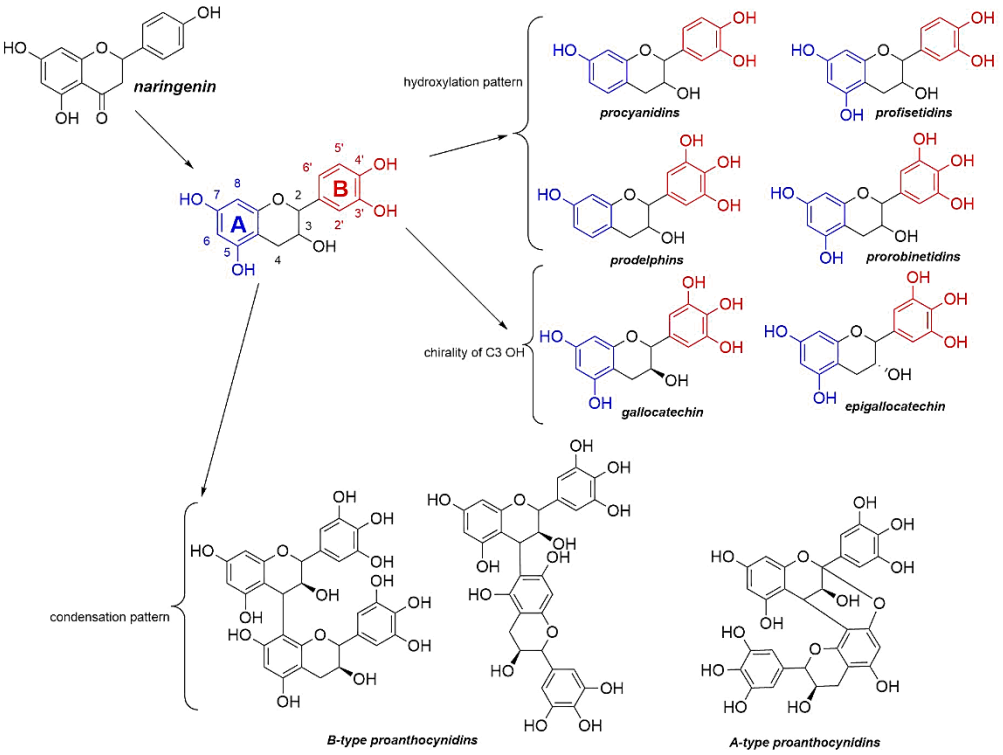

Fig. 3 Main elements of variability in proanthocyanidins group. Just the main subgroups and elements of variability are displayed.

1.1.1.3) Complex tannins and phlorotannins

Complex tannins embrace the structural and chemical features associated with both HT and CT groups.[18,31] They are probably synthetised via the interaction of the anomeric transient carbocation of an open-chair HT(such as vescalagin) with the electron rich A-ring of a flavan-3-ol unit (Fig. 4a).[31,43] Since the first demonstration of their natural occurrence, a considerable number of these secondary

metabolites have been identified[43] in different natural sources containing both high amount of HT and CT.[34]

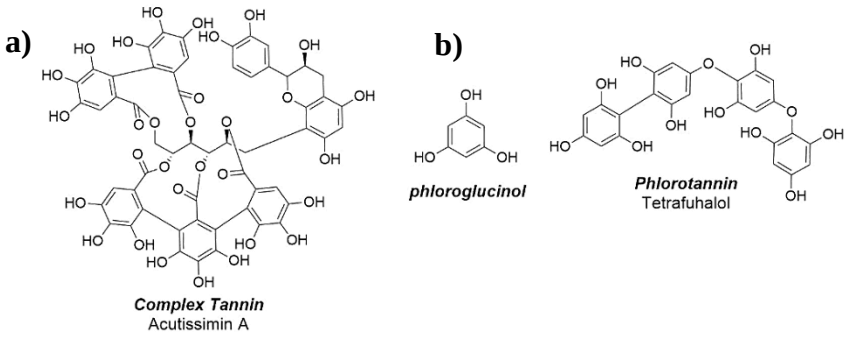

Fig. 4 a) Structure of one flavanol-ellagitannin (Complex tannin); b) Structure of phloroglucinol and of one phlorotannin

Phlorotannins instead are often omitted in the literature related to tannins since they can be isolated just from marine brown algae.[16] Phlorotannins are oligomeric or polymeric phloroglucinol derivatives in which phloroglucinol units are connected by biphenyl bonds (fucols), diaryl-ether bonds (phlorethols, hydroxyphlorethols, fuhalols) or both (fucophlorethols) (Fig. 4b).[16,21]

1.1.2) Elements of variability

Gall extracts can be considered as a complicated mixture of polyphenolic substances. High performance liquid chromatography (HPLC) analyses performed on gall extracts, have revealed a relatively high concentration of phenolic acids such as gallic acid, ellagic acid, different isomers of dihydroxybenzoic, vanillic, caffeic, syringic, ferulic and chlorogenic acids.[10,44] The range of possible phenolic compounds present in gall extracts is however much more extended including also tropolone-containing molecules such as purpurogallin and flavonoids such as catechin.[10,45] Interestingly, recent studies performed on commercial gallnut extracts seem to suggest an higher content of GT and dimers and trimers of gallic acid while no significative amount of flavonoid has been detected (Fig. 5).[24]

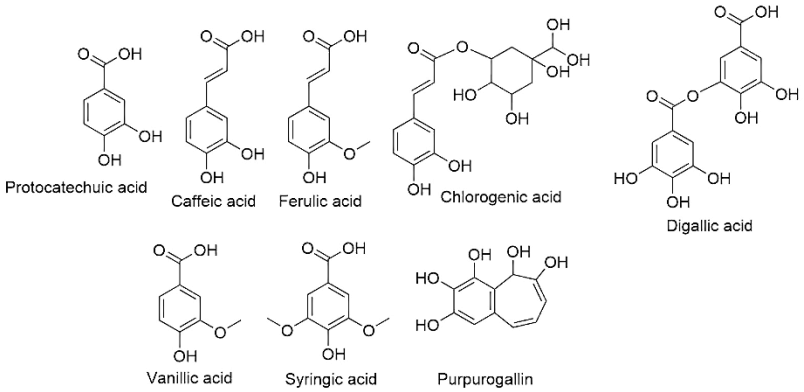

Fig. 5 Some of the other polyphenolic compounds present in gall extracts

The most important factors affecting the overall composition of gall extracts are:

a) *<u>Vegetal matrices (tannin source) nature and provenance</u>*

As previously mentioned, original recipes involved different tannin sources. The structural differences in polyphenols deriving from various sources, result in different binding capabilities and stabilities of iron-polyphenolic complexes. This element is important with respect to the conservation of IGI-containing manuscripts. In fact, it has been noticed a different efficacy in the iron-removal phytate treatments on inks prepared using different tannin sources (this differences it is enhanced after artificial

aging).[11] Moreover, there is evidence that also the geographical provenance of the gallnuts can be associated with slight structural differences of the contained tannins. In particular, the role of these differences in terms of esterification degree and stereochemistry can be interesting for both a diagnostic and an archaeometric point of view. Analyses performed on galls from different provenance contain different amount of GT[46] and, more recently, ^{31}P NMR analyses of Chinese and Turkish oak galls, have revealed structural differences on the extracted tannic acid.[24,47]

b) Extraction methods

The methods used to obtain the tannins extract for the IGI preparation were extremely variable, as mentioned in the first paragraph. In fact, as reported by *Teixeira et al.*, even if the same type of tannin source is used, extracts prepared using different extraction methods exhibit different ratios of hydrolysis products of the initial tannins.[28] Not only the solvent used, but also the time of maceration, the temperature, the type of galls processing and the ratio between the solvent and the tannin source, turn out to be relevant parameters affecting the nature of the polyphenols contained in the extract.[29]

Regarding this aspect it is important to underline that, often, gallnut polyphenolic content analyses results are referred to extracts obtained with alcoholic solution, acetone[10] and other modern extraction techniques which are significantly different from the traditional extraction methodologies employed for the preparation of gall inks. Ultrasonic bath, ultrasonic probe assisted extraction,[48] microwave assisted extraction and supercritical carbon dioxide polyphenolic extraction[20] are for instance important procedures used nowadays in the polyphenolic extraction and isolation at the industrial level.[49] Gallnuts extracts obtained under this condition could display important differences in respect to the ones obtained with simple aqueous based methods traditionally used for IGI preparations.

1.1.3) Study of polyphenols: an overview of the possible analytical approaches

Nowadays, a huge variety of analytical methods for the identification and quantification of polyphenols in complex systems such as the vegetal matrices are available (schematically reported in Fig.6).[50–52] In the evaluation of the best analytical procedure for the characterization of natural organic substances however, many aspects should be taken into account: sample pre-treatments, running-time of the analysis, costs and required equipment are just some of the practical elements that should be balanced to the more technical ones such as sensitivity, accuracy, structural information content etc.[53] Chromatographic techniques for instance has become a dominating analytical tool for the polyphenolic separation, identification and quantification, especially in the agri-food industry.[50,52] Nevertheless, often in these methods sample, time- and chemicals-consuming pre-treatments (such as pre-concentration and purification in HPLC and derivatization in GC) are required.[50–52] Innovative analytical tools such as the use of bio-sensors or supercritical fluid chromatography (SFC), despite their interesting potentialities, are nowadays used just for specific applications and their diffusion is quite limited.[51]

Moreover, it should be remarked that the prepared aqueous extracts are containing a wide range of natural organic substances and therefore their characterization is a challenging task that should be properly addressed possibly using a multi-analytical approach.

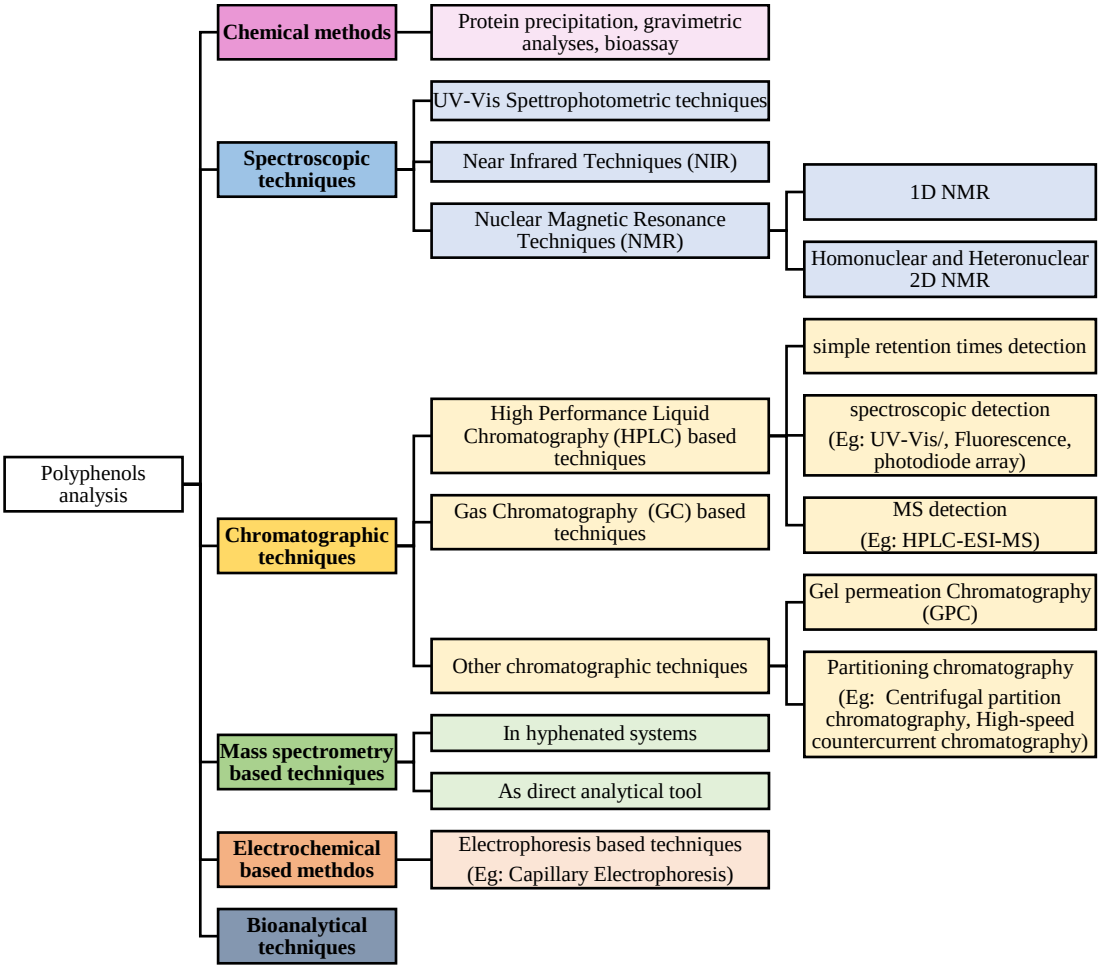

Fig. 6 Schematic summary of the most relevant analytical techniques for the polyphenols analyses and characterization. [50–52]

NMR and MS are the most used analytical tools, among the ones reported in the scheme in Fig.6, in all those studies in which structural detailed information needs to be obtained and for this reason a brief overview of their use in this field is presented in the following brief paragraphs.

1.1.3.1) NMR techniques in the in the characterization of vegetal biomolecules

NMR is based on the evidence that the magnetic dipoles associated with nuclear spins, in presence of an external strong magnetic field (B), tend to be oriented either in the direction of the field or opposed to it, thus creating multiple energy states. These states are discrete and associated with the nuclear spin, I. When I≠0 (as for ^{13}C, ^{1}H, ^{15}N, ^{31}P etc) the nucleus is "spin active" and 2I+1 energy states are present, each of them having an energy E described by the equation reported below (eq.1):

(1) $E = -\hbar\gamma B m_I \rightarrow \Delta E = -\hbar\gamma B = h\nu_R$

where ħ is the compact form $\frac{h}{2\pi}$ and therefore a constant, γ is the gyromagnetic ratio and it is constant for a given nucleus, and m_I is the spin quantum number characterizing the orientation of the magnetic moment in the magnetic field and it varies from I to -I in integral steps.

This very simple quantum mechanical concept, properly elaborated and studied, constitute the basis of the well-known NMR techniques in one dimension, two above all, the popular ^{1}H NMR and ^{13}C NMR. In the early 1970s the introduction of two-dimensional NMR (2D-NMR) gave to the scientists another important tool to determining more precisely the structure of complex molecules. A detailed explanation of 2D-NMR principles is outside the scope of this chapter. However, these techniques can be seen qualitatively as an array of 1D-NMR resulting from a series of frequency pulses which enable

to highlight the NMR cross-peaks that link two resonance signals. 2D-NMR techniques themselves constitute a huge set. Some of them, the so-called "inverse NMR techniques", are particularly interesting for the study of complex biomolecules. A considerable enhancement of sensitivity is obtainable when nuclei with a low magnetogyric ratio like ^{13}C are detected through their effects on the more sensitive nuclei, like ^{1}H. Protons not coupled to the ^{13}C nuclei are suppressed so that only protons directly bonded to the ^{13}C nuclei produce cross-peaks in the 2D spectrum. The most important techniques which imply this method of acquisition are the Heteronuclear Multiple-Quantum Coherence (HMQC), Heteronuclear Single-Quantum Coherence (HSQC) and Heteronuclear Multiple-Bond Connectivity (HMBC). Both HMQC and HSQC are based on the correlation between coupled heteronuclear spins (^{1}H-X) across a single bond. However, HSQC gives a better resolution in the indirect dimension (^{13}C and ^{15}N) as compared to HMQC due to the transfer of magnetization from the proton to the second nucleus via an Insensitive Nuclei Enhanced by Polarization Transfer (INEPT). Moreover, HSQC signals are singlets, while the HMQC spectra usually give multiplets due to homonuclear (^{1}H–^{1}H) couplings. For these reasons, HSQC is preferred in the case of large biomolecules, due to the possibility of resolving crowded spectra.
Without going into details, HSQC is a 2D heteronuclear chemical shift correlation map between directly bonded (J-coupled) ^{1}H and X-heteronuclei (such as^{13}C and ^{15}N)[A] resulting from a pulse sequence consisting of four independent blocks of pulses. Due to a large number of pulses, the precise technical settings of HSQC experiments (the so-called "programs" or "methods") requires special care and should be performed by a specialized operator.

NMR, therefore, is an extremely versatile analytical tool in which data-acquisition modes or/and instrumental parameters can be manipulated or modified to meet the needs of different analytic projects and to extend applications in specific fields.[53] Numerous NMR methods have been developed for the study of botanical biomolecules both improving the acquisition methodologies enabling to obtain more readable and easy-to-interpret data, and/or implementing new technologies to overcome practical constraints such as the extraction process of the analytes from the matrices.[53,54]
The use of 2D-NMR techniques, and in particular [^{13}C-^{1}H]-HSQC methods, turned out to be a powerful analytical tool in the characterization of tannins and complex polyphenolic substances such as lignin.[24,38,42,55,56] In the study of condensed tannins for instance, conventional 1D ^{1}H and ^{13}C NMR do not allow a proper detailed assignment and quantification of individual signals due to broad and often unresolved signals, long acquisition times, and low signal-to-noise ratios. HSQC techniques instead, combining the sensitivity of ^{1}H NMR with the higher resolution of ^{13}C NMR, are in principle the best qualitative methods to reveal the resonance frequencies of the different proanthocyanidin units and the interunit bonding patterns.[42] Whitin a multi-analytical approach, HSQC presents clear advantages in the characterization of polyphenolic compounds, but still detailed qualitative and especially quantitative information regarding the phenolic groups structures are difficult to get.[57]
The detailed analyses of hydroxyl groups, and in particular phenolic ones, can be obtained with 1D ^{31}P NMR of phosphitylated polyphenols.[24,35,36,42] Since its introduction in the early 90s, phosphitylation followed by ^{31}P NMR spectroscopy analysis turned out to be a promising technique for the analysis of hydroxyl groups in different kinds of materials and lots of research efforts have used or adopted the proposed technique for the analysis of lignins and other biomass-related products. The initial protocols have been optimized and systematized through time as to improve the resolution and the quality of the spectra as well as to solve other practical issues related to the samples typologies.[47,57] A typical ^{31}P NMR experiment involves the phosphitylation of hydroxyl groups in the substrate using an appropriate phosphorous-containing reagent, 2-chloro-4,4,5,5-tetramethyl-1,3-2-dioxaphospholane (TMDP),

[A] The resulting cross-peaks are also defined J-couplings signals. For this reason, in the following chapter they will be defined also as $J_{C\text{-}H}$ signals.

followed by quantitative NMR spectroscopy and finally data processing which eventually can involve the calculation of the amounts of different hydroxyl groups.[47,57] The phosphorus-containing reagent in fact is able to react with free hydroxyl groups and the so ^{31}P labelled hydroxyl functionalities (aliphatic, phenolic, and carboxylic) can be readily detected and quantified with ^{31}P NMR experiment. The scheme in Fig.7 synthetically reports the passages of the ^{31}P NMR analytical protocol for hydroxyl groups analysis with an epigallocatechin gallate example.

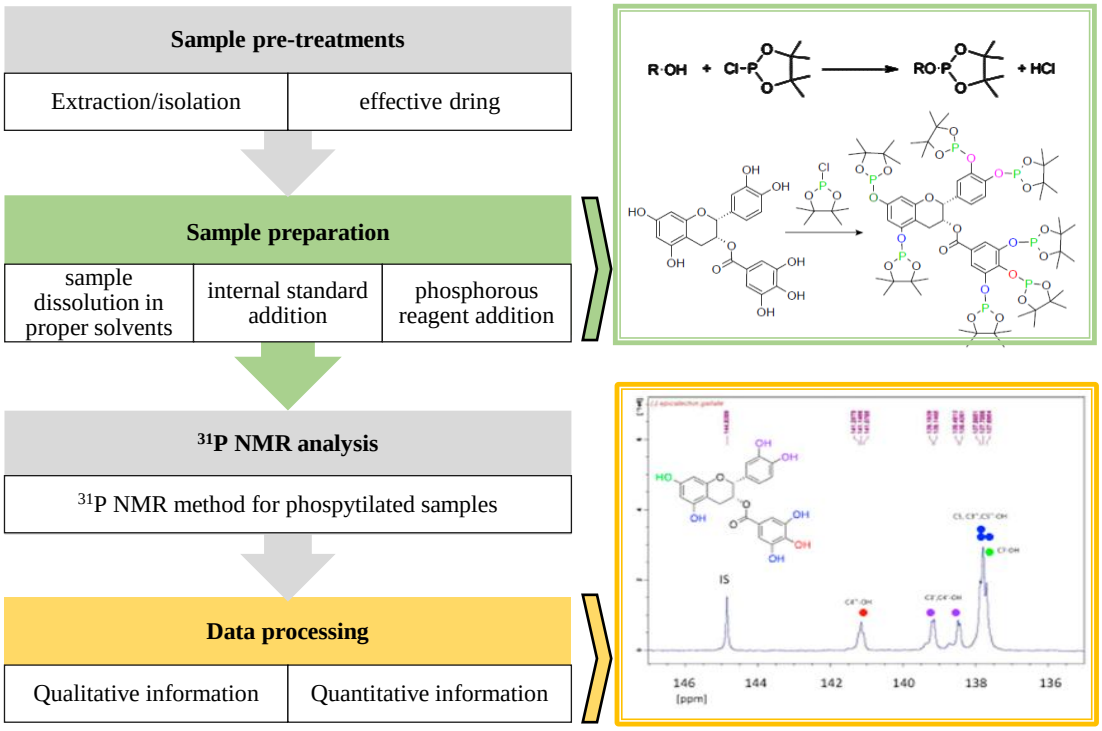

Fig. 7 Synthetic scheme of the protocol for hydroxyl groups analysis via ^{31}P NMR.

Both HSQC and ^{31}P NMR present some practical limitations. In both cases the samples should be properly solubilized in suitable solvents such as pyridine, pyridine/deuterated chloroform mixtures or deuterated dimethyl-sulfoxide and in the case of ^{31}P NMR the expensive TMDP reagent is required. Moreover, being NMR technique, appropriate NMR instrument are necessary.

1.1.3.2) Mass spectrometry in the study of polyphenols and other secondary metabolites

MS is currently one of the most versatile and sensitive instrumental methods applied to structural characterization of plant metabolite mixtures.[58–61] In particular, versatility of mass spectrometric methods is based on the possibility of application of different physical phenomena for ionization of analysed molecules, generation of their fragments and separation of the created ions. In this regard, the application of various mass spectrometric techniques, including different systems of ionization, analysis of both positive and negative ions of analytes, fragmentation of the protonated/deprotonated molecules and in some cases addition of metal ions to the studied compounds before ionization and fragmentation, may improve structural characterization of natural products.[60,61] Resolution of the applied mass spectrometers plays an important role in structural studies of mixtures of the target compounds isolated from biological materials. For this reason, several high resolution mass spectrometry (HRMS) approaches have been developed and successfully implemented in natural product researches for the identification, quantification and structural elucidation of a broad variety of metabolites with diverse physicochemical properties (e.g polarity, volatility, thermolability, molecular weight).[58–61]

I) Ionization methods

Electrospray (ESI) or heated electrospray (HESI) ionization sources are the most popular and widespread used interfaces in HRMS instruments. ESI-based ambient ionization techniques are intended for the analysis of both small molecules and macromolecules exhibiting moderate polarity, whereas ambient ionization sources based on atmospheric pressure chemical ionization (APCI) are mainly used for the analysis of less polar and small molecules. These methods have been successfully used for the detection of a broad variety of secondary metabolites in plant natural products, including phenolics, flavonoids, terpenoids, alkaloids, coumarin, and saponins.[60,61] Alternatively, electronic impact (EI) ionization has historically been the standard ionization interface in MS instruments hyphenated to GC. Due to the highly reproducible mass fragmentation obtained by EI, the hyphenation GC-EI-HRMS represents a powerful tool and the first choice for identification and structure elucidation of unknown volatile and semi-volatile organic compounds.[60] Matrix-assisted laser desorption/ionization (MALDI) is a soft ionization technique based on desorption phenomena used in the analysis of high molecular weight compound and/or high polymerization degree, such as proteins, polysaccharides and other biopolymers including tannins. Together with direct analysis in real time (DART), it is mainly reported for stand-alone HRMS configurations.[60] Potentialities of MALDI-MS systems have been emerged in several studies regarding hydrolysable and condensed tannins structural elucidation[56,62–65] and it has also the great advantage of being a fast analytical method which requires few pre-treatment steps.[56] Without going into details, MALDI is based on three basic steps: 1) the incorporation and isolation of analytes in a matrix, 2) the excitation of the matrix with a suitable laser producing the plume by physics desorption/ablation, and 3) the ionization of the analytes by ion-molecules reactions.[60]

II) Mass detection systems

Time of flight (TOF) spectrometers are probably the mass analysers most extensively reported in literature for the analysis of plant natural products.[60] Moreover, often in this field of application tandem mass spectrometers (MS-MS) are used, especially for untargeted analysis of complex plant extracts, due to their capability of providing accurate mass data, and structural information from ions fragmentation. In this regards, hybrid tandem mass analysers such as quadrupole-TOF (Q-TOF) are the most mentioned in literature and they often are successfully used in the (U)HPLC-ESI-Q-TOF configuration,[59–61] even if triple quadrupole systems (QqQ) have been proved to be efficient systems as well.[59] Other common methods for studying the fragmentation are the ones based on the collision induced dissociation (CID) and higher-energy collision dissociation (HCD) ion trap (IT) systems followed by the proper mass analysis such as TOF or FT-MS systems such as Orbitrap.[B]

1.2) Iron(II) salt as inorganic component of the iron-gall inks

The addition of an iron(II) salt to polyphenolic-rich extracts allows the formation of the complexes responsible for the dark colour of IGI. In most of the historical recipes, "green vitriol", or simply "vitriol", have been used to refer to iron(II) sulphate heptahydrate ($FeSO_4 \cdot 7H_2O$). Actually, other sulphates such as copper and zinc sulphate used to be referred as vitriols.[2,5,12] Additionally to the green vitriol commonly used at the time, "copper green", copper(II) hydroxycarbonate ($Cu_2(OH)_2CO_3$) could be also added. Consequently, the presence of other cations, especially copper(II), can be detected in IGI.[4,11]

Another factor to bear in mind is represented by the wight ratio of vitriol and galls. In particular, an extremely variable range, from a slight excess of galls weight to a huge excess of iron salt one, is reported in historical recipes.[2,5,67]

[B] Orbitrap and linear trap (LT) Orbitrap are recent mass spectrometers (introduction in 2005) characterized by increased acquisition speed, higher resolving power, mass accuracy, and sensitivity. For the curiosity of the reader, an overview of the principles of these mass analysers and their potentialities can be found in the accurate description of *Zubarev and Makarov,* ***2013.***[66]

1.3) Binder and additives in iron-gall inks

Other additional constituents of IGI are binders and additives. The most commonly used binders in the ink preparation were chosen not to be affected by a relevant volume reduction after the drying process (commonly known as light binders). In IGI historical recipes, Arabic gum (AG) is the most commonly mentioned binder.[2,4,5] From a chemical point of view, AG is a vegetal polysaccharidic extract, rich in galactose, arabinose, rhamnose, containing also glucuronic acid. The amount of AG is extremely variable in historical recipes with respect to the amount of galls and iron salts. Interestingly, it has been observed that Arabic gum is able to reduce the pH dropping and to increase the stability of the ink with time.[68] The binders used for the production of inks vary according to the availability of materials in the geographical area and the final desired characteristics for the ink. It is therefore not surprising that the use of other vegetable gums, such as tragacanth and mastic gum (or mastic), or other substances such as animal jellies, animal glues, egg white, mucilage and in some cases even honey is documented too.[2] Additionally, the amount of AG used was extremely variable with respect to the iron sulphate and gall one.[67]
Additives were used to modulate the final properties of the ink. For instance, dyes and pigments were used in small quantities in some cases to modulate the colour or, even in relevant quantities, defining the final inks as "composite inks".[4] In some archivistic studies on Spanish recipes, hematite[67] and indigo[5] resulted as commonly used pigments. The addition of carbon black, gold scraps,[2] lapis lazuli, Prussian blue[15] or other colorants is well documented too. Urine, potassium nitrate (saltpetre), alum (in particular rock alum) and other organic and inorganic materials were frequently added because of their etchant properties.[5,11,23] Other additives were added also to modulate the viscosity of the ink. The most common ones were sugar and honey.[2,12] However in one article published in Harper's Bazar at the end of the Nineteenth century, a recipe elaborated by some chemists mentions the use of glycerine as a secondary binder, and phenol or chopped cloves as anti-fermentative.[14]

2) The chemistry of iron-polyphenolic complexes: an overview

2.1) Formation mechanism

The formation of iron-gall complexes is generally described as a two-step mechanism:[3]

a) HT and their hydrolysis products initially bind the Fe^{2+} mainly via catechol and galloyl groups instantaneously forming the dark soluble complexes. The formation of the Fe(II)-polyphenolic complexes is generally faster than the free Fe(II) cations autoxidation and therefore the polyphenols typically bind preferentially these cations instead of Fe (III) ones.[69] Due to its octahedral geometry, Fe^{2+} can coordinate up to three catechol or galloyl groups.[70,71] With this respect, it is important to underline that this step is strongly pH-dependent; in fact, the variation of the pH of an aqueous solution of a polyphenolic ligands results in the modification of its coordination sites depending on its hydrolysis degree,[72–77] determining the actual stoichiometry of the final complex (Fig.8).[25,70,75,77–80]

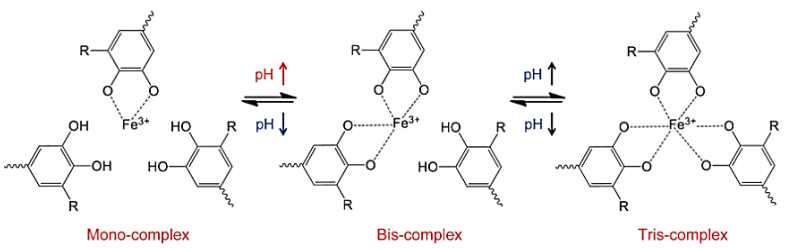

*Fig. 8 General trend for iron to ligand stoichiometry in iron-catecholate complexes. Figure adapted from Kim et al., **2021**. NB: the complexes displayed in figure are Fe(III) based. However, there are no significative reasons to hypothesize a different binding mechanism.*

Various studies on gallates and catecholates[70,78,79] have highlighted that when the pH of a ligand solution is below 4, resulting in a structure fully protonated (GAH_4),[72,73,81] the stoichiometry of complexes is 1 : 1 (iron to ligand). Differently, when GA is partially deprotonated, in a pH range between 4.5 and 6.5, the formed complexes are characterised by 1:2 and 1:3 iron to GA stoichiometries. However, it has also been demonstrated that in the pH range between 3.5 and 5.5 GA-iron complexes are still characterized by a 1:1 stoichiometry with the most reactive protonation form being GAH_2.[78] Lastly, under alkaline conditions, when GA is predominantly deprotonated (HGA^{3-} and GA^{4-}), it tends to form 1:3 iron to ligand complexes.[70] These different iron to gallic acid ratios result in different hues of the final complexes, ranging from blue-green (1:1) to purple (1:2) and dark red-brownish colours (1:3).[70,82,83C] It is remarkable that the complexation itself drives to the ligand deprotonation. The mentioned studies are generally conduced in buffer solutions, which are quite far from the medieval ink preparation conditions. For this reason a strong acidic pH and consequently 1:1 iron to polyphenolic ligands ratio is generally expected.[5,78,84,85]

It is relevant to underline that the mentioned studies are referred to simple systems in which model polyphenolic compounds are used. It will be therefore important to investigate the pH dependence in the iron-polyphenols complexes formation also in the case of more complicated polyphenolic structures eventually present in gall extracts such as PGG, TA and condensed or complex tannins. For instance, it has been demonstrated that epicatechin-gallate and epigallocatechin, in strong acidic environment (pH range 1-3) are capable to form 2:1 iron to polyphenols complexes with Fe(III) due to their multiple binding sites (Fig.9).[80,86]

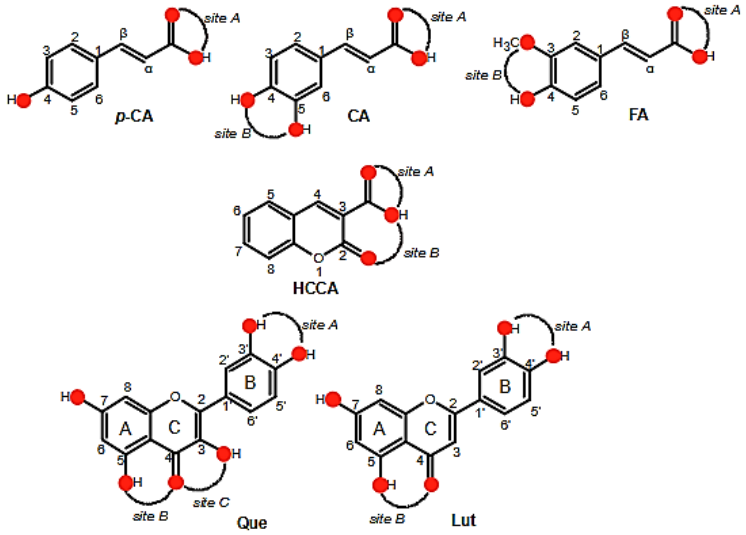

*Fig. 9 Binding sites involved in Al(III) and Fe(III) complexes formation of some polyphenolic compounds. p-CA=para-coumaric acid, CA=caffeic acid, FA=feroulic acid, HCCA=coumarin-3-carboxylic acid, Que=quercitin, Lut=luteolin. Figure adapted from Malacaria et al., **2016***

Moreover, the most commonly studied iron-polyphenolic complexes in literature are the Fe(III)-catechol ones, and only very few studies are focused on the chemistry upon the Fe(II)-galloyl complexes formation.[78,87] More specifically, the role of the carboxylic acid of gallic acid in the complex formation should be better defined. In fact, the proposed complexation mechanism just rarely

[C] Concerning the actual expected iron-polyphenolic stoichiometries according to preparation pH conditions, the available literature is often not coherent since different results can be obtained with different methodologic approaches. It would be extremely useful therefore to dedicate an effort to critically revise all the available literature, and eventually perform other (systematic) experimental studies to define more properly (once and forever), at least for simple model compounds, the iron to ligand trends, possibly considering both Fe^{2+} and Fe^{3+} ions.

involves the carboxylic group, which instead seems to cooperate in the formation of the final structures which will be further discussed below.[80,88–91]

b) Due to its weak acidic character, Fe^{2+} does not form as stable complexes with deprotonated polyphenols as Fe^{3+}does. This difference can be related to the different acidic Lewis character of Fe^{3+}. For instance, the pKs for iron(II)-(mono)catecholate is about 7.95, while the one for iron(III)-(mono)catecholate it is about 20.00[D].[70,87,92] Therefore, as polyphenolic ligands strongly stabilize Fe^{3+} over Fe^{2+}, Fe^{2+} in polyphenolic complexes is rapidly oxidized by atmospheric O_2 to give dark-bluish insoluble Fe^{3+}-polyphenolic complexes. This process is commonly referred as *autooxidation* (Fig.10). Typically, Fe^{2+} oxidation occurs quite slowly under normal conditions, but because of the coordination of polyphenol ligands to Fe^{2+}, the iron reduction potential is lowered, resulting in the enhancement of the autooxidation rate.[69,70,87] Some interesting relations between the polyphenols structure and the autoxidation rate of the complex have been observed. Polyphenolic acids in fact promote an higher rate of autoxidation of the complexes if compared to their corresponding esters or phenols without carboxylic group.[93] Unambiguously, it has been observed that the oxidation of Fe(II) ions was indeed facilitated by phenolic acids bearing catechol group than their counterpart with galloyl moiety.[87,93] The complexes autoxidation kinetics have been studied from different prospective resulting the proposal of different kinetics equations.[68,87]

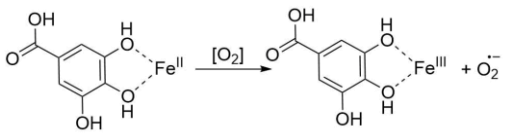

Fig. 10 Autooxidation process in a Fe(II)-GA complex

2.2) Structure

A critical aspect of the studies focused on the complexes formation mechanism and structures, lies in the fact that they have been conducted just on gallic acid instead of considering also tannins. Furthermore, the gallate iron(III) complexes were often synthetized with methods far different from those used in the preparation of IGI. With respect to iron(III)-gallate complexes, in 1990s *Wunderlich* demonstrated that a dark insoluble polymer together with some dark polymeric crystals can be obtained from the reaction of $FeCl_3$ with gallic acid using a silica gel method at room temperature. The stoichiometry proposed for these complexes was $Fe(C_7O_5H_3)\cdot 2H_2O$. Since the Wunderlich synthesis implies the direct use of an Fe^{3+} precursor, the results obtained have not been widely accepted in the cultural heritage science field.[89] In 2006 *Cheetham and Feller* have been able to synthetize bluish-black rod-shaped crystals of iron(III) gallate from $FeCl_2\cdot 4H_2O$, gallic acid monohydrate and NaOH using an hydrothermal method.[89–91] The results of diffractometric analyses of some selected single crystals confirmed the Wunderlich structural model: crystalline structures consisting of hexagonal arrays of slightly twisting chains of MO_6 octahedra, connected by the organic groups forming a scaffold (Fig.11).[90,91] More recently, *Ponce et al.* demonstrated that the main colouring agent in IGI is indeed an amorphous form of the Wunderlich complex[E].[89]

[D] Also in this case, the available data in literature are dispersed and often incoherent due to the different methodologies used for the calculations of such instability constants (or formation constants). For the aim of this thesis however, it is enough to observe that all the methods agree on the fact that the binding is favoured for Fe(II) cations but the stability of the resulting complexes is much lower in respect to the ones of Fe(III).

[E] In this case the synthesis has been carried out starting from $FeSO_4\cdot 7H_2O$ and gallic acid monohydrate using different molar ratios.

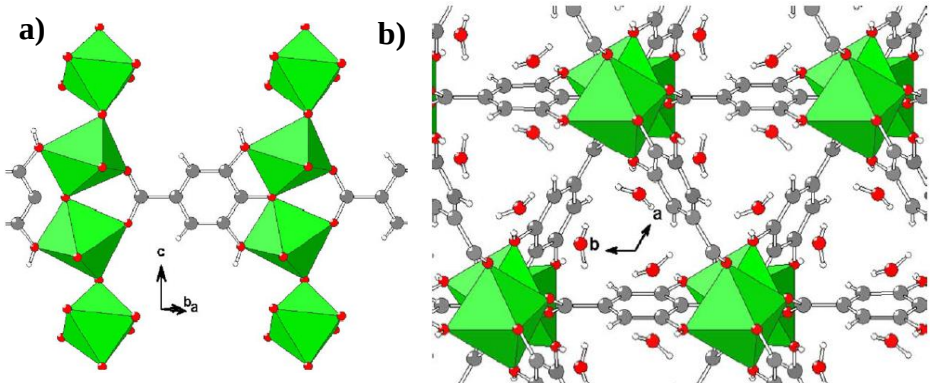

Fig. 11 9 a) Section of the structure of Ni(II) gallate dihydrate in a plane containing the c axis. Chains of NiO6 octahedra are connected by roughly planar gallate groups. The structures of the other gallates (such as the Fe(III) ones) are analogous. B) View down the c axis of the gallate structure. Unbound water molecules occupy trigonal channels between chains of MO_6 octahedra. Figure adapted from Feller, R. K. et al., ***2006.***

It is important to highlight that, according to this structural model, the carboxyl group participates in the formation of iron-gallate complexes. This elucidation re-opens the debate upon the formation mechanism, which has been described considering just the catechol/galloyl coordination site and further studies are necessary to better understand the role of carboxylic acid groups in the coordination of iron cations.
In this thesis the structure of iron-polyphenolic complexes will be discussed and therefore, for the help of the reader, some basic concepts related to the iron-complexes structures and their direct implications are reported in the Box 1 "Iron complexes chemistry - A brief description" at the end of this chapter.

2.3) Characterization of iron-polyphenolic complexes in Iron-gall inks

It is important here to stress an aspect which will be then fundamental in the definition of the methodological approach: the difference between the identification and the characterization of IGI.

The identification of IGI on historical manuscript is an important task of conservation scientists and it mainly involves those analytical techniques capable of clearly identify IGI on different support with a minimum invasiveness.[94–97] On the other side, the characterization of IGI is aimed to access specific aspects of these materials such as their precise chemical structure,[28,89,98,99] the most common degradative patterns,[84,100–102] their response to conservation treatments,[11,85] etc. Obviously, to pursuit different goals, different analytical tools have been used (schematically reported in Fig.12)[F].[103]

[F] Please note that a complete description of the analytical techniques used in the study of IGI is outside the aim of the current thesis. For a general overview of the most used analytical tools used in this field, with a suitable bibliography, see the references *Goltz et al.,* ***2012*** and *Corregidor et al.,* ***2019***.

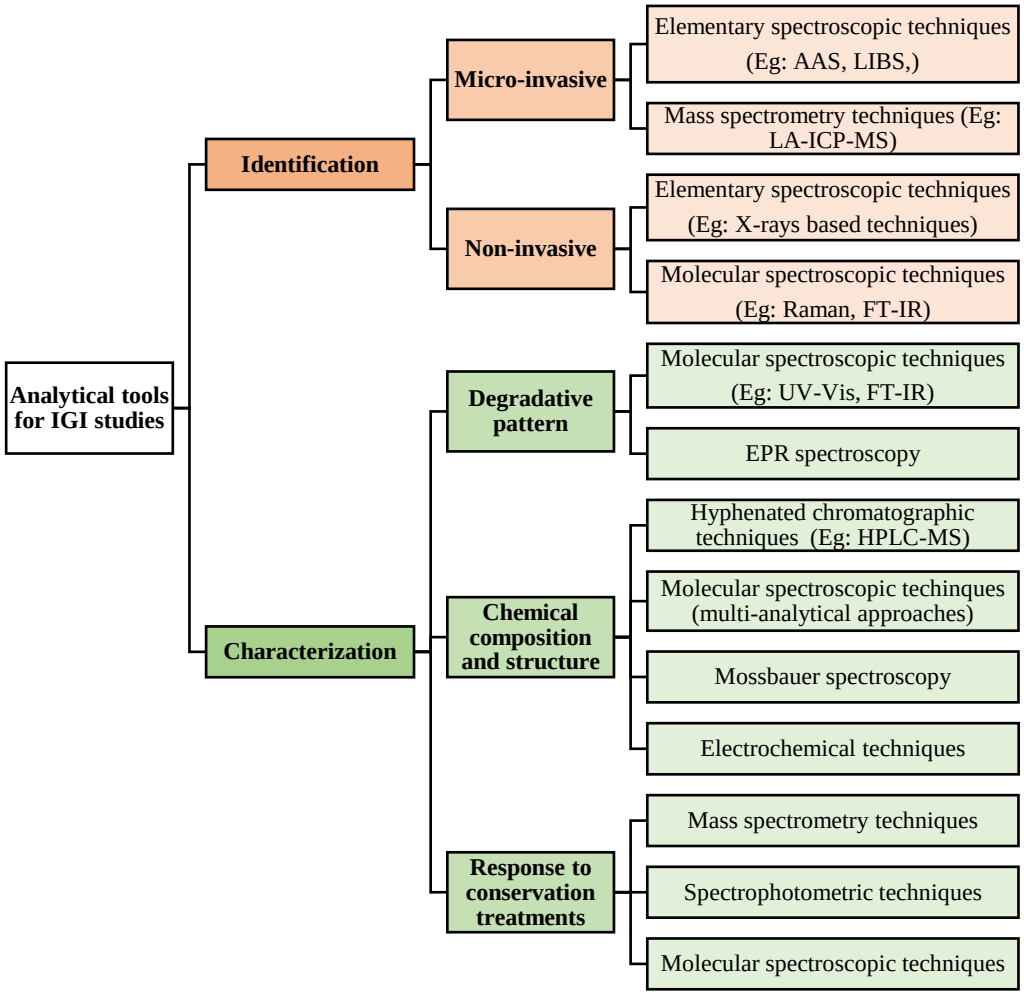

Fig. 12 Schematic summary of the most used analytical tools for the identification and the characterization of IGI.

Regarding the IGI characterization, most of the studies take advantage of multi-analytical approaches mainly based on molecular spectroscopic techniques such as Raman and FT-IR.[5,89,95,97,104]

Raman spectroscopy, in particular, is one the most used non-invasive method to identify the presence of IGI. The characteristic peaks of iron-polyphenolic complexes are generally quite visible and easily detectable in different supports.

However, in the usage of this technique in a characterization study, the Raman intrinsic limitations should be considered. The most important aspects in this respect are listed below:

- *Raman spectroscopy as surface technique*

  If this fact could be an advantage in the identification part, this is not the case for characterization studies. The results obtained with surface techniques can in fact be affected by many external factors such as morphology of the surface, optical properties of the bulk material (refraction and reflection phenomena), humidity, heterogeneity of the sample surface, consistency of the sample (powder, compact solid, liquid drop etc) and many others uncontrolled variables. For this reason, to have meaningful and statistically relevant results (in characterization studies), a massive amount of spectra are required.

- *Level of information details*

  Being a vibrational molecular technique, Raman spectroscopy can give information about the presence/absence of specific functional groups of interest. With a proper and meticulous study and using suitable references, Raman can give very useful information but the level of structural details cannot compete with the ones provided by mass spectrometry or NMR techniques. For instance, it would be quite hard to distinguish (with an acceptable level of certainty) GA and one of its

oligomers (and even more for a mixture of GA oligomers) just using Raman spectroscopy. To improve the potentialities of Raman from this point of view, it is not unusual to read about models based on ratios between peaks intensities and/or signal position shifts. These models have generally a quite limited applicability (local validity in statistical terms), especially considering the aspects mentioned in the previous point and the possible presence of other interfering substances. When a secondary and more reliable technique (such as MS) cannot be used to validate the model, it would be too speculative to completely rely on these kinds of models.

- *Fluorescence*

  Unfortunately this is an important limitation of Raman in the study of many organic materials, especially in the case of electron rich compounds as in this case. Fluorescence is a phenomenon related to the non-radiative emission of part of the absorbed radiation (the so-called inter-system crossing) which can interfere with the Stokes Raman signals[105].

  The final effect of this phenomenon is the non-quantitative emission of the radiation, causing the worsening of the baseline and a lowered sensitivity. This effect is encountered very often in organic materials but, in most of the cases, for identification of IGI does not constitute a real problem since the main peaks related to iron-polyphenolic complexes are generally quite visible. Concerning the characterization studies instead, in which a higher level of spectral details is needed, fluorescence constitute an important technical issue[G]. Setting aside the automatic fluorescence attenuation systems of some Raman software (which in any case could provide misleading results), the baseline correction needed in the case of strong fluorescence is often performed manually. This post-processing operation is obviously very useful to obtain nice and readable spectra, but on the other side it is a quite risky manipulation: it is often biased by the expectation of the scientist performing the data treatment. The position and, most importantly, the intensities and relative intensities of the peaks can dramatically change, the profile of the peaks can change as to provide misleading information (such as noise signals becoming a proper peak) etc.

2.4) Degradation patterns

Degradation IGI can be considered as the counterpart of chemical modifications of the different substances present in such systems. For instance, it has been observed that the Fe^{3+} resulting from the polyphenolic complexes autoxidation can be then reduced into Fe^{2+}.[70,87,92] This process involves the oxidation of the polyphenolic species into semiquinones which can be further oxidised to quinones (Fig.13).[69,70,87,108] Additionally, it has been also observed that the formation of quinones is favoured by low molar ratio [polyphenols]/[Fe^{3+}].[93] However, no Fe^{2+} accumulation due to this process has been noticed in the studied systems since its successive re-oxidation is promoted by iron-polyphenolic interactions.[87,93]

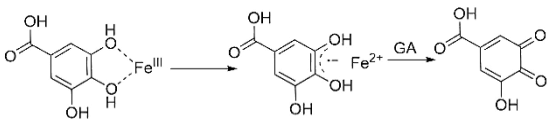

Fig. 13 Reduction of Fe(III) with formation of quinones via radicalic mechanism

[G] There are some attempts to overcome the fluorescence issue in organic electron rich molecules. In the field of IGI study, the most promising methodologies are the ones that take advantage from the localized surface plasmon resonance effect induced by noble metal colloids (Surface Enhanced Raman Scattering, SERS) or noble metal coated tips (Tip Enhanced Raman Scattering, TERS). For the curiosity of the reader see the interesting peer-reviewed papers *Wei*, ***2015***; *Espina*, ***2022*** and *Kurouski*, ***2014.***[105–107]

Nevertheless, the most well-known and mentioned degradative processes in manuscripts are related to hydrolysis reactions promoted by the ink acidity and the oxidative Fenton-type reactions which can cause severe damages to the ink support, which for medieval manuscripts are mainly cellulosic (paper) or proteinaceous (parchment)(Fig.14).[109,110] In fact, Fe^{2+} or Cu^{+} cations, together with other transition metal species eventually present on the support, can undergo a series of redox and Fenton-type reactions catalysing the formation of reacting oxygen species (ROSs) such as the hydroxyl radical.[70,111] Some of the main radicals formed during these processes are listed below:

Fig. 14 Degradation in a paper manuscript due to iron-gall inks induced reactions. Adapted from Gimat A. et al, ***2016***

(1) $Fe^{2+} + O_2 \rightarrow Fe^{3+} + H_2O_2$

(2) $Fe^{2+} + H_2O_2 \rightarrow Fe^{3+} + HO\bullet + HO^-$

(3) $Fe^{3+} + H_2O_2 \rightarrow Fe^{2+} + HOO\bullet + H^+$

(4) $Fe^{2+} + O_2 \rightarrow Fe3+ + O_2^{\bullet-}$

(5) $Fe^{2+} + H_2O_2 \rightarrow Fe(H_2O_2)^{2+} \rightarrow Fe^{IV}O_2^{2+} + H_2O \rightarrow Fe^{2+} + 2HO\bullet$

The so formed radicals rapidly react with the organic compounds present in the ink and/or in the support. The main steps of ROSs mediated oxidations are summarized in the following reactions.[101,109]

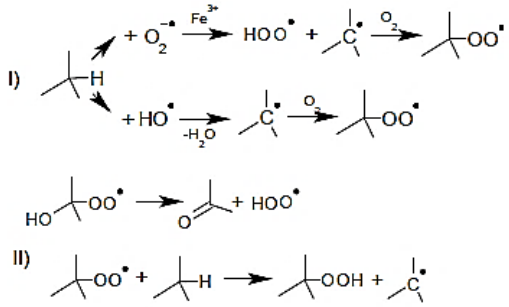

Both oxygen and hydroxyl radicals can interact with trisubstituted carbon atoms resulting in hydrogen extraction and the formation of a tertiary radical species. This radical is quite stable and can interact with additional molecular oxygen driving to the formation of peroxyl radicals. These radicals, finally, can generate additional radicals or undergo oxidation reactions forming carboxyl and carbonyl groups depending on the nature of carbon substituents.

It is also interesting to underline that several studies have demonstrated the possibility to observe autocatalytic oxidation processes via Fenton reactions in presence of quinones and semi-quinones, which are organic species that might be present in the system as previously reported (Fig.15).[112,113] The ROSs formed in this type of reactions may oxidise in different ways the ink support. Cellulose oxidation for example can lead to two groups of effects: simple modification of the glucopyranose units with the formation of aldehyde, carboxyl, and keto groups (eventually associated with ring openings) and oxidative cleavage of the β-glycosidic bonds resulting in the breakdown of polysaccharide chains[109]. Parchment oxidation, instead, primarily involves modifications of the side chains of amino acids resulting in an alteration in the charge balance of the collagen tertiary structure.[84,110,114] It should be underlined that oxidative processes and hydrolytic ones generally act synergistically and the study of the exact mechanisms of degradation is therefore quite complicated.

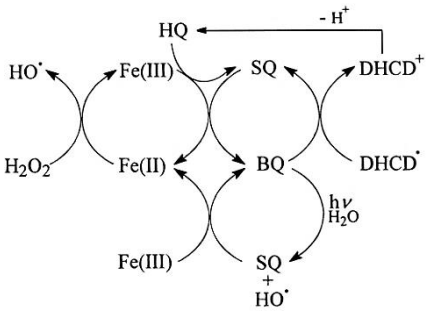

Fig. 15 Role of quinones in autocatalytic Fenton-like reactions. HQ=hydroquinone (1,4-dihydroxybenzene), BQ=quinones, SQ=semiquinones, DHCD=dihydroxy cyclohexadienyl (cation and radical). Figure adapted from Chen et al., ***1997.***

2.5) Modern fields of application

Formation of iron-polyphenolic complexes does not require particular experimental conditions or expensive equipment and their biologically tuneable physicochemical properties provide a platform for the engineering and assembly of advanced materials for potential use in a wide range of applications.[115,116] The so-called metal polyphenols networks (MPN) can be successfully used for the fabrication of nano-films, nano-capsules (or nano-shells) and nano-coatings having a great affinity with a large range of substrates ranging from inorganic materials to cell membranes.[83,108,115,117–119] For this reason, MPN-based molecular and bio engineering methods have started to be effectively used in a wide range of fields of applications ranging from the renewable energy technologies[108] to bio-imaging.[115] More in general, it has been also observed that catechol−Fe^{3+} complexes possess unique combination of mechanical features including high mechanical stability, fast reformation kinetics, and environmental sensitive mechanics. These properties can be exploited for the creation of innovative hybrid materials with high strength such as adhesive hydrogels.[77,120,121] Moreover, recent studies are focusing in the sorbent properties of iron-tannate microstructures in the field of water depuration technologies.[122] Lastly, strategies based on metal-catechol interactions, turned out to be interesting in the field of chemical modification of iron oxides surfaces (in particular iron oxides nano and micro particles)[H].[123–125] In the following scheme (Fig. 16) some of the modern applications of this chemistry are reported.

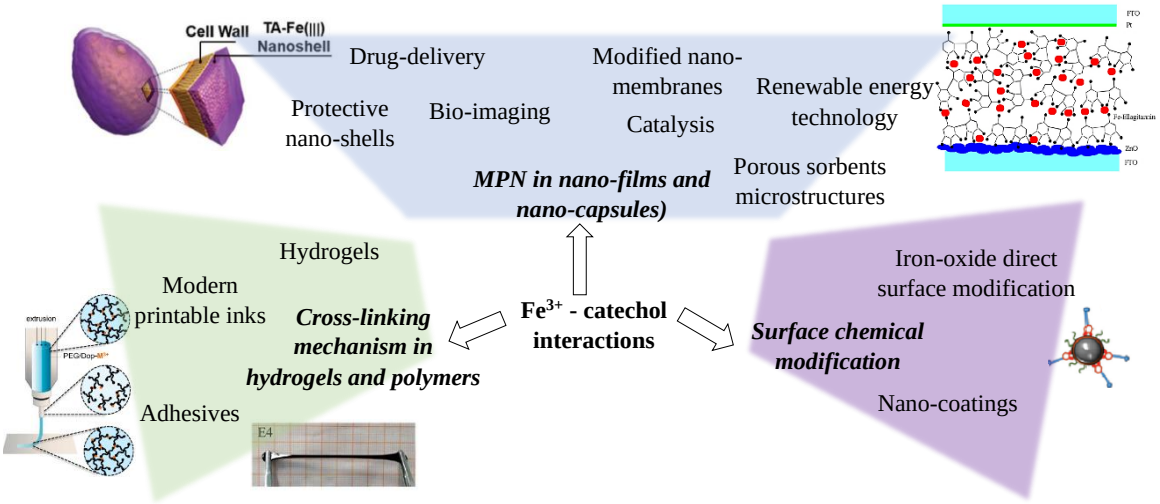

Fig. 16 Some of the modern applications of iron-catechol coordination chemistry.

Closing this introductive chapter, the main elements regarding the chemistry of IGI has been described, in particular focusing on the main aspects of IGI occurring iron-polyphenolic complexes. In the wide scientific literature on this field however there are still several gaps. The current thesis project therefore is exactly integrated in this optic of filling these knowledge gaps, as will be discussed in the next chapter.

[H] In these studies, several compounds bearing catechol groups have been involved, such as dopamine, trihydroxy benzaldehyde and hydro cinnamic acids. However, there are no reasons to doubt that the same results can be obtained with natural polyphenols from vegetal sources.

Box 1

Iron complexes chemistry – A brief description

Iron(II) and Iron(III)-polyphenolic complexes formation in aqueous systems can be defined more properly as substitution reaction in octahedral coordination compounds, since iron (at RT) tends to form octahedral aquo-complexes. These reactions generally proceeds so fast that it is almost impossible to study their precise mechanism, but in general they follow a dissociative pathway: the formation of the final complex is preceded by an intermediate complex having a lower coordination number and largely dissociated leaving groups (Fig.a).

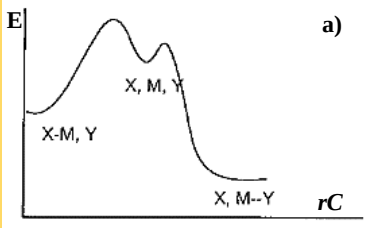

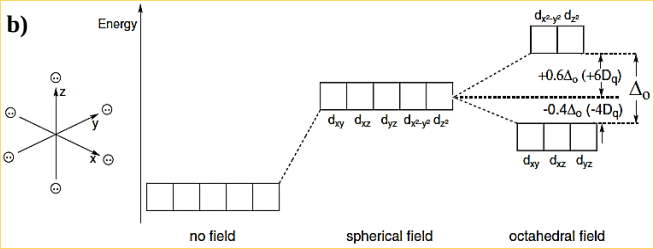

Coordination compounds structures and physicochemical properties can be described with different approaches. One of the still most used approach to discuss the properties of coordination compounds is the *Crystal field theory*, to which reference will be made later in the thesis. Without going into details, the main idea is that the degeneracy of the 5d orbitals of iron cations can be lost in coordination compounds (as to say when charges are introduced in specific locations around the 5d orbitals). The result of this phenomenon is therefore the formation of an energy gap called *crystal field splitting* (generally reported as Δ) between the lower and the higher energy d orbitals. An emblematic case is the octahedral field experienced by iron cations in presence of 6 point-charges introduced symmetrically along the x, y and z axes, each equidistant from the central ion at the vertices of an octahedral array. The loss of d orbital degeneracy results in their splitting in the lower energy diagonal set of orbitals (also defined as t_{2g}) and the higher energy axial set (also defined e_g)(Fig.b). The precise description of this outcome would require an important physical and mathematical explanation which is outside the aim of this thesis. Anyway, this model can be used to explain also other coordination environments geometries (Fig.c) and these aspects will be referred to later on in the current thesis.

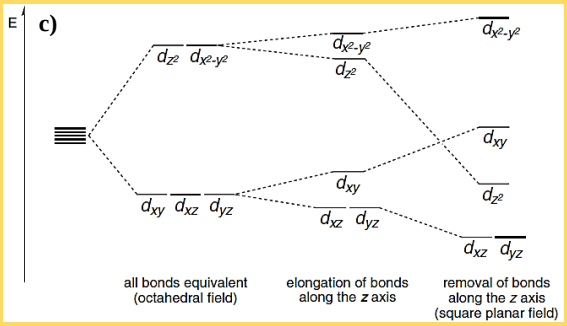

There are other theoretical approaches to study the structure and the properties of iron complexes but the Crystal field theory is the one which will be mostly referred to in the next chapters of this thesis.

Aim of the Thesis and definition of the methodological approach

1) Aim of the thesis

Starting from the state of the art upon IGI, the current thesis project is aimed at deepening the knowledge about this type of inks focusing on two of the most unexplored aspects in this field of study. The first part of the thesis project has been focused on the characterization of polyphenols-rich extracts, a crucial aspect for the study of IGI. The second part of the study, instead, was aimed at properly characterize iron-polyphenolic complexes. The novelty elements of this thesis project lie in the methodological approach implemented, including the use of analytical techniques not commonly used in the field of scientific studies on cultural heritage materials. The transversal goal of the current thesis is therefore to probe the potentialities of the innovative multi-analytical approach used and to highlight the critical aspects to optimize in future studies.

2) Definition of the methodological approach

In the following paragraphs the definition of the general methodological approach will be illustrated and discussed as to justify the choice of the operative workflow which can be summarized as follows(Fig.17):

(1) Preparation of freeze-dried aqueous extracts starting from 5 different galls samples: one sample of Aleppo oak galls and 4 samples of Italian oak galls.
(2) Characterization of the extracts via ^{31}P NMR and HSQC
(3) Preparation and isolation of iron-polyphenolic complexes using both simple polyphenols as model compounds and the freeze-dried galls extracts prepared in the step 1.
(4) Characterization of the iron-polyphenolic complexes prepared in step 3 via CW-EPR and Raman spectroscopy as auxiliary technique. In the case of CW-EPR both the solid and the supernatants (referred in the following chapters also as liquid) resulting from the isolation procedure have been analysed while the Raman characterization involved just the solid samples.

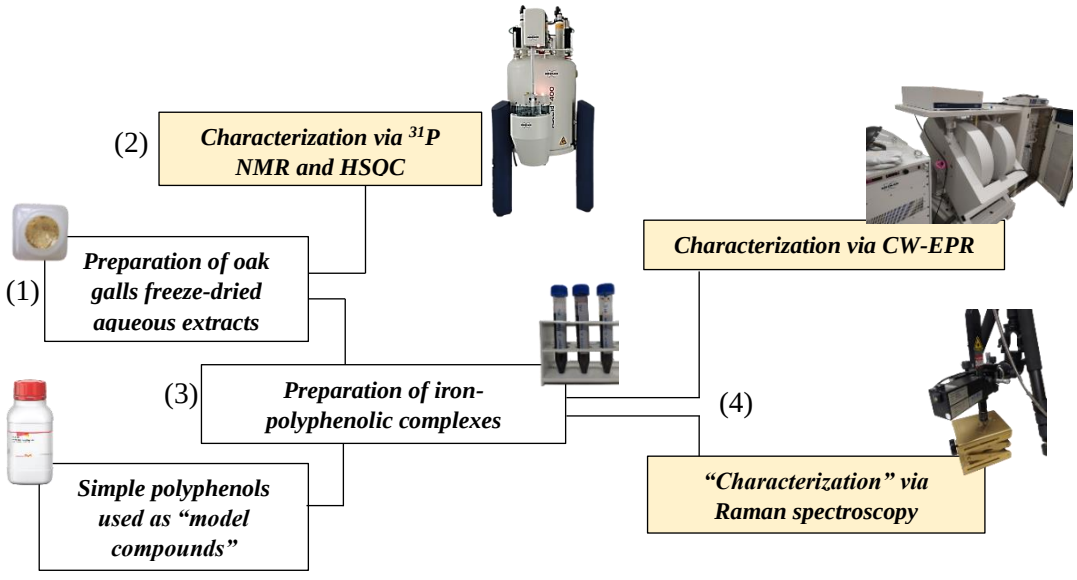

Fig. 17 Schematic representation of the thesis project workflow

All the technical aspects and the accurate description of the protocols for the preparation of the samples and the analyses are instead reported in the experimental section. The results reported in the following chapter are just referred to the characterization of the extracts and of the iron-complexes (actually few observations related to the preparation of the complexes are reported too).

2.1) Preparation and characterization of oak galls extracts

As previously mentioned in the introduction chapter, the oak galls extract composition represents one of the main elements of variability in the IGI preparation. In order to access this variability, the first step of the methodology has been the preparation of oak galls extracts. Considering what has been discussed in the introduction about the nature of this type of extracts, the accurate reproduction of gall extracts according to historical IGI recipes would have introduced in the study numerous variables (related to the presence of substances such as wine, vinegar, additives etc) whose role in the final extract composition necessitate an appropriate and time-consuming study.

The first step of the methodological approach therefore has been the preparation of gall extracts with a more systematic and simplified approach having as main variable to be evaluated just the typology of galls. In this study five different oak gallnuts samples have been considered: Aleppo oak galls and four typologies of Italian oak gallnuts with a slightly different provenience. Starting from oak galls therefore, oak galls aqueous extracts have been prepared in laboratory using a systematic procedure (properly described in the "Experimental section" chapter) and then freeze-dried. The in-depth characterization of the so-prepared gall extracts necessitated the use of suitable techniques for the accurate identification and quantification of polyphenolic species present. Considering the aspects reported in the Introduction chapter related to the characterization of plant extracts, and taking into account also a series of technical constraints, it has been decided to characterize the prepared freeze-dried extracts via ^{31}P NMR and HSQC.

2.2) Preparation of iron-polyphenolic complexes

In order to access detailed information about the structure and eventually the degradation patterns of iron-polyphenolic complexes in IGI, the first step to consider is the preparation of suitable mock-ups samples. As illustrated in the first chapter of the thesis, the historical recipes for IGI preparation involve the use of binder(s) and additives (see paragraph 1.3 in the "Introduction" chapter). However, in order to achieve the aim of the current project, a simplification and systematization of the preparation procedures is not only suggested but necessary to have a proper control of almost all the variables involved in the formation of the iron-polyphenolic coordination compounds. For this reason, in this stage of the study, neither the use of binders nor the one of additives has been involved.

Moreover, it has been decided to operate in two directions: on one side iron-polyphenolic complexes have been prepared using simple polyphenols, and in particular GA and EA, and the other side iron complexes have been synthesized using as source of organic ligands two of the freeze-dried oak galls extracts previously prepared.

All the technical details regarding the practical aspects of the preparation and isolation of the complexes are properly addressed in the "Experimental section" chapter but some very important and key aspects have to be introduced here.

As briefly introduced and discussed in the previous chapter, the first step of the formation of iron-polyphenolic complexes is strongly pH-dependent (see paragraph 2.1 in the "Introduction chapter"). This aspect is enough to state that an accurate study of iron-polyphenolic complexes ***must*** involve the pH control conditions in the complex formation step. In other terms, the pH conditions control in this stage is not optional but ***formally required***. This aspect has been fundamental in the definition of the methodological approach and surprisingly it also represents a novelty in the study of iron-polyphenolic complexes in IGI.

It is true that polyphenolic substances, and in particular polyphenolic acids such as GA and EA, are characterized by pH values in between strongly and mildly acidic[126,127] and that the final pH of IGI is typically strongly acidic.[5] However, considering the whole variety of historical recipes for IGI preparation several elements affecting the pH in this iron complexes formation step emerge including:

a. Composition of the extracts (including all the substances coming from the natural matrices and the ones introduced with the extraction solvents, especially in the case of vinegar and wine);
b. Concentration of the acidic species in the extracts, or in other terms, ratios galls: extraction solvent used for the extract preparation;
c. Typology and concentration of pH-affecting additives and binders (see paragraph 1.3 in the "Introduction chapter").

Considering these aspects, it has been decided to prepared iron complexes not only in a single pH condition, but to evaluate the effect of pH in the formation and, more properly, in the final structure, of iron-polyphenolic complexes, working with three controlled pH-conditions. These have been selected starting from considerations regarding the binding capabilities of different protonation states of the ligands involved in the formation of iron-polyphenolic complexes in IGI, and in particular GA and EA (see paragraph 2.1 in the "Introduction" chapter). Therefore, iron complexes prepared using both simple polyphenols and oak galls extracts have been prepared in three pH-controlled conditions (as to say in aqueous buffers): pH 4, as to have completely protonated ligands, pH 6, to have mainly partially deprotonated ligands, and pH 12, to have mainly strongly and completely deprotonated ligands. Unfortunately, due to low solubility in aqueous media of EA, it has not been possible to prepare Fe-EA complexes in controlled pH gradient. In this case it has been decided to prepare complexes starting from EA methanol solution and EA water/methanol (1:1) fine dispersion as to check the occurrence of important differences in the complex's structures[I].

All the iron-polyphenolic complexes have been then isolated. The isolation procedure has been optimized in this study since no information about oxidation times and separation procedures are available in scientific literature. The isolation procedure involved the use of centrifugation cycles which enabled to obtain solid precipitates, that then have been properly dried in mild conditions, that will be simply referred to as "solids" in the following chapters, and supernatant fine dispersions, for brevity defined "liquids" in the presentation and discussion of the results[J].

2.3) Characterization of iron-polyphenolic complexes

Regarding the characterization of the prepared iron-polyphenolic systems, an innovative analytical approach has been used which involves the use of electron paramagnetic resonance spectroscopy (EPR), and Raman spectroscopy, which has been used just as an auxiliary technique. A quick monitoring of the prepared complexes with Raman spectroscopy can in fact reveal easily anomalies due to technical issues in the preparation and/or isolation of the complexes and can also provide a general overview of the systems such as unusual rough ratios between signals intensities. However, it is the implementation of EPR in this field of study which actually constitutes the novelty element of this second part of the investigation.

EPR is a spectroscopic technique still not completely valorised and explored in many fields of applications, including the Conservation Science one. Being a spectroscopic technique not so popular in common analytical laboratories, the following paragraph will give to the reader a brief (and absolutely not exhaustive) overview of the basic principles of this technique.

2.3.1) Electron Paramagnetic Resonance (EPR): an innovative analytical tool in the IGI characterization

Electron spin resonance (ESR), also called EPR, is a spectroscopic technique confined to the study of species having one or more unpaired electrons. Among the large number of these paramagnetic systems,

[I] All the technical aspects regarding the preparation of iron-polyphenolic complexes, including the proper definition of "pseudo-stoichiometric regimes" are properly addressed in the "Experimental section" chapter.
[J] All the technical aspects regarding the isolation of iron-polyphenolic complexes are properly addressed in the "Experimental section" chapter.

the most important ones are free radicals, transition metal ions, ions and molecules having odd number of electrons.

Similarly to NMR, EPR is based on the energy separation of the electron spin states induced by an external magnetic field, B_0, in the so-called Zeeman Effect. Without going into details, it useful to remind that electrons are characterized by an orbital magnetic momentum, related to the electron intrinsic angular momentum due to its motion around the nucleus, and a spin magnetic momentum, derived by the spinning of the electron around its own axis. The predominant contribution to the total magnetic moment, μ, is indeed the spin angular magnetic moment, M_s, which always has discrete values and that can be also defined starting from the spin direction vector m_s (eq.2-3):

(2) $M_s\hat{z} = \left(\sqrt{s(s+1)}\hbar\right)\cos\theta \; = m_s\hbar$

(3) $\begin{cases} M_s\hat{z} = \left(\sqrt{s(s+1)}\hbar\right)\cos\theta \\ \mu = -g\mu_B M_s \\ \mu_Z = \mu\cos\theta \end{cases} \rightarrow -\boldsymbol{g\mu_B M_s}$

Where "s" is the spin quantum number, "ħ" is the compact form of the Plank constant divided by two pi, "g" is a dimensionless factor called Landé factor, which for a single electron is 2.0023, and "μ_B" is the basic unit of magnetic moment of the electron, known as Bohr magneton (which is equivalent to eħ/2m where m is the mass of the electron.

When an electron is placed in a magnetic field B_0, this interacts with the electron magnetic moment creating an energy gap related exactly to the discrete values of M_s. An external radiation with a proper frequency could promote the transition between the two spin states[K] (the selection rules for the allowed EPR transitions is $\Delta m_s = \pm 1$)(eq. 4, Fig.18).

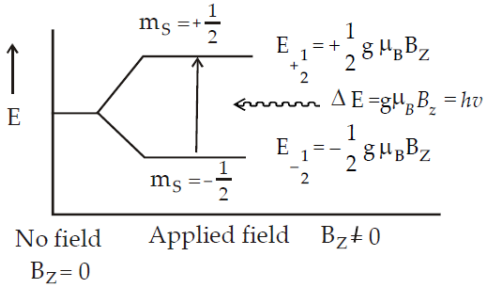

Fig. 18 Transition between two spin states of a free electron (single ESR peak detection).

(4) $\begin{cases} E = -\mu B \\ \mu = -g\mu_B M_s \\ \Delta E = E_{\mu'} - E_{\mu''} \end{cases} \rightarrow \Delta E = g\mu_B B \rightarrow \begin{cases} \Delta E = g\mu_B B \\ \Delta E = h\nu_R \end{cases} \rightarrow \nu_R = \frac{g\mu_B B}{h} \rightarrow g = \frac{\nu_R(GHz)}{B(mT)} * 71.448$

Where μ' and μ'' are referred to different magnetic moment values due to M_s and ν_R is the resonance frequency. Please note the linear relation between the resonance frequency and the applied magnetic field. In the current thesis project, it has been used an instrument operating with a value of B of 34GHz: this result in tuning microwave frequencies of isolated electrons (g≈2) in the range of 9.5/9.75 MHz.

Systems operating in these conditions are said to work in the X-Band. EPR instrumentation operating with higher magnetic fields (and therefore higher frequencies) are available and commonly used in ESR. During the discussion of the results for instance there will mention the necessity to conduct further study in the Q-Band: this corresponds to work at B values of around 130MHz and higher tuning frequencies.

[K] Sometimes, in analogy to NMR, they are referred to as α-spin state, the one with a higher energy, and β-spin state, the one with a lower energy.

For technical reasons, the signal detection in most of ESR techniques follows a different route from the conventional spectroscopic techniques. After a first step of tuning, the sample placed in a cavity (suitably constructed to have an optimal impedance) experiences a constant microwave frequency while the magnetic field strength is modulated (varied) sinusoidally with a certain frequency called "modulation frequency". If there is an EPR signal, the field modulation quickly sweeps through part of the signal and the microwaves reflected from the cavity[L] are amplitude modulated at the same frequency. This process is commonly referred to as "phase sensitive detection" and it normally results, as it would be notice in the presentation of the results, in signals with a typical derivative shape (Fig.19).

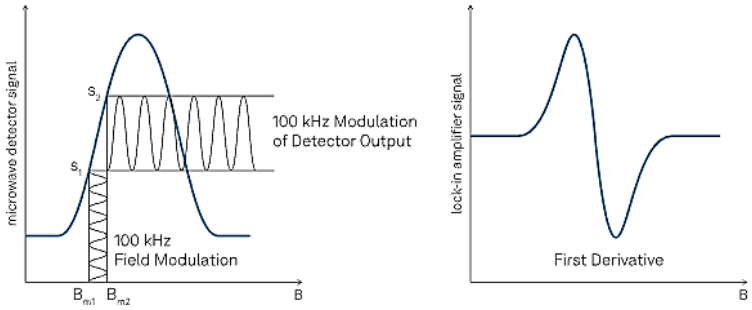

Fig. 19 Phase sensitive acquisition method of ESR signals

ESR spectroscopy can be practically actuated both in Continuous Wave (CW) and pulsed modes: in the first case microwaves at low power are continuously sent to the sample while in the latter the sample are exposed to a series of short and intense microwave pulses. Then, a series of technical variants has been introduced to better explore different kind of samples and spin-state systems, including the well-known techniques Electron Nuclear Double Resonance (ENDOR) and Electron Spin Echo Envelope Modulation (ESEEM).[129]

The potentialities of EPR techniques are numerous and the fields of application range from technological materials study and development to biochemistry and medicine. In the following scheme, some of the most important applications are reported (Fig. 20).[128,130,131] Due to the versatility of EPR in fact, it is possible not only to study different systems obtaining valuable information about structure, typology and abundance of paramagnetic centres, but it is also possible to take advantage of techniques such as ENDOR, ESEEM and spin labels methods, to have precious information of their chemical microenvironment.[128]

[L] The cavity in which the sample is placed is "critically coupled" with a microwave guide. When an absorption of energy from the sample occurs the standing wave frequency inside the cavity is not coupled anymore with the waveguide and a reflection occur. The readers can find further and more detailed information in *Lund et al., **2011***[128] and in the common EPR instrument manuals.

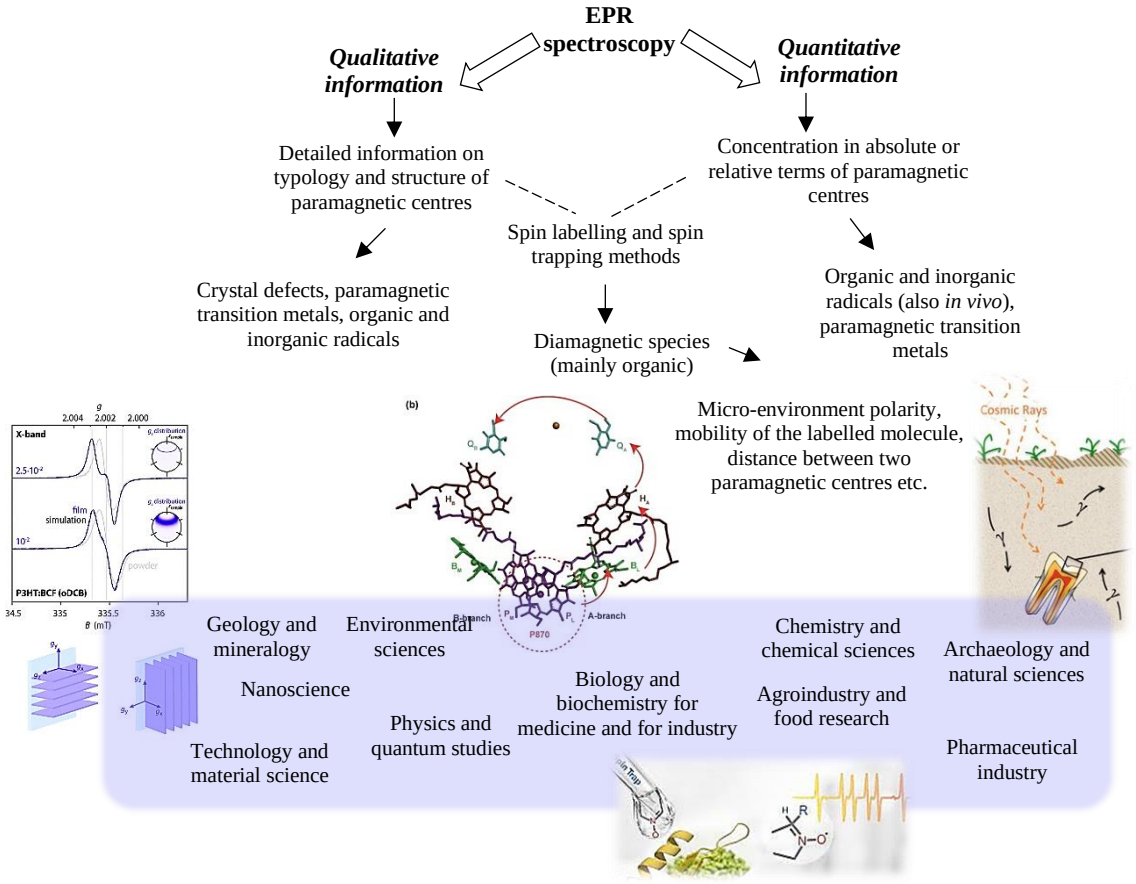

Fig. 20 Some of the most important information that can be obtained using EPR and some of the possible fields of application of the mentioned above in the text.

In the case of paramagnetic transition metal in solid complexes, like the ones involved in the current thesis project, ESR can be useful to elucidate the coordination environment and in particular the coordination site symmetries within the complexes. Basically, when a transition metal with an odd number of electrons is placed in a crystal field, the spin levels may be split even in the absence of a magnetic field: this phenomenon is called "zero field splitting" (ZFS) or "fine structure". For species with an odd number of unpaired electrons, therefore the spin degeneracy of every level remains doubly degenerate. This is known as Kramer's degeneracy. When the metal instead posses an even number of unpaired electron, the degeneracy can be totally quenched by the crystal field. For an explicative example of this phenomenon, please see the box "*Practical description of Fe^{3+} spin states system*" reported at the end of this chapter.

The very last point to mention in the description of the Landè factor g is not necessarily isotropic and needs to be treated as a tensor g^M. The anisotropy of g is a source of important information to define the coordination site geometries of the paramagnetic centres.

The ESR methodology used in the current thesis project has been a CW-EPR in X-band. In particular, the study has involved two blocks of measurements: a first block in which an overall monitoring of the iron complexes has been performed at RT and at 100K, and a second block in which instead selected iron complexes have been investigated more in depth with temperature gradient and time monitoring

[M] A complete description of EPR spectroscopy and in particular of the g factor would require a quantum mechanical approach. For the aim of the current thesis project however it is sufficient to bear in mind that the electron spin Hamiltonian which can better fit the properties of unpaired electrons in such systems (solid samples containing paramagnetic centres) must consider g as anisotropic and therefore as a tensor described by a 3x3 matrix. For the curiosity of the reader, valid books for all the theoretical part of ESR, including the quantum-mechanic picture, are *J.W.Orton*, ***1968*** and the famous *Abragaam and Bleaney*, ***1970.***[132,133]

experiments. The selection of the samples used in the second block of measurements has been carried out starting from a first general interpretation of the results obtained in the first block.

Box 2

Practical description of Fe^{3+} spin states system

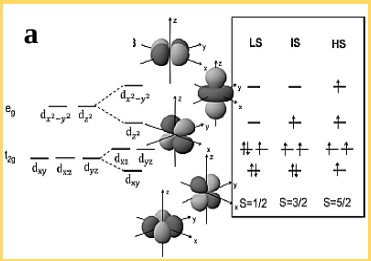

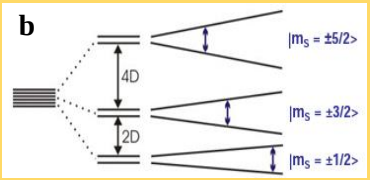

Electronic configuration of Fe^{3+} is $4s^2\ 3d^5$ and the allocation of the 5 electrons in the d-orbitals depends on the strength of the crystal field it experiences. For high crystal fields the final electronic configuration is $t_{2g}^5\ e_g^0$ or in other terms $3d_{xy}^2\ 3d_{xz}^2\ 3d_{yz}^1\ 3d_{z^2}^0\ 3d_{x^2y^2}^0$ resulting in the so-called low-spin state (LS) S=1•1/2=**1/2**. In low crystal filed the electronic configuration is the opposite: $t_{2g}^3\ e_g^2$ $(3d_{xy}^{\mathbf{1}}\ 3d_{xz}^{\mathbf{1}}\ 3d_{yz}^{\mathbf{1}}\ 3d_{z^2}^{\mathbf{1}}\ 3d_{x^2y^2}^{\mathbf{1}})$ resulting in the high-spin state (HS) S=5•1/2=**5/2**.

Considering the orbitals in t_{2g} and e_g as no longer as degenerate, as occur in distorted coordination sites, another electronic state, called intermediate-spin state (InS), is allowed: $3d_{xy}^2\ 3d_{xz}^{\mathbf{1}}\ 3d_{yz}^{\mathbf{1}}\ 3d_{z^2}^{\mathbf{1}}\ 3d_{x^2y^2}^0$ and the final S=3•1/2=**3/2 (**Fig.a). In the case of iron complexes the general electronic system results in a null orbital angular momentum (L=0). In terms of M_s, setting aside the spin-orbit coupling interaction which for the iron-group should be cosider a first order perturbation, this situation simply results in M_s=±1/2 for LS, M_s=±3/2 for InS and M_s=±5/2 for HS. In presence of ZFS interactions these three states are no-longer degenerate even in absence of the exteral field B resulting in 3 Kramer's pair. Without going through the quatum-mechanics description, it can be state that the Zeeman effect "acts" on systems in which the 5d orbitals have already lost their degeneracy: for transition metals the spin systems, and the resulting EPR spectrum, are always strongly dependent on their electronic configuarations and in particular on the crystal field splitting magnitude.

Concluding, in ESR mainly two situations for Fe^{3+} can be observed:

1) Low ZFS or "high symmetrical systems" does not allow the formation of Kramer's pair (spherical crystal field – *see Box1, Iron complexes chemistry – A brief description*). The five degenerate d-orbitals are splitted via Zeeman effect and this result in the EPR line at g≈2.
2) High ZFS, indirectly related to high crystal field and therefore strong coordination interactions, allows the formation of 3 well separated Kramer's pairs (Fig.b). What happen is that transitions in lowest and highest-energy Kramer's pairs are strongly anisotropic and consequently their signals can be hardly visible.
   The consequence of this phenomenon is that the transitions in the central Kramer's pair (M_s=±3/2) is the only isotropic one and can be visible at g values which depend on the distortion of the coordination site. This distortion magnitude is generally measured through the E/D ratio, also called "rombicity parameter". The extreme limit of this effect is when E/D is amost 0.33 resulting in a g value of about 4.3 (Fig.c).

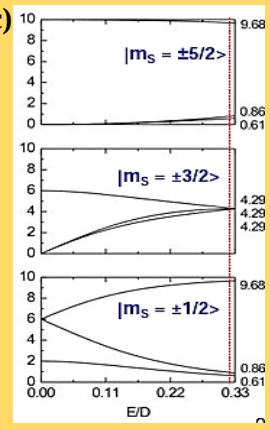

Results and discussions

1) Oak galls extracts preparation and characterization

As illustrated in the previous chapter, the first step of the methodological approach has been the preparation of gall extracts with a more systematic and simplified approach in respect to those actually mentioned in IGI preparation recipes, having as main variable to be evaluated just the typology of galls. The extraction procedure selected involved a simple solid-liquid extraction at room temperature (RT) using Milli-Q water as extraction solvent. The ratio between vegetal matrices and solvent has been set at 35mL of Milli-Q per gram of crushed galls. At the end of the extraction period, for each sample, the insoluble part has been separated from the clear extract solution via filtration and centrifugation. Finally, they have been freeze-dried as to obtain powders suitable for the characterization step[N]. In the following table (Tab.1) the extended names and the abbreviations for the mentioned samples are reported.

Tab. 1 Extended names and abbreviations of oak galls extracts samples used in the following chapters of the thesis.

Sample number	Extended name	Freeze-dried extract sample abbreviation
1	Aleppo oak galls, Turkey (distributed by Kramer Pigmente)	Ex1
2	Oak galls manually collected in Zavattarello (PV), Italy	Ex2
3	Oak galls manually collected in Menconico (PV), Italy	Ex3
4	Oak galls manually collected in Ticino Valley Natural Park (NO), Italy	Ex4
5		Ex5

1.1) ^{31}P NMR results

The characterization via ^{31}P NMR turned out to be more than important for the identification and the quantification of the different polyphenolic classes present in the gallnuts aqueous extracts. In Fig. 21 the spectrum related to the Extract 1 (Aleppo gallnuts extract) is reported.

[N] The precise description of the oak galls samples and the aqueous extracts preparation steps is properly addressed in the "Experimental section" chapter.

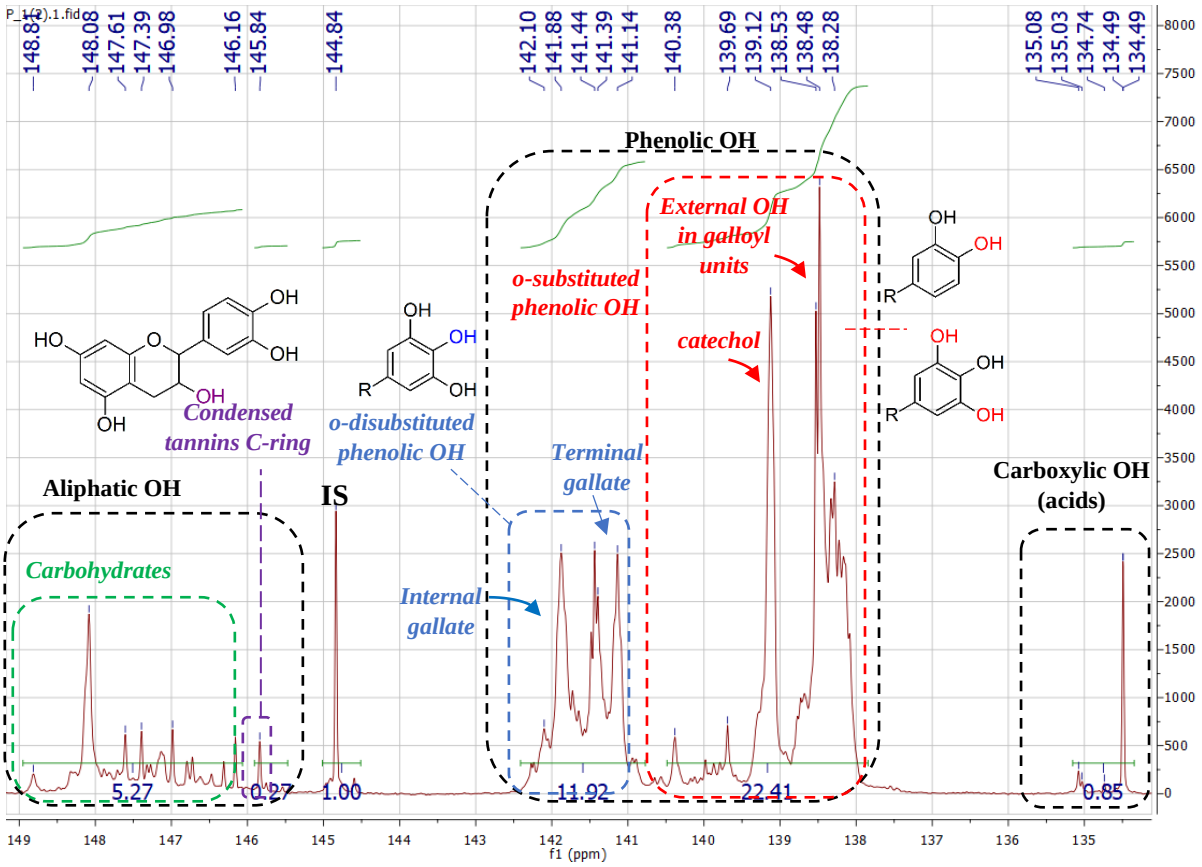

Fig. 21 ^{31}P NMR spectra of Extract 1 after phosphitylation with Cl-TDMP. The position of the main peaks is reported in the upper part of the spectrum while in the bottom part the results of the integrations are reported below the green horizontal lines. IS= internal standard main peak.

As can be seen from the spectrum reported, hydroxyl groups can be divided (according to the chemical shifts of related labelling phosphorus) in at least three major regions: the aliphatic OH region (~149.0-145.25ppm), the phenolic OH region (~144.0-137.0ppm) and the carboxylic OH region (135.5-134.0ppm).[24,35,36,47,56,57] These regions can be then further subdivided in smaller regions according to previous studies on model compounds.[35,36,38] In this case the aliphatic OH region for instance include a spectral area in which the signals related to hydroxyl groups of carbohydrates usually can be found (~149.0-146.0ppm) and in another area, which in this case is poorly populated, related to aliphatic OH of proanthocyanidins and their derivates (145.25-146.0ppm).[36] The second major group of OH signals, the one of phenolic OH, can be subdivided according to the substitution of the hydroxyl groups: in this specific case at least two clear sub-regions can be identified: the one related to ortho-substituted phenolic OH (~140.6-137.6ppm) and the one of ortho-disubstituted (~142.5-141.1ppm). Based on the comparison with literature spectra, other and more detailed assignments can be proposed. The region of ortho-disubstituted OH can be for instance further divided in at least two region: the peaks with a higher chemical shifts, such as the peaks in the spectral range 142.2-141.8ppm, can be attributed to ortho-disubstituted OH in gallate units positioned more internally in HT structures, while those that can be found at slight lower chemical shift can be instead attributed to more terminal units.[36] The assignments of some peaks turned out to be not that simple: the peaks in the spectral range 140.5-139.5ppm for instance, according to scientific literature[36,57] they can be still attributed to ortho-substituted phenolic OH but their precise assignment is not perfectly clear. Another critical point is concerning the peaks in the lower limit of the aliphatic OH region: according to literature the peaks in the range 146.0-145.5ppm, as previously mentioned, should be attributed to those aliphatic OH in proanthocyanidins and condensed tannins. In this case however it is also possible to merge these peaks with those related to carbohydrates.

In order to have a clearer picture of the real content of Ex1, the quantitative results should be considered[O]. The following table (Tab.2) reports the results of the integration of the peaks and the final results in terms of concentration of specific OH classes.

Tab. 2 Quantitative results of ^{31}P NMR analysis of Ex1. O-substituted/disubstituted standing for ortho-substituted/disubstituted.

	Aliphatic OH			**Phenolic OH**			**Carboxylic OH**
	Carbohydrates (149-146ppm)	C-ring in Proanthocyanidins (146-14.5ppm)	Total	o-substituted (140.6-137.6ppm)	o-disubstituted (142.5-141.1ppm)	Total	
Area*	5.27	0.27	5.54	22.41	11.67	34.08	0.85
mmol/g	1.57	0.08	**1.65**	6.66	3.47	**10.13**	**0.25**

*Area calculated by MestreNova software

What can be observed is that the majority of hydroxyl groups are indeed related to phenolic OH. Their total concentration is about 10.13mmol/g which is not so far from the results obtained by *Melone F. et al.* in a previous work related to ^{31}P NMR quantification of OH groups in samples of TA extracted from different sources (Fig. 22).[35] Considering the results mentioned in that study and comparing them to the ones reported in Tab.3 a similar ratio between o-substituted and o-disubstituted phenolic OH can be noticed with a slight higher ratio ortho-disubstituted/ortho-substituted phenolic OH in the samples analysed in the mentioned study (0.52 in the case of Ex1 while 0.59 in the Turkish galls TA) suggesting an average slightly lower dimension of the HT present in the analysed Ex1[P]. However, considering the different nature of the samples (in the case of the mentioned study the authors used commercial tannins while this study is focused on aqueous galls extracts), the obtained results can be defined as quite in accordance with the presence of an important amount of TA, which is an extremely important evidence for the aim of this study and will be further discussed in the following sections.

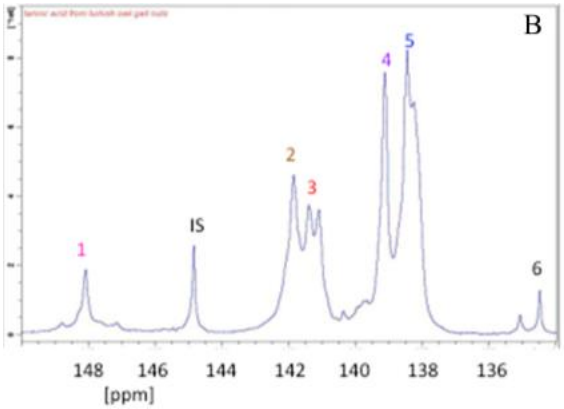

Fig. 22 ^{31}P NMR spectrum of TA from Turkish gallnuts reported in the mentioned study of Melone F. et al.

Another element which could be tremendously important is the presence of a small amount of proanthocyanidins. When present, their concentration should be in the order of a tenth of millimole per gram of sample: in this case just the signals related to the aliphatic OH are visible while the possible presence of signals related to the phenolic OH of the A and B ring of these polyphenolic species are not clearly visible or distinguishable from the other signals. It would be useful therefore to implement further analyses to elucidate the structure of these proanthocyanindins.
Obviously, the presence of un-esterified small polyphenolic units such as GA and EA cannot be excluded. The important evidence that however suggest a minor quantity of hydrolysed (un-esterified) polyphenols is the low concentration of carboxylic acid OH: in GA for instance the concentration of carboxylic hydroxyl groups should be not so different from the one of ortho-disubstituted phenolic OH. This is not the case in the spectrum acquired for Ex1 in which the intensity of ortho-disubstituted phenolic OH (in terms of area), just considering the peaks with a chemical shift close to the one of GA,[36] is about 3.5 times the one of carboxylic OH. Finally, another important evidence suggesting the predominance of proper HT

[O] The procedure for the quantification of hydroxyl group is properly described in the "Experimental section" chapter.
[P] An higher orto-disubstituted/orto-substituted phenolic OH ratio in fact suggest lower concentration of ortho-substituted phenolic OH, the ones more generally prone to the formation of depside bonds due to steric constraints.

is the presence of the intense peak related to catechol groups: this can be related to simple polyphenols carrying catechol moieties or, more probably, the presence of esterified units. If so, the depside bond should be more frequent in the ortho-substituted phenolic OH leaving free catechol moieties in the internal gallate units. To understand more clearly the ratios of all these considerations, a final scheme with some structures of TA and HT is reported in Fig.23.

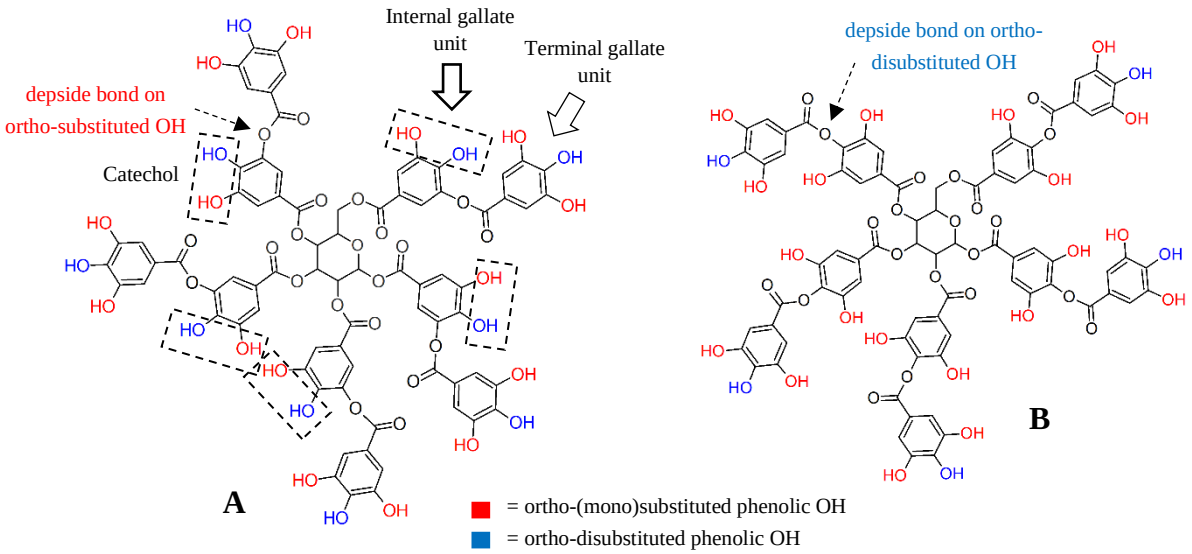

		A	B
orto-(mono)sub	cat.	5	0
	non-cat	10	20
	tot	**15**	**20**
orto-disub	internal	5	0
	external	5	5
	tot	**10**	**5**
orto-disub/orto-sub ratio		**0.66**	**0.25**

Fig. 23 Example of two TA structure. In the structure A all the depside bonds are on o-substituted phenolic OH while in the structure B are all on o-disubstituted ones. The table reported below is roughly representing how the relative ratios between the specific phenolic OH change accordingly to the structure.

The most interesting results however emerged from the ^{31}P NMR characterization of the Italian gallnuts extracts (Ex2-Ex5). In Fig.24 the spectrum related to the sample Ex2 is reported. As can be clearly noticed, the overall appearance of the spectrum is quite different from the previous one. Qualitatively, the major differences between the spectrum of Ex1 and the one of Ex2 are focused on the region of phenolic OH: the area of o-disubstituted OH in this case should be considered a bit wider due to the presence of weak signals in the spectral range 142.5-141.9ppm. According to literature data,[36,42] these signals can be attributed to o-disubstituted OH in B rings of proanthocyanidins (highlighted in the spectrum with a yellow arrow). Actually, in some studies[42] this region is extended in its upper limit until about 143.5ppm[Q]. In any case, the signals related to hydroxyl groups in B rings of proanthocyadins can be found in the whole spectral region 142.5-138.0ppm,[35,36,47] but just the ones shielded at higher chemical shifts can be associated to these molecules while, as mentioned before, in the rest of the region, signals related to numerous other compounds can be present.

[Q] In some cases the spectral range[38,57] 143.5-142.5ppm is attributed to syringil units in lignin while in some other cases,[42,47] as mentioned in the text, the peaks present in this spectral range are still attributed to B-ring of proanthocyanidins carrying galloyl moieties (gallo/epi-gallocatechin).

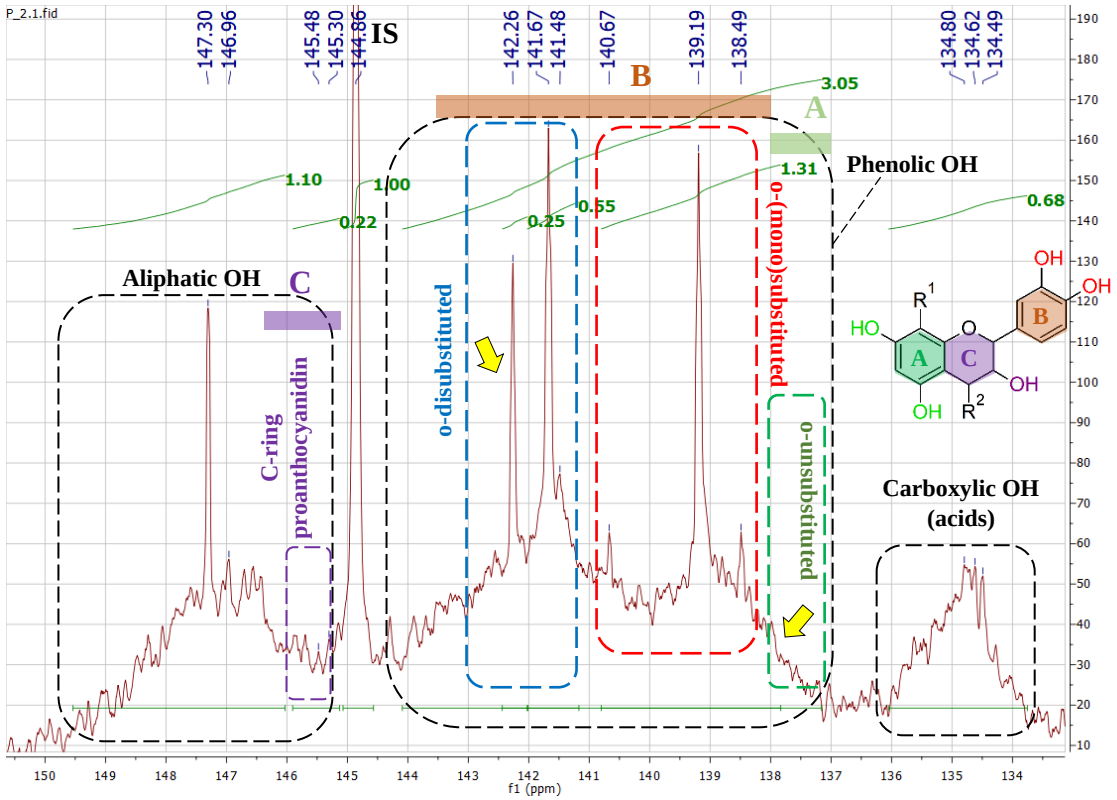

Fig. 24 ^{31}P NMR spectra of Extract 2 after phosphitylation with Cl-TDMP.

Another important element is the presence of some signals, still quite weak, in the region 138.0-137.0ppm (highlighted with a yellow arrow in the spectrum). These peaks can be instead attributed to ortho-unsubstituted phenolic OH like the ones generally present in the ring A of proanthocyanidins.

These features are more visible in the ^{31}P NMR spectra acquired on Ex4 and Ex5, as can be seen from the enlargement of the polyphenolic OH region of the spectrum acquired on Ex4 reported in Fig.25 (all the complete ^{31}P NMR spectra of the Extracts 3 to 5 are reported in Appendix A in Fig. 1 to 3).

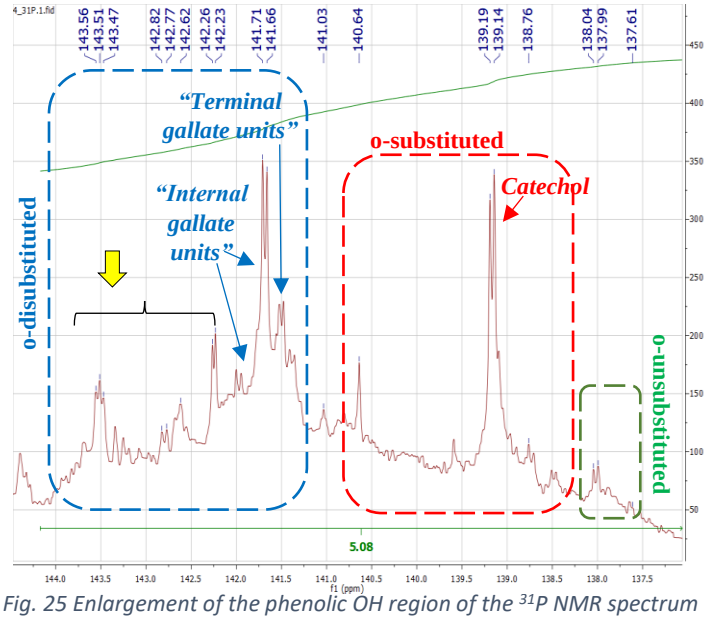

Fig. 25 Enlargement of the phenolic OH region of the ^{31}P NMR spectrum of Extract 4 after phosphitylation with Cl-TDMP

The interpretation of the ^{31}P NMR of Italian oak galls extracts however, is in general more complicated than the previous case. It is interesting for instance to notice that, considering the ortho-(mono)substituted phenolic OH, there is always an absolute predominance of signals attributable to catechol moieties. This aspect would be quite regular in case of high concentration of proanthocyanidins carrying a catecholate group in the B ring (profisetidins and procynidins)[36,42]. However, if this was the case, the signals related to the A ring should be significantly more intense. Another aspect to underline instead regards the ortho-disubstituted phenolic OH: the signals generally attributed to more external gallate units (around 141.4-141.2ppm) are significantly less intense in respect to all the other signals related to more internal ortho-disubstituted phenolic OH.

All these elements seem to suggest an overall situation which is more complicated than just a mixture of simple HT (such as GT) and CT. The presence of other polyphenolic species related to the bio-synthesis of tannins such as (hydro)cinnamic acids cannot be excluded as well as the one of more complicated tannin structures such as the ones of complex tannins and ET.

Based on the spectral range for the specific hydroxyl group mentioned above, it has been possible to have a semi-quantitative overview of the OH content in the Italian gallnuts extracts, here reported synthetically in Tab. 4 and the plots in Fig. 26 (for the complete results of the quantitative analyses see Tab. 1-4 in Appendix A).

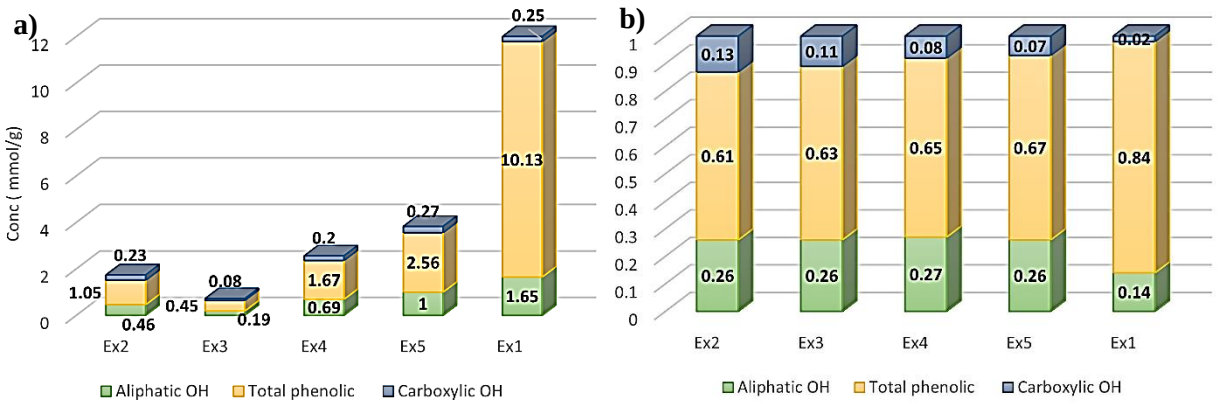

Fig. 26 Quantitative results of ^{31}P NMR characterization graphical description a) Plot of the Aliphatic, total phenolic and carboxylic hydroxyl groups content in all the analysed extracts. b) Plot the normalized (by the sum), aliphatic, total phenolic and carboxylic OH group concentrations in all the analysed extracts.

Tab. 3 Summary of the quantitative results of the ^{31}P NMR analyses of the Italian gallnuts extracts (Ex2-Ex4).

			Ex2	Ex3	Ex4	Ex5
			Concentration (mmol/g)			
Aliphatic OH	Carbohydrates (149.5-146ppm)		0.38	0.16	0.59	0.86
	C-ring proanthocyanidins (145.25-146ppm)		0.08	0.03	0.10	0.14
Phenolic OH	**ortho-disubstituted**	Syringil like moieties (143.5-142.5ppm)	/	/	0.33	0.43
		B-ring proanthocyanidins (142.5-141.9ppm)	0.09	0.05	0.09	0.17
		Gallate units (142.0-141.1ppm)	0.19	0.11	0.34	0.56
	ortho-substituted	(140.6-137.6ppm)	0.45	0.18	0.65	1.15
	Total phenolic (143.5-137.6ppm)		1.05	0.45	1.67	2.56
Carboxylic OH	Carboxylic acids (136.0-133.0ppm)		0.23	0.08	0.20	0.27

The plots reported in Fig. 27 clearly highlights the fact that, considering that, normalizing the amount of hydroxyl groups in each category by the total hydroxyl content (sum of all the groups), a clear difference can be noticed between the Italian gallnuts extracts and the Aleppo one. Please note that, in absolute terms, the content of aliphatic OH in Ex1 is higher than the one in Ex2-5 and its carboxylic OH content is in accordance with the ones in Ex2-5 (about 0.25mmol/g). The observed difference is in fact induced

by the much higher amount of phenolic OH[R]. The differences among the group of Italian galls extracts can be highlighted instead considering the sub-classes of polyphenolic OH moieties: the subregion which is more relevant in this sense, is the one related to ortho-disubstituted (Fig. 27). As expected, the composition of Ex4 and Ex5 are more similar one another, while Ex2 and Ex3 seem to have a slightly lower content of total ortho-disubstituted phenolic OH in which the contribution of the peaks in the area related to B ring of proanthocyanidins is not negligible.

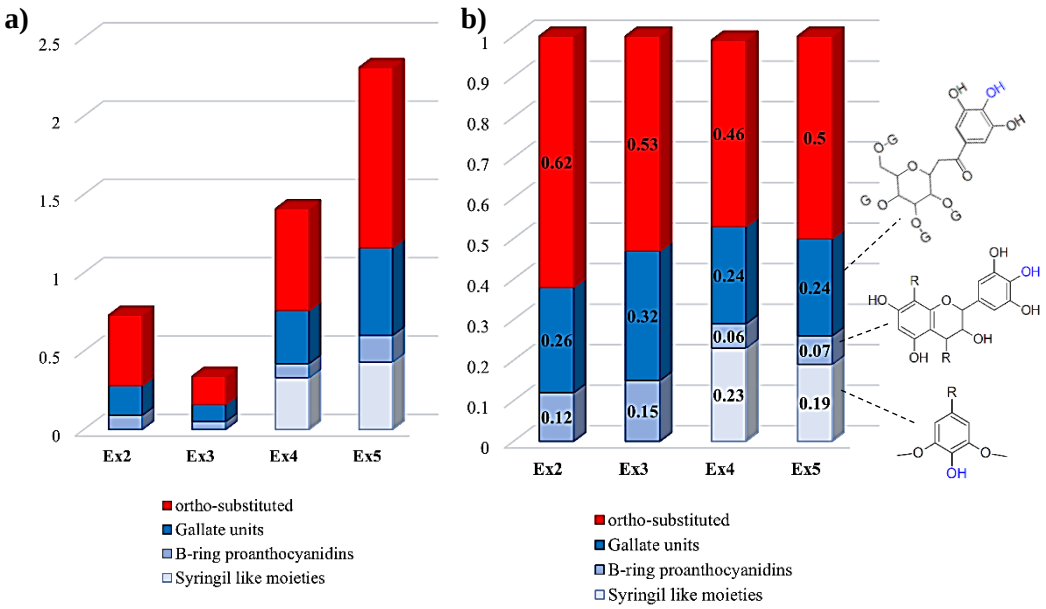

Fig. 27 Plot of the a) non-normalized and b)normalized (by the sum) content of each sub-class of phenolic OH in the Italian galls extracts.

Considering the content of proanthocyandins, it is interesting to notice that the concentration of aliphatic OH related to C-ring and the one of ortho-disubstituted phenolic OH related to B-ring seems to be coherent with the presence of a small amount of gallo/epigallocatechins, where the ratio between these concentrations should be theoretically around 1. One of the most problematic aspects is the fact that no clear and intense peaks which could be related to the A-ring ortho-unsubstituted hydroxyl groups[S].

It should be remarked that the results of the quantitative ^{31}P NMR characterization are strongly dependent on the overall quality of the spectra and also on the possibility to clearly define the integration areas boundaries. This task is quite problematic in those spectra characterized by a noisy background such as in the case of Ex2-Ex5.

1.2) HSQC results

The characterization via HSQC enabled to obtain useful qualitative detailed information about the extracts composition. In Fig.28 the HSQC spectrum related to Ex1 (together with the assignments of the main cross-peaks) is reported. Cross-peaks have been assigned starting from scientific literature and reference spectra.[38,42,56,134,135]

[R] This difference is totally in accordance with the differences in terms of extraction yields observed during the preparation of the extracts and mentioned in the "Experimental section" chapter.

[S] For epigallo/gallocatechin for instance a ratio of about 2:1:1 for A-ring to B-ring to C-ring would be expected. For the curiosity of the reader, see reference ^{31}P NMR spectra of proanthocyanidins and condensed tannins in the published works of *Crestini et al.* ***2016,*** *Melone et. al* ***2013*** and *Meng et al.* ***2019.***

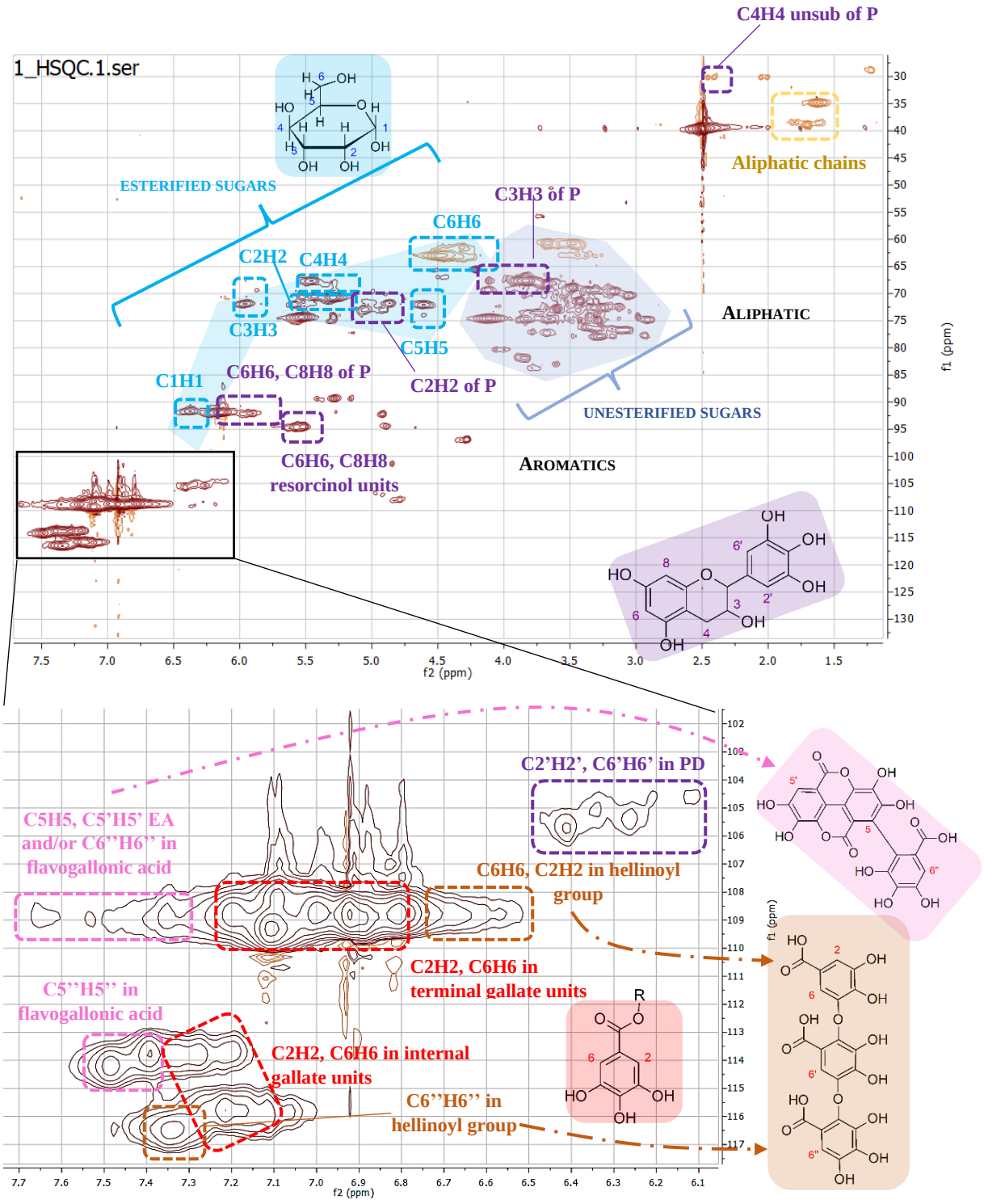

*Fig. 28 HSQC spectrum of Ex1. Assignments mainly based on Zhen et al. **2021**. EA= ellagic acid; P=proanthocyanidins, PD=prodelphins*

The spectrum reported is not dissimilar from the ones reported in literature related to commercial tannic acids.[24,56] In the region typically related to aliphatic J_{C-H} couplings, the signals of carbohydrates have been split in the ^{13}C coordinate as to define a sub-region related to esterified sugars[24,56,134], and another one related to free sugars.[134] The density of signals in the latter case does not allow a proper detailed assignments of all them in this sub-region. However, their intensity suggests a non-negligible concentration of free-sugars in the extract. In the same region however, signals of aliphatic J_{C-H} related to the C-ring of proanthocyanidins seem to be present too. The presence of a small amount of

proanthocyanidins in the extract is confirmed by the C2'H2' and C6'H6' cross-peaks related to the B-ring (in particular of prodelphins – PD) and the C6H6 and C8H8 signals related to the A-ring, in the aromatic region.[32,42,56] Weak signals related to C4H4 coupling in isolated proanthocyanidins (monomeric) seem to exclude the presence of high molecular weight CT.

Considering more closely the aromatic region of the spectrum, a first point to observe is the presence of all the signals related to C2H2 and C6H6 couplings in both internal and terminal gallate units of GT,[24,38,56] coherently with the previous hypothesis of an important amount of TA. Another important element to underline is the presence of a series of $J_{C\text{-}H}$ coupling signals attributable to C5H5 and C5'H5' of EA and their biosynthetic precursors such as flavogallonic acid and hellinoyl group.[56] This evidence is particularly interesting considering that these types of tannins bear an important amount of catechol groups and very few pyrogallol moieties, providing therefore a new interpretation of the relatively high proportion of catechol groups in the ortho-(mono)substituted phenolic OH observed with ^{31}P NMR analysis.
It should be remarked that for some of the assignments proposed, especially the last ones regarding the ET characteristic moieties, further analyses should be implemented to prove their actual structure and possibly their concentration. In evaluating and interpreting the results in fact, it should always be considered the complexity of natural substances. The initial sources used for the preparation of the extracts were not commercial and purified tannins. For this reason, small quantities of substances related to the bio-synthesis of tannins, such as (hydro)cinnamic acids, cannot be excluded by default.[136]
The quite important difference in composition between Ex1 and the other extracts already emerged from the ^{31}P NMR characterization, turned out to be evident also via HSQC. Regarding the Italian galls extracts, several similarities among their spectra have been observed. In Fig. 29 the HSQC spectrum acquired on Ex4 is reported together with the assignments of the main signals as visual guide in the following discussion.[32,42,56,135]

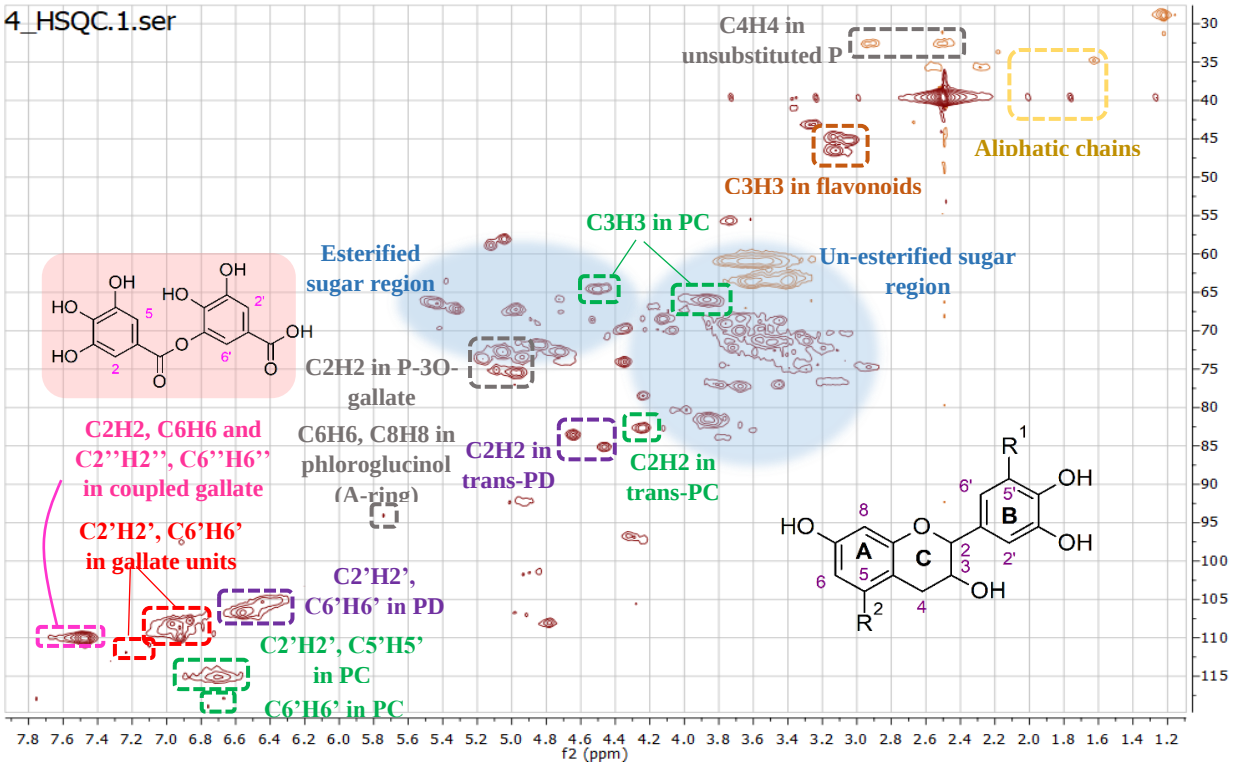

Fig. 29 HSQC spectrum of Ex4. Assignments of the main signals based on Zhen et al. ***2021.***

As can be clearly noticed, more signals related to proanthocyanidins have been observed in respect to the previous case, even if those referred to the aliphatic $J_{C\text{-}H}$ couplings in procyanidins (PC) and PD C-rings, could be overlap with esterified and unesterified sugars signals. Regarding the structures of the proanthocyandins present in Ex2-Ex5, both PC (bearing a catechol group in B-ring) and PD (bearing

instead a pyrogallol group in B-ring) seem to be present. What is interesting to notice is that in all the spectra no evident signals related to C4-C8 bonds have been observed, suggesting also in this case low molecular weight and isolated proanthocyanidins. On the other hand, the C6H6 and C8H8 signals of phloroglucinol and/or resorcinol (A-ring) are not intense as expected (especially in comparison with the signals related to B and C rings)[T].

It can be hypothesised therefore the presence of complex tannins, such as Acutissimin A (Fig. 30), in which the C8 of the proanthocyanidins is engaged in the bonding with the sugar core of the tannin while C4 remains un-bonded. It is difficult to prove the occurrence of this kind of tannins without a preliminary separation: signals related to hexahydroxy diphenyl, or similar moieties, characteristics of this sort of complex tannins, can be found in the same spectral region of PD B-ring signals or C2H2 and C6H6 signals of gallates. About this last point, it should be underlined that the signals of gallates units in HT are difficult to distinguish from the ones of isolated gallic acid or the gallate units in structures such as (epi)(gallo)catechingallate (D-ring).[42,56] Their occurrence in the extracts in fact seems to be confirmed by the signals related to C2H2 (C-ring, aliphatic region). Regarding gallate units, very weak signals attributable to internal gallate units of HT (in the spectral range δ_1~7.15-7.40ppm and δ_2~113.6-116.0) have been observed, suggesting the predominance of low molecular weight HT or even isolated gallic acid.

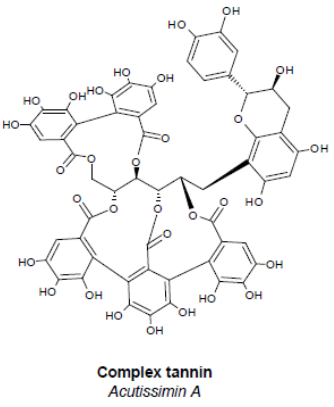

Fig. 30 Model structure of a complex tannin containing a procyanidin unit.

Regarding the structure of B-rings therefore, as already mentioned, the occurrence of both cross-peaks related to catechol (more intense and always visible) and pyrogallol moieties (less intense but still visible in all the spectra) suggest the co-presence of PC and PD. In the spectra acquired on Ex4 and Ex5 it can be noticed the presence of a signal which is in intermediate position between the C2'H2', C6'H6' of PD and C2H2, C6H6 of gallate units (Fig. 31). The precise attribution of this signal has not been possible just starting with the available reference data, but it could be related to pyrogallol units in slightly different molecules.

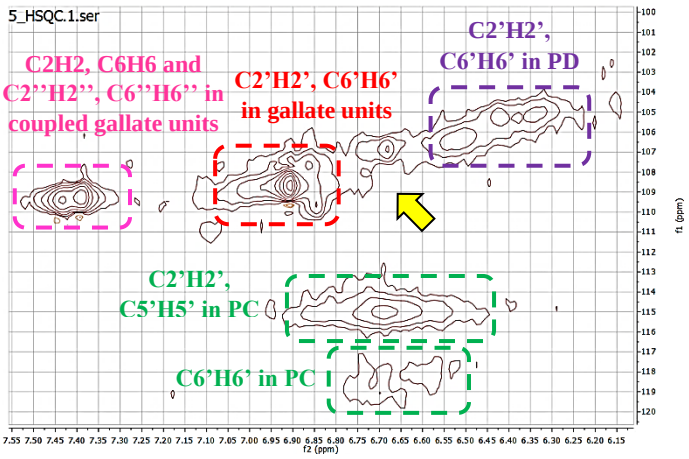

Fig. 31 Enlargement of the aromatic region of the HSQC spectrum acquired on Ex5.

The most critical aspect in the reconstruction of the most probable structures of proanthocyanidins in these extracts is the nature of the A-ring: in the discussion regarding the ^{31}P NMR results turned out that just few and low intense signals related to ortho-unsubstituted phenolic OH (characteristics of both phloroglucinol and resorcinol moieties of A-rings) can be observed. With HSQC it has been possible to see the presence of few and low-intensity signals related to phloroglucinol moieties[U]. The final picture is

[T] No signals related to the other main type of A-ring structure, resorcinol, have been observed. **It should be remarked that signals intensities are both related to their abundance in the extracts as well as to the specific relaxation times.**

[U] Please note that the low intensity of the signals related to A-ring in ^{31}P NMR spectra suggest the presence of resorcinol moieties while the HSQC results are more in accordance with the presence of pholoroglucinol groups.

even more complicate considering that no signals related to C4H4 for C4 engaged in C4-C8 have been observed suggesting the presence of isolated proanthocyanidins or complex tannins. In the first case an higher intensity of the C6H6 and C8H8 signals in HSQC and of ortho-unsubstituted phenolic OH in ^{31}P NMR would be expected. On the other hand, the hypothesis of the presence of complex tannins fits quite hardly with the so low intensity of signals related to the A-ring observed in the ^{31}P NMR analyses of all the Italian galls extracts. However but it could work considering the predominant catechol signals in the ortho-(mono)substituted phenolic OH region of ^{31}P NMR spectra and the other HSQC signals. About this last point, in the spectral area δ_1~7.40-7.70ppm and δ_2~109.5-111.0 in fact signals attributable to C2H2, C6H6, C2'H2' and C6'H6' in coupled gallic acid units, such as di- or tri-gallic acid, are visible[V]. It should be remarked that this spectral area partially overlap with the ones in which signals related to C5H5 and C5'H5' of ellagic acid could be found. In any case, it can be said that the presence of signals in this range of chemical shifts can be related to the presence of ET or their precursors bearing characteristic moieties derived from different types of oxidative couplings of gallic acid units (see the paragraph 1.1.1 in the Introduction chapter).[137,138]

As previously mentioned, the complexity of the starting natural sources composition does not allow to exclude the presence of compounds related to the bio-synthesis of tannins, but also the presence of small amounts of lignin and other polyphenolic substances.[55,136,139,140] This complexity is reflected also in the signals in the aliphatic region of the spectra, which in some cases are difficult to precisely interpret. Please note for instance the signals highlighted in the spectral range δ_1~3.00-3.10ppm and δ_2~43.5-48.20ppm in the spectrum reported in Fig.31. According to some literature references, these cross-peaks could be associated with C3H3 occurring in flavonoids such as naringenin,[141] or more in general with C in α in respect to a carbonyl group.

1.3) Merging the data: the composition of oak galls aqueous extracts

The data resulting from both the ^{31}P NMR and HSQC analyses of galls aqueous extracts provided a clearer general picture of their chemical composition. In accordance with the preliminary observations coming from the preparation procedure, properly reported in the "Experimental section" chapter, an important difference between Ex1 and the Italian galls extracts (Ex2-5) emerged.

Regarding the composition of Ex1, all the data suggest the presence of an important amount of TA and similar GT, un-esterified sugars, and a small amount of proanthocyanidins. The HSQC characterization enabled to define the proanthocyanidins in the extract mainly as isolated PD. According to the quantitative ^{31}P NMR results the concentration of these compounds in the extract should not exceed one tenth of millimoles per gram of freeze-dried extract. The HSQC results highlighted also the presence of a small amount of ellagic acid or more in general products of oxidative couplings of gallic acid units related to ellagitannins.

The composition of Ex2-5 appears instead much more complicated to reconstruct. All the data are in accordance with a non-negligible amount of proanthocyanidins, in this case both PC and PD, un-esterified sugars and low-molecular weight GT or even isolated gallic acid units, this last option supported by the slightly higher proportion of carboxylic hydroxyl group emerging from the quantitative ^{31}P NMR results. Moreover, both HSQC and ^{31}P NMR seem to be in accordance with the presence of ET. A clear picture of the proanthocyaninds and ET structures is however difficult to provide due to uncertainties in the HSQC signals assignments.

Once again it must be underlined that the sample analysed are not commercial products, and therefore purified, tannins. It is crucial to take into consideration that the composition of natural substances involves

[V] For these small polyphenolic compounds, no reference HSQC data are present in scientific literature. These (maybe speculative) considerations have been therefore proposed starting from simulated spectra.

also the presence of other polyphenolic and non-polyphenolic substances such as precursor of tannins, lignin/lignin fractions, flavonoids, fatty acids and ceres (vegetal waxes in general), must not be excluded.

2) Iron-polyphenolic complexes: preparation and characterization

3.1) Preliminary observations in the preparation step

As illustrated in the "Aim of the thesis and definition of the methodological approach" chapter, the preparation of iron-polyphenolic complexes involved the synthesis in pH-controlled regimes of iron complexes of simple polyphenols, in particular GA and EA, used as "model compounds" and the preparation of iron complexes using the oak galls aqueous extracts, in particular Ex1 and Ex4, as source of polyphenols. Just in the case of iron-gallic acid (Fe-GA) and iron-ellagic acid (Fe-EA) coordination compounds, starting from literature data, it has been possible to proceed in a "pseudo-stoichiometric" regime as to better characterize the resulting complexes. For iron-polyphenolic complexes prepared starting from oak galls extracts (Fe-Ex) this can obviously not be achieved and therefore an iron-excess condition should be assumed. Due to technical constraints but also to increase the number of complexes to obtain a clearer picture of the pH role in the final structure of the complexes, Fe-GA complexes at intermediate pH conditions have been prepared. As already mentioned, the preparation and isolation of these complexes required a proper optimization since no literature information is available regarding these practical aspects[W]. For this reason, it is appropriate to report some of the most notable aspects concerning these steps.

2.1.1) The relation between the iron complexes colour and their preparation pH conditions

In accordance with the literature data used for the construction of the protocols, it has been observed a clear relation between the pH conditions at which the complexes have been prepared and their colour. Even if these differences in colour are visible also in the Fe-polyphenolic complexes precipitates, due to the dark colours of these precipitates, they appear more evident in the complexes remained in solution, especially in diluted systems, as can be seen in Fig.32. Even if for the complexes prepared using as source of polyphenols the oak aqueous extracts at pH 4 and pH 6 the differences in colours appear less evident (also due to the initial colour of the extracts), all the complexes prepared in strong acidic pH conditions (pH $\leq$ 4) turned out to be dark bluish, the ones prepared in slight acidic pH conditions (pH 6) purple, while the ones prepared at strong alkaline pH (pH 12) dark reddish.

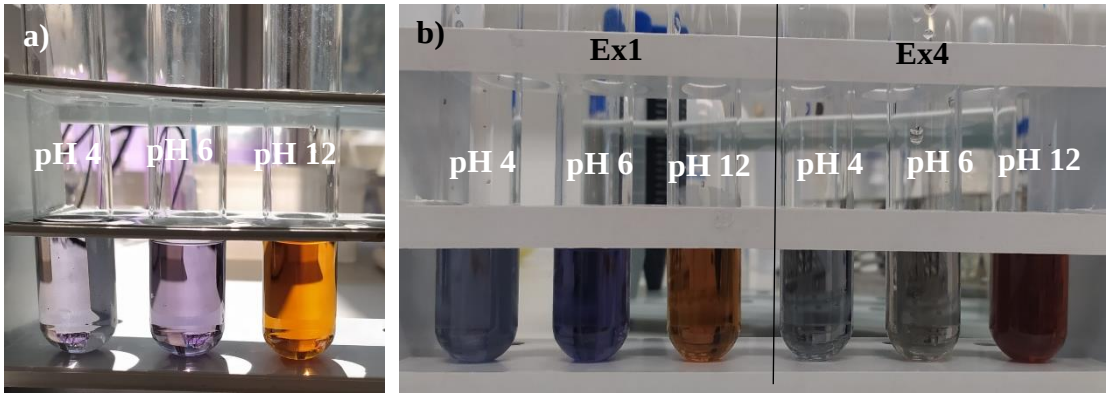

Fig. 32 Diluted iron-polyphenolic complexes-containing solutions. a) Fe-GA b) Fe-Extract

The rough visual observation of their colours can itself provide initial evidence upon the structural differences induced by the pH conditions.

[W] The protocols used for the preparation and isolation of the iron-polyphenolic complexes are properly described and discussed in the "Experimental section" chapter.

The differences in the complexes colours results from the contribution of two structural aspects: a significant difference in the overall HOMO-LUMO gap (of the complexes and not of the single ligands) and the well-known phenomena of internal electron transitions occurring within the complex. For instance, in general it can be said that, for each ligand set, the higher the energy gap induced by the ligands field (or in other terms the higher the energy separation of d orbitals due to crystal field effect) the higher will be the energy required for the *d-d electronic transitions*. Qualitatively (and roughly), the higher the energy required for the electronic transition and the lower the absorbed radiation wavelength and consequently the higher the transmitted one. This very rough assumption fits quite well with the hypothesis of a higher binding capability of deprotonated polyphenols resulting in higher energy separations between e_g and t_{2g} d orbitals. However, considering the nature of the electron rich organic ligands involved (presence of ligands' π, π^* and n orbitals), metal-to-ligand and ligand-to-metal electrons and charge transfer phenomena cannot be excluded. A detailed theoretical explanation is however outside the aim of the current thesis project and a proper study of the electronic transitions in iron-polyphenolic complexes would require a proper and detailed study.

2.1.2) The relation between the Oxidation rough yields and complexes preparation pH conditions

As will be properly described in the "Experimental section" chapter, the Fe(III)-polyphenolic solid precipitates isolated via centrifugation and drying, have been weighted and their mass has been used to calculate a rough but practical yield defined as "Reaction and Oxidation rough yield" (ROry)[X]. A separate set of Fe-GA complexes prepared in pseudo-stoichiometric regime and isolated in the most accurate way as possible, has confirmed the general trend of ROry across all the complexes prepared (Tab.4, Fig.33).

Tab. 4 Preparation details of Fe-GA complexes in pH-controlled regime and ROry values

Pseudo stoichiometric Fe-GA		**pH 4**	**pH 6**	**pH 12**
GA (Sigma Aldrich™)	Mass (mg)	53.30	53.53	58.43
	Pure (mmol)	0.342	0.308	0.337
$FeSO4•7H_2O$ 350g/L	Volume (µL)	174.4	63.0	57.4
Fe-GA solid precipitate	Iron to ligand ratio*	1:1	1:2.5	1:3
	Expected mass (mg)	77.19	59.04	62.51
	Obtained mass (mg)	72.24	45.18	14.27
	ROry (% mg/mg)	**93.6**	**76.5**	**22.8**

[X] All the practical aspects about the definition of ROry are referred to the "Experimental section" chapter, paragraph.

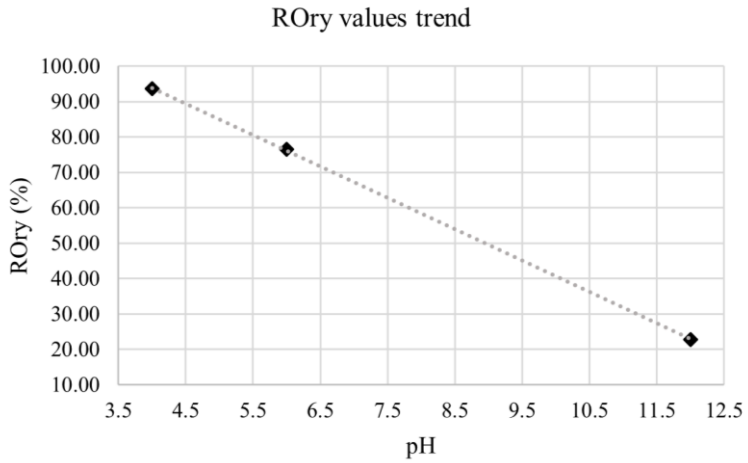

Fig. 33 RORy values trend according to the preparation pH-conditions

As can be appreciated from the plot in Fig.33, RORy values decrease with the increasing of the preparation pH conditions. Considering the fact that RORy can be used as an indicator of the oxidation rate more than a proper reaction yield value[Y], as expected their value turned out to be higher for complexes prepared in strong acidic conditions, and therefore having a 1:1 iron to ligand stoichiometric ratio, and significantly lower for those prepared in strong alkaline pH conditions, having a 1:3 iron to ligand ratio. In other words, being the oxidation the kinetically limiting stage of the insoluble Fe(III)-polyphenolic complexes formation[Z], RORy can be used to confirm the fact that the oxidation rate is depending on the structure of the Fe(II) complex itself. In accordance with literature data,[70,87,142] the oxidation rate is lower when Fe(II) is strongly coordinated by two or three ligands while is significantly higher when it is coordinated by a single ligand. In fact, it has been possible to observe that precipitation in the pH 6 and pH 12 supernatant solutions was continuing to take place after the separation from the precipitated at the fifth day[AA]. These elements, together with the evident colour differences mentioned in the previous paragraph, are therefore interesting indicators of the structural differences induced by the preparation pH conditions.

3.2) CW-EPR results

2.2.1) Iron-gallic acid coordination compounds

Regarding the Fe-GA complexes, as properly described in the "Aim of the thesis and definition of the methodological approach" and "Experimental section" chapters, the EPR study started with a general monitoring of the prepared complexes both at RT and 100K. In Fig. 34 the spectra acquired at RT on the solid Fe-GA complexes prepared both in pseudo-stoichiometric and iron excess conditions are reported

[Y] It is important to bear in mind that the formation of Fe(III)-polyphenolic complexes follows a double step mechanism (see paragraph 2.1 in the "Introduction" chapter) and therefore it is quite difficult to define a global yield for the whole mechanism.

[Z] Being in a octahedral coordination geometry (d_6 preferred geometry), the formation of the Fe(II)-polyphenolic complex due to substitution of the aqueous ligand is a very fast reaction and its kinetic is therefore difficult to study.[87]

[AA] The separation after the fifth day from the preparation of the complex has been arbitrary set. All the details of the isolation procedure, including this aspect, are properly described in the "Experimental session" chapter.

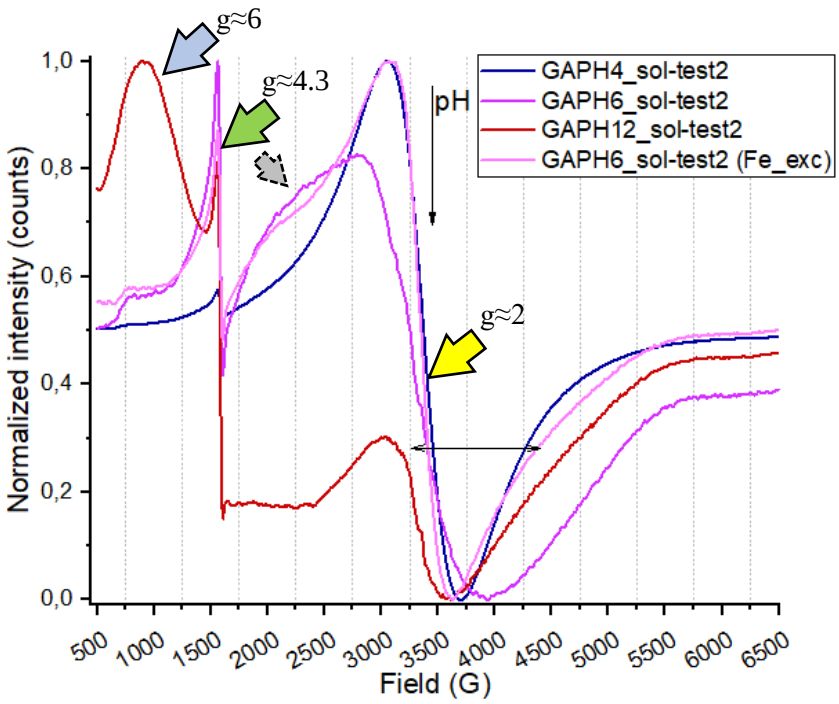

Fig. 34 EPR spectra of Fe-GA solid complexes in pseudo-stoichiometric and Fe-excess conditions.

As can be easily observed, a clear relation between the pH and the geometries of the coordination sites is evident. In all these spectra at least two signals are present. The symmetrical gaussian signal at g≈2 (around 3500G) is commonly referred to the HS Fe^{3+} in an octahedral or pseudo-octahedral site ("spherical"/quasi-symmetrical coordination environment)[143–145] and it is therefore associated with weak coordination with the ligands (it can be referred to perfect octahedral sites just in the case of isolated and narrow signals – Fig.35a). The intensity of this signal (highlighted with a yellow arrow), is decreasing with the increasing of the pH conditions of the complexes preparation as to confirm the higher coordination strength of Fe-GA complexes prepared in alkaline conditions (proposed stoichiometry $Fe(GAH^{3-})_3$). As can be observed, there are some differences in the exact position (g-shifts) and amplitude (line width) of the g≈2 signal. The small shifts of this signal are related to variation in the ZFS parameters and could be properly interpreted just using appropriate simulation tools enable to reconstruct the most precise spin Hamiltonian of these systems. The variation in the line width instead describes the different "heterogeneity degree" of the pseudo-spherical coordination sites. In other terms, in the same area of g≈2, weak Fe(III) coordinations produce a broad resonance peak, while octahedral and pseudo-octahedral coordination geometries (independently from their strength) produce a more defined and sharp signal.

Concerning both g-shifts and linewidth no clear trends with the pH have been observed. Note that the g≈2 signals in the Fe-GA EPR spectra at pH 6 (both pseudo-stoichiometric and excess iron complexes) do not appear to be perfectly symmetrical (dotted grey arrow). This feature indicates the possible presence of iron oxide signals around 2000-2500G which disturb the readability of the signal.

The second main signal is the generally narrow peak at g≈4.3 (around 1500G, highlighted with a green arrow). This signal is instead associated with InS Fe^{3+} in rhombic coordination sites, or, more in general, distorted octahedral sites,[143–145] and related to the an E/D ratio close to 0.3 for the M_S=|3/2> Kramer's pair (Fig. 35c)[BB].[143,146] In this case the observed relation is the opposite of the previous one: the intensity of the signal is increasing with the increasing of the complexes preparation pH due to a

[BB] See the Box "Practical description of Fe^{3+} spin states system" in the "Aim of the thesis and definition of the methodological approach" chapter.

higher coordination which results in distorted sites. However, in the Fe-GA prepared at pH 6, the g≈4.3 signal is present together with a still quite intense one at g≈2, and a small shoulder at g≈6 is noticed too. Interestingly, this combination of signals is generally observed in tetrahedral coordination sites, which are typically observed in iron-containing glasses or in frozen solutions (Fig. 35b).[145,147,148] Further and more detailed studies are required to understand the reason of this unusual coordination site geometry of Fe(III).

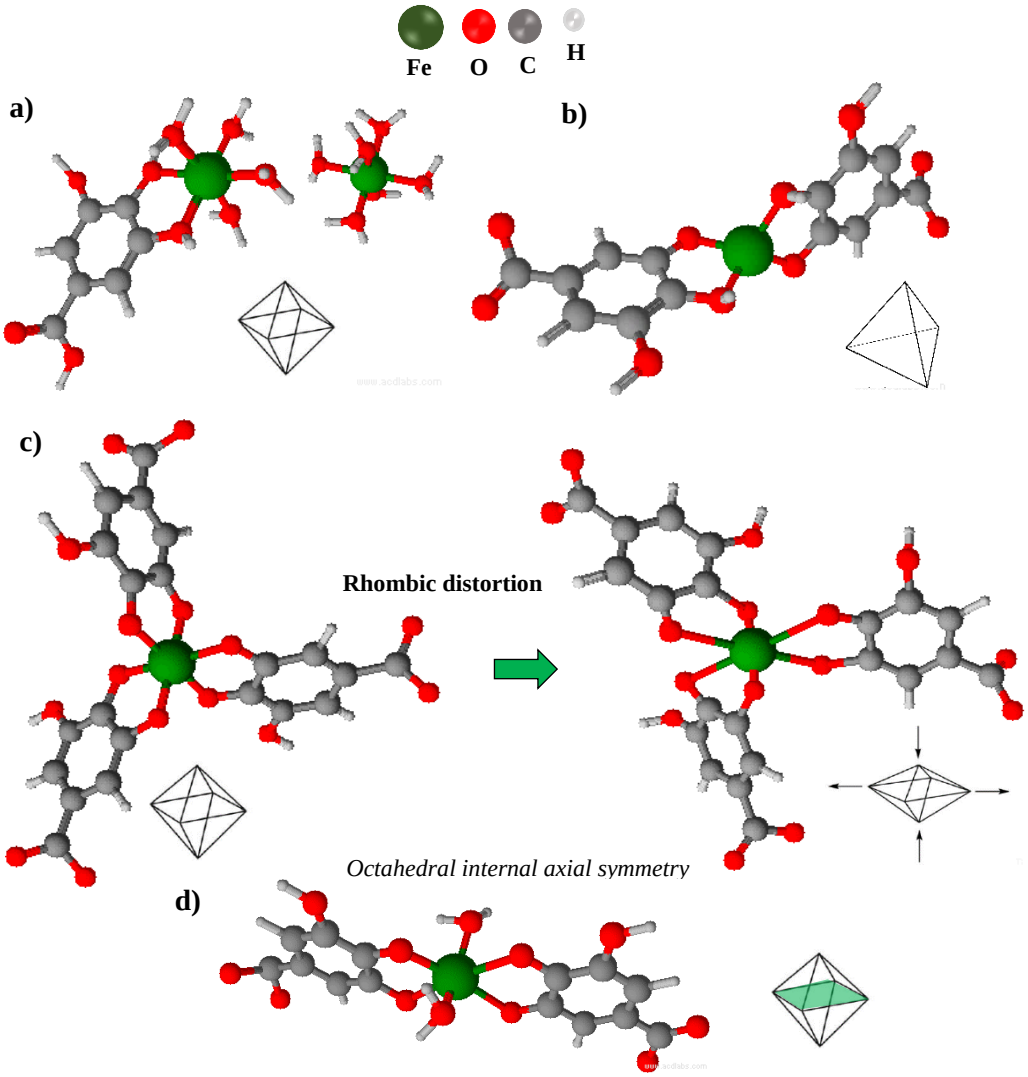

*Fig. 35 a) Octahedral coordination site of iron in Fe-GA complex (1:1 iron to ligand ratio) and in hydrated condition (hexa-aquo complex). b) Tetrahedral coordination site of Fe-GA complex (1:2 iron to ligand ratio). c)Rhombic distortion in Fe-GA complex. Proposal model for a 1:3 iron to ligand Fe-GA complex. In the reported models it has been assumed that just the catechol groups are involved in the formation of the complex. d) Octahedral coordination site with internal axial symmetry in Fe-GA complex (1:2 iron to ligand ratio). **Please note that all the proposed models are just a visual guide for the discussion but are far from the reality**. In the case of Fe-GA solid particles/crystals, the contribution of the carboxyl group in the formation of the final 3D structure cannot be neglected.*

In general, considering these two signals therefore, for higher complexes preparation pH conditions, higher intensities of g≈4.3 and lower intensities of g≈2 are observed. As will be briefly mentioned in the "Experimental section" chapter (paragraph 4.1), due to practical issues during the stabilization of the alkaline conditions, complexes at intermediate pH conditions have been prepared. Despite the lack of control of the pseudo-stoichiometry (which in any case should be considered in iron excess conditions), EPR spectra have been acquired on these complexes (see Fig.1 Appendix B). As expected, these spectra suggest that the excess of iron is in pseudo-octahedral coordination environment. In

future studies it would be interesting to study quantitatively the pseudo-octahedral to rhombic signals ratio as to determine after a suitable calibration the exact excess of iron for instance.[143,147,148]

In addition to these signals, just in the Fe-GA solid complex prepared at pH 12 an additional signal at g≈6(around 750-1000G, highlighted with a blue arrow), which could be referred to internal symmetries of octahedral coordination sites (Fig. 35d), can be observed.[146] At first sight, these types of internal symmetries are more expected to be found in Fe-GA complexes having a 1:2 iron to ligand ratio. However, it is important to remind that other factors which have not been considered in this study, could contribute to this type of situation: the role of carboxylic acid groups, the possible presence of dimers or oligomers of GA formed at alkaline pH and/or other modifications of the ligands structure and, most importantly, the final 3D internal structure of the Fe-GA particles. For these reasons, further and more detailed study are necessary to elucidate the nature of the observed axial internal symmetry in iron octahedral coordination sites.

Concerning the liquid samples analysed (supernatants resulting from the complexes isolation methodology), the first element to underline is that the signals observed are all referred to fine solid particle (probably in the order of hundreds of nanometres) containing HS and InS Fe(III)[CC](Fig.36).

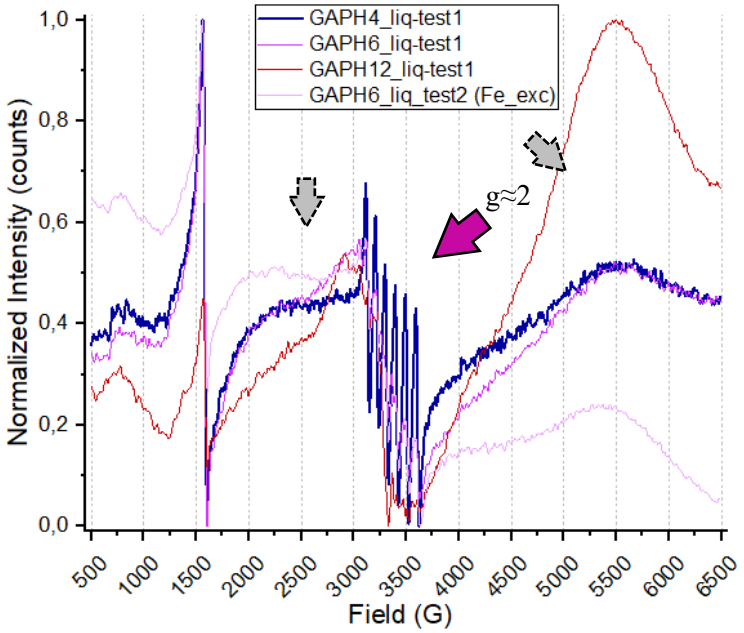

Fig. 36 EPR spectra of Fe-GA complexes in the liquid samples both in pseudo-stoichiometric and Fe-excess conditions.

The extremely interesting fact emerged from the results of these samples is that the Fe(III) coordination environment is mainly tetrahedral independently from the pH conditions of the complexes preparation. This unusual situation seem to suggest that the formation of the larger Fe-GA solid particles involves an intermediate step in which the growing particles (difficult to separate and therefore still present in the supernatants) are characterized by Fe(III) in tetrahedral coordination sites. However, it is important to underline that the exact explanation of this evidence requires other and more detailed studies.

One of the most evident features of the spectra reported in Fig.36 is the presence of a clear sextet centred at g≈2 with a separation of the peaks of about 90G (highlighted with a purple arrow) which is related to Mn(II) hyperfine splitting of the M_s=|1/2> interacting with the nuclear spin of the manganese nucleous.[143] Manganese turned out to be present in traces in the iron(II) sulphate used for the preparation of the complexes (see Fig.2 Appendix B) and its presence has been easily revealed with

[CC] Due to intrinsic constrains of CW-EPR, it is not possible to observe Fe(II) species, which generally are diamagnetic, and Fe(III) at the molecular level due to fast relaxation times.

EPR. What is interesting to notice is that the presence of Mn(II), which appears weakly coordinated with the ligands (the six peaks are quite sharp and well defined in all the spectra), has not been revealed in the solid Fe-GA samples. This fact suggests the presence of an initial step during the formation of the final iron-gallic complexes, in which Mn(II) is able to enter in the growing particles substituting iron in the complexes formation.

Also in this case is evident the presence of different signals (dotted grey arrows) referred to iron oxides ($Fe^{III}_xO_y$) particles[DD]. An important aspect to highlight in this sense is that, due to the super-paramagnetic behaviour of micro and nanoparticles of iron oxides, their corresponding resonance signals can be found at different fields.[149,150]

As will be further discussed, the position of these signals is strongly temperature and size dependent. The iron oxides signals having a broad shape and situated at high fields are commonly referred to iron oxides "bulk" (indicating an order of magnitude of hundreds of micrometres). Finally, also in this case the spectra acquired on the Fe-GA complexes at intermediate pH and in iron excess conditions confirm the fact that the excess of iron is mainly in octahedral coordination sites.

The EPR spectra acquired on both solid and liquid Fe-GA samples at 100K are reported in Fig.37.

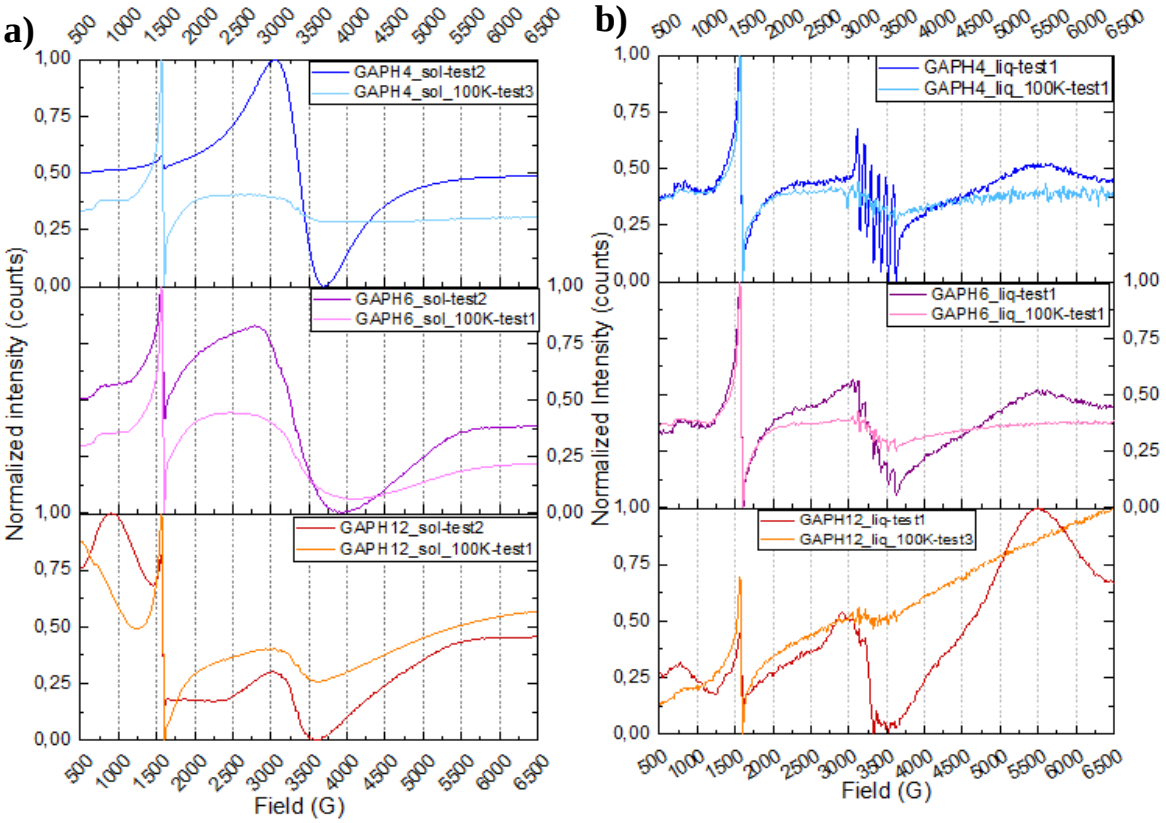

Fig. 37 EPR spectra acquired at RT and 100K on pseudo-stoichiometric a) solid Fe-GA samples b) liquid Fe-GA samples

Comparing the spectra of Fe-GA solid samples acquired at RT and 100K (shown in Fig. 37a), it is interesting to notice that the Fe(III) signal at g≈2 is strongly reduced due to the frozen solvent effect which force the system to acquire a more distorted coordination geometry. For the same signal, coupled with the reduction of the intensity, an increasing of the line width has been noticed as expected. The line width of this signal is in fact strongly dependent on the temperature. Since g≈2 signal is related to

[DD] Please notice that the formation of iron-oxides particles is favoured at alkaline pH conditions and therefore the contribution of these species should be particularly taken into account in the interpretation of EPR spectra of iron complexes prepared in alkaline conditions.

the weak Fe(III) spherical coordinations, decreasing the temperature is possible to record an higher heterogeneity in this type of coordination sites, which is resulting in a wider linewidth. In solid Fe-GA samples prepared in iron-excess conditions, in which, as mentioned before, the excess of iron is mainly in octahedral coordination sites and the signal at g≈2 is therefore predominant, this phenomenon is even more evident. In Fig. 38 the temperature gradient experiment results referred to one of the Fe-GA solid complexes prepared in iron-excess conditions clearly demonstrates this behaviour: this phenomenon of line width opening has been used in the second block of measurements (see "Experimental section" chapter) in this case to check the symmetry of the signal in order to see if other contributions in the g≈2 area were present[EE].

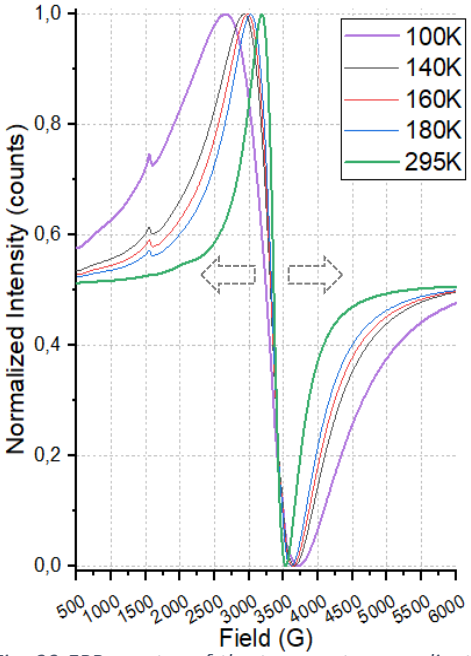

Fig. 39 EPR spectra of the temperature gradient experiment on the Fe-GA complex prepared with the intermediate pH 10.3 in iron-excess condition.

Concerning the spectra reported in Fig.37a, there is another interesting element to discuss. Regarding the comparison between the spectra acquired at RT and 100K on the Fe-GA complexes prepared at pH 12, it is evident that the signal initially attributed to the axial distorted coordination site of Fe(III) at g≈6 underwent an important shift. This displacement has been properly addressed in the second block of measurements with a temperature gradient experiment, here reported in Fig. 39. A part from the already mentioned effect of the g≈2 line width increasing, what emerged is that the signal around g≈6 is actually composed of two contribution: one related to an axial internal symmetry in the octahedral coordination sites of Fe(III) complexes (red arrow) which remain fixed (but more shifted at g≈9) independently from the temperature, and the one related to $Fe^{III}_xO_y$ that on the contrary is shifted at lower fields decreasing the temperature. The temperature influence in the $Fe^{III}_xO_y$ resonance signal positions is therefore proved to be useful in those situations in which the possible presence of iron-oxides particles can disturb the readability of the spectra.

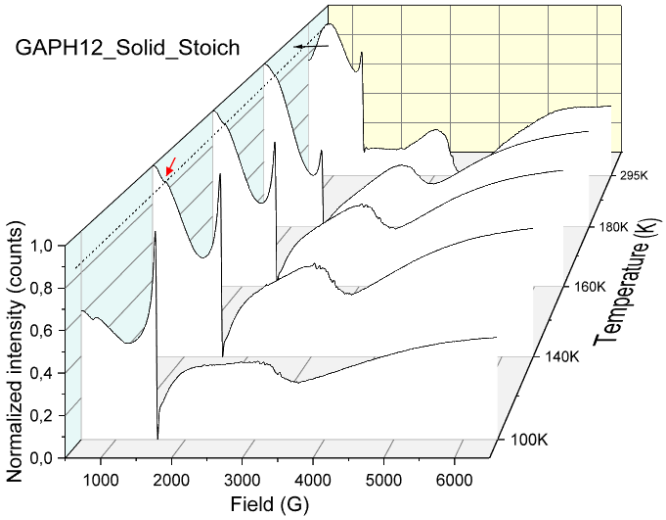

Fig. 38 EPR spectra of the temperature gradient experiment on the Fe-GA complex prepared at pH 12 in pseudo-stoichiometric condition.

Regarding instead the comparison between the spectra of Fe-GA liquid samples acquired at RT and 100K (proposed in Fig. 37b) no dramatic changes are observed. The main differences are in the intensities of the signals related to Mn(II) which are strongly reduced. This reduction is due to the fact that at lower temperatures manganese is more strongly coordinated with the ligands: each line is

[EE] Regarding the temperature effect on the signal at g≈2 in Fe-GA complexes prepared in iron-excess conditions at different pH see also Fig. 3 Appendix B.

therefore further split by the zero-field interaction which affects the six hyperfine signals causing the apparent increasing of the line width and the consequent reduction of the signal.[143]

Concluding the section related to the Fe-GA complexes characterization, it is important to mention the results of the time monitoring experiment performed on the Fe-GA complex prepared at pH6 in pseudo-stoichiometric conditions. The experiment highlighted that the same type of coordination sites of Fe(III) are observed in time and the major changes in the spectra are due to differences in the iron-oxides contribution (see Fig. 4 Appendix B).

The following table (Tab. 5) summarize the results of the CW-EPR characterization of Fe-GA complexes mentioned above.

Tab. 5 Summary of the most notable results regarding CW-EPR characterization of Fe-GA complexes

		pH 4	pH 6	pH 12
Solid	**RT**	Predominantly ***pseudo-octahedral*** coordination sites	***Tetrahedra***l coordination site (contribution of pseudo-octahedral and rhombic can not be excluded)	Predominantly tetrahedral and ***rhombic coordination with internal axial symmetries***
	Low T	Predominantly tetrahedral coordination site		
Solid particles in the supernatants	**RT**	Predominantly tetrahedral coordination site		
	Low T			

2.2.2) Ellagic acid coordination compounds

As described in the "Aim of the thesis and definition of the methodological approach" and "Experimental section" chapters, for the preliminary testing of Fe-EA complexes, the various pH conditions applied for the other complexes were not considered. It is nevertheless, important to take into account that the pH of this compound is known to be acidic (pK_a from 5.42 to 12.4)[126]. The main goal of this part of the study was therefore to notice eventual differences between Fe-EA complexes prepared starting from EA MeOH solution and EA dispersed in MeOH/H_2O (1:1).

As can be seen from the spectra reported in Fig. 40, no dramatic differences between the coordination site geometries of paramagnetic centres in Fe-EA complexes prepared in the two different conditions can be observed. This evidence seems to suggest a similar structure between the complexes formed in MeOH and the ones formed in MeOH/H_2O dispersion and therefore still adsorbed on insoluble EA particles.

All the features present in the reported spectra have been already described and discussed in the previous paragraph and therefore they will not be discussed again. Also regarding the differences in between the spectra acquired at RT and the ones at 100K, the typical trends discussed for Fe-GA are observed for Fe-EA complexes too. As can be noticed from the spectra in Fig. 40 also in this case bulk $Fe^{III}_xO_y$ signals are visible.

What is interesting to notice instead is that, even if in the utilised condition for the Fe-EA preparation the complete protonation of EA can be assumed[FF], the coordination environment of the HS (and InS) Fe(III) seems to be in all the cases tetrahedral as suggested from the signals at g≈2, g≈4.3 and g≈6 (Fig. 41). Another interesting element to notice is that the typical Mn(II) signals are in this case

[FF] Please note that, since pH can be defined just in aqueous solutions, it is not possible to clearly define a pH value of the methanol and methanol/water ellagic acid solutions and dispersions.

observed also in the EPR spectra acquired on the solid Fe-EA complexes (highlighted with purple arrows in Fig.40).

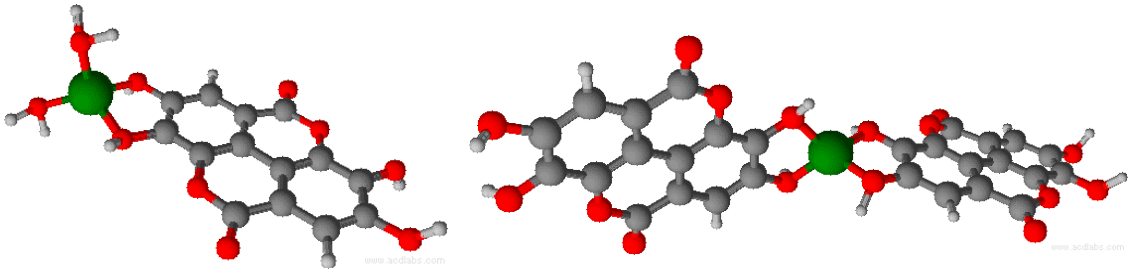

Fig. 40 Fe-EA models for 1:1 and 1:2 iron to ligand ratios with tetrahedral coordination site. Also in this case, it must be underlined that ***these models are just a visual guide for the discussion and they are far from the real structures of the complexes.***

Both these evidences support the fact that the final structures of Fe-EA complexes are different from those of Fe-GA complexes and seem to suggest that these structure are more prone to include Mn(II)[GG]. Also in this case however, further and more detailed studies are necessary to elucidate the actual structure of these complexes.

2.2.3) Iron-polyphenolic complexes from oak galls aqueous extracts

The preparation and the characterization steps for iron-polyphenolic complexes using as source of polyphenols the oak galls aqueous extracts (only Italian and Aleppo oak galls extracts have been used) followed basically the same procedure used for Fe-GA complexes, with the only difference that in this case all the complexes have been prepared with large iron excess.

The CW-EPR study of these complexes as usual started with a monitoring stage with spectra acquisitions at RT and 100K both of the solids and the supernatants. In Fig. 41 the spectra acquired on the solid samples are presented.
The first aspect to bear in mind in the examination of these spectra is that the situation represented is given by the sum of different complexes present in the sample and therefore just general comparisons and observations can be proposed. Starting with the spectra acquired at RT for instance, the comparison between Fe-Ex1 (meaning the complexes present in the sample obtained using the Extract 1) and Fe-Ex2 (meaning the complexes present in the sample obtained using the Extract 2) highlights some interesting aspects. The complexes prepared at pH 4 and pH 6 for instance are characterised by strong signals at g≈2 and g≈4.3 with a weak shoulder at g≈6, suggesting in both cases a predominant tetrahedral structures of iron coordination sites. Just in the case of Fe-Ex1 prepared at pH4 it can be hypothesized the presence of proper pseudo-octahedral coordination sites due to the stronger intensity of the g≈2 signal. The narrowing line width of this signal in the Fe-Ex1 complex seems to suggest an higher coordination strength (and therefore less heterogeneity) and also the effective g for the g≈2 signal is slightly different from Fe-Ex4. However, in this sense it is also important to bear in mind that these complexes have been prepared in strong iron excess conditions and therefore the unknown iron excess (whose amount can be different due to different polyphenolic composition of the extracts) can affect differently the g≈2 signal. What can be noticed in any case is that the increasing of the g≈2 line width due to temperature effect is not so dramatic (see also temperature gradient experiment result in Fig. 5 Appendix B) suggesting a good coordination strength between the ligands and the Fe(III) centres.

[GG] As mentioned in the previous paragraph, Mn(II) can be considered an impurity introduced with the iron(II) salt.

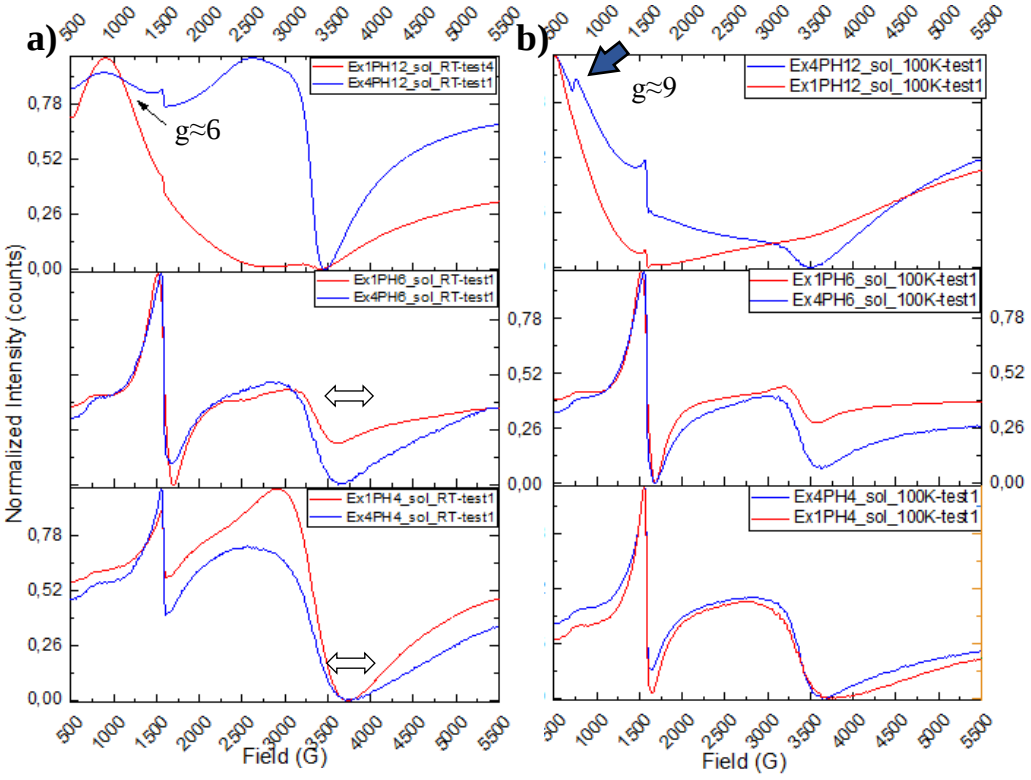

Fig. 41 EPR spectra of the solid iron-polyphenolic complexes of Ex1 and Ex4 acquired at a) RT b)100K. For clarity in these and in all the following spectra related to Fe-Ex complexes, spectra represented with red lines indicate complexes of Ex1 while blue lines are used for iron complexes of Ex4.

Apparently the most important differences can be noticed in the Fe-Ex complexes prepared in alkaline conditions. Unfortunately, however, the spectra acquired at RT on both Fe-Ex1 and Fe-Ex4 are dramatically disturbed by the presence of $Fe^{III}_xO_y$ related signals.

Regarding the spectra related to Fe-Ex4 it can be observed from the spectrum at RT a strong signal related to Fe(III) in pseudo-octahedral coordination sites and a quite weak signal related instead to distorted/rhombic coordination geometries of the paramagnetic centres. Moreover, the separation of the iron oxides contribution form the g≈6 signal induced by lower T, seems to highlight the presence of axial internal symmetry in the octahedral coordination sites due to the emerged g≈9 signal (see also temperature gradient experiment result for this sample in Fig.6 Appendix B).

The situation in the case of Fe-Ex1 appears slightly more complicated. The iron-oxide signal in the Fe-Ex1 spectrum acquired at RT completely dominates upon the other signals keeping from properly see the intensity and the position of the signals at g≈2 and g≈4.3. The spectrum acquired at 100K enables to recognize the g≈4.3 signal but the signal at g≈2 and the intensities of these signals are still not recognizable. In this case the use of experiments in higher fields (Q-Band EPR) would be necessary to eliminate the $Fe^{III}_xO_y$ interferences.

The EPR spectra acquired on the supernatants (Fig. 41, see also Fig.7 Appendix B) are not dissimilar from the ones related to Fe-GA complexes described above. The predominant geometry of the Fe(III) coordination sites in all the Fe-Ex samples is the tetrahedral even if contribution from rhombic coordinations cannot be excluded. The presence of Mn(II) hyperfine splitting lines have been observed: from clear sextet with narrow peaks when the affinity with the ligands is not so strong (Fe-Ex at RT prepared at pH4) to unclear low signals when the affinity is higher (Fe-Ex at 100K prepared at pH12). Also in these spectra, signals related to bulk $Fe^{III}_xO_y$ are present. The spectra shown in Fig.42 seem also to suggest an higher affinity of Mn(II) in the complex prepared with the Ex1 in respect that the one related to Ex4, as to say that Fe(III) can be more easily substituted by Mn(II) in the complexes

Fe-Ex1. Due to the poor statistic however, this is a highly speculative consideration and further study should prove these points.

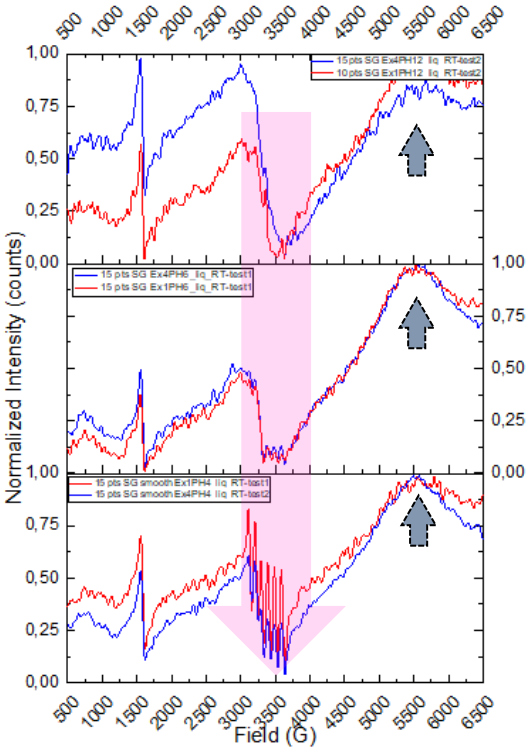

Fig. 42 EPR spectra of the supernatant Fe-Ex complexes acquired at RT. The bottom panel is referred to complexes prepared at pH4, the middle one at pH6 and the upper one at pH12.

2.2.4) General considerations about CW-EPR characterization results

At the end of the discussion of CW-EPR results, some elements should be remarked.

- *pH dependency on Fe(III) coordination sites*
  A relation between the pH conditions of iron-polyphenolic complexes preparation and the geometry of the iron coordination site observed in the isolated solid complexes, especially in the case of Fe/GA coordination compounds.
  Slight shifts in the g values of the main signals turned out to be related to the pH conditions of the complexes preparation too, as well as to the nature of the ligands (especially for Fe-Ex).
- *Solid vs Liquid samples*
  In all the studied liquid samples, the coordination environment of iron seems to predominantly tetrahedral (glassy phase) independently from the pH conditions of the complexes preparation.
  Mn(II) signals, deriving from manganese impurities in the iron sulphate salt, have been observed mainly in the liquid samples, a part from the Fe-EA complexes.
- *No signals related to radicals have been observed*
  This last point is extremely important for future studies since it suggests that stable organic radicals (expected in this type of molecules rich in aromatic groups) are formed during the aging processes and are not immediately present within the ink. Moreover no signals of Fe^{IV} have been observed as well suggesting that Fenton type reaction did not occurred in the working conditions.
- *Model compounds vs Extracts iron polyphenolic complexes*
  This is probably one of the most important result emerging from the EPR investigation. Iron-polyphenolic complexes prepared starting from GA, displayed different coordination site geometries of HS and InS Fe(III) according to the pH conditions (Tab. 5) while for complexes

prepared starting from oak galls extracts, this turned out to be not the case. For Fe-Ex in fact the coordination sites structures are predominantly the tetrahedral ones with a contribution of distorted octahedral sites with an internal axial geometry in the case of the complexes prepared at strong alkaline pH conditions.

It should be remarked that the proposed interpretation of the results of the CW-EPR investigation is so far, solemnly qualitative. Further and more detailed calculations and simulations are necessary for the clarification of data and give answers to open questions merged during these preliminary studies. All of the additional investigation will be planned in/for future projects. The comparison between different EPR spectra has been carried out in a qualitative way too: the use of internal standards could be therefore useful in future studies to have a fixed reference in the EPR interpretations[HH]. As mentioned during the description of the results, the presence of the iron-oxides particles signals can really hide or disturb the proper iron-complexes signals. For this reason, further studies should be carried out considering the possibility to explore Q-Band and W-Band frequencies, in which these signals can be really separated from the ones of major interest.

3.3) Raman analyses results

This part of the study involved the acquisition of a series of Raman spectra in order to probe the real potentialities of Raman spectroscopy in the characterization of iron-polyphenolic complexes. As properly illustrated in the "Experimental section" chapter, the spectra have been acquired just on solid samples.
In Fig. 43 the spectra acquired on Fe-GA complexes prepared both in pseudo-stoichiometric and iron-excess conditions are reported[II]. The assignments of the main peaks is reported in Tab.6.[5,89,151–154]

[HH] The use of an internal standard for the analysis of solid samples in capillaries is not easy to implement. Practical constrains should always be considered during the evaluations of possible improvements of the procedure.
[II] The reported spectra have undergone a mild manipulation including manual correction of the baseline, smoothing and normalization.

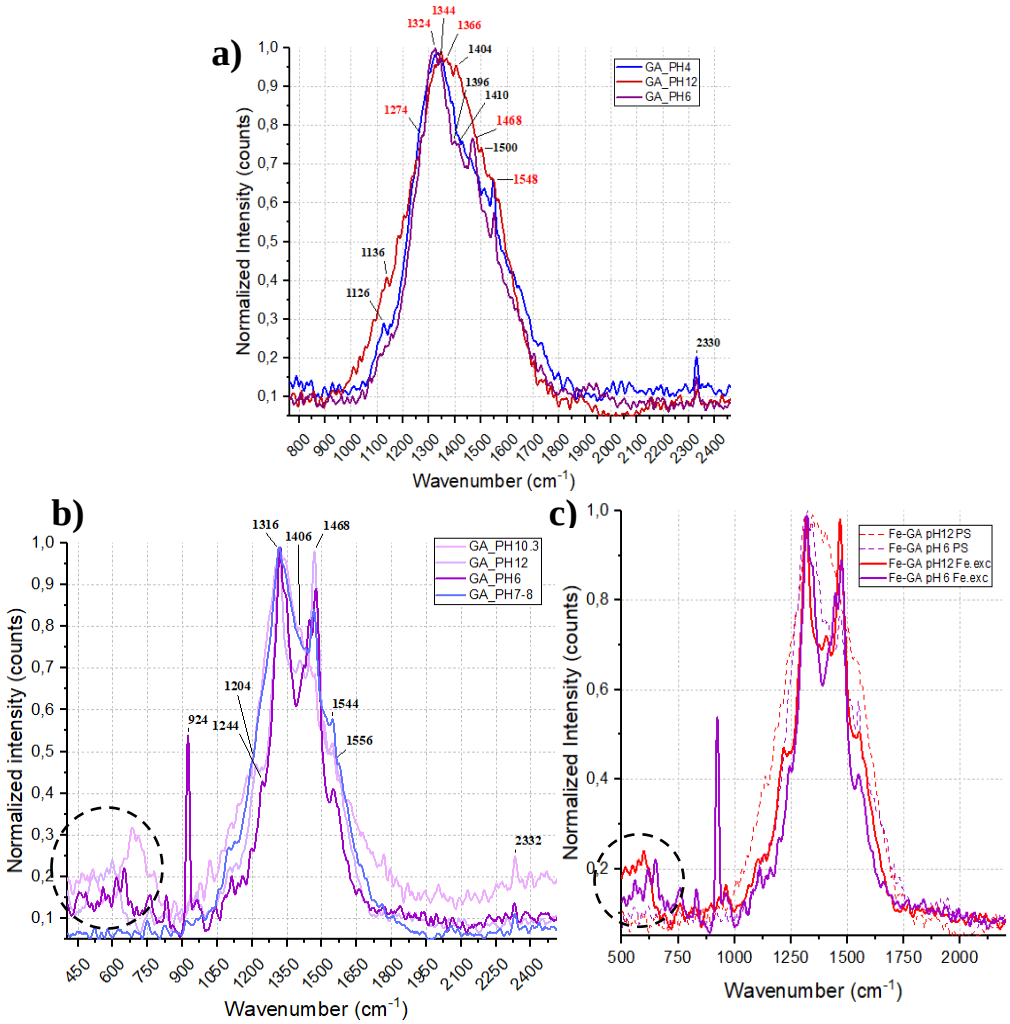

Fig. 43 Raman spectra of solid Fe-GA complexes prepared in a) pseudo-stoichiometric conditions b) iron-excess conditions. c) comparison between spectra acquired on Fe-GA pH 12 and Fe-GA pH 6 prepared in pseudo-stoichiometric conditions (PS) and iron excess (Fe.exc). The peaks highlighted in red in the panel a, are those considered characteristics in IGI identification.

Tab. 6 Main IGI related peaks assignment table (literature data). The peaks reported in bold are the ones generally considered characteristic of IGI and used for their identification on real manuscripts.

Peak position (cm^{-1})	**Assignment**	**Reference**
~1560-80	$\nu_{as}COO^-$ coordinated or νC=C quadrant stretching	5,89
1470-1480	νC=C of aromatic rings, βCH or νC=C of aromatic rings and βOH	106,151
1430-1450	ν_sCOO- coordinated or βC-OH and βCH or νC=C of aromatic rings and βOH	5,89,106,151
1350-1315	(doublet) νC=C aromatic rings, νCO or νCO(carboxylic), $\nu_s COO^-$ or ν(C-OH), βCH or βCH, βOH and νC=C aromatic ring	5,89,106,151,152
1230-1245	νC=C of aromatic rings, νCO ester, βCH	151,152
1270-1280	β(oop)C=O	107
1090-1120	νCO alcohols or β(oop)CO alchols	151,152

ν= stretching (asymmetrical and symmetrical), β= bending (β(oop)=bending out of plane)

It is quite evident from the spectra reported in Fig.43 that there are some differences among the spectra acquired on complexes prepared at different pH but with the same iron to ligand condition (iron-excess and pseudo-stoichiometric, Fig 43a-b) but also important differences can be noticed between those acquired on complexes prepared at the same pH but with different iron to ligand conditions (Fig. 43c). The comparison proposed in Fig. 43c is quite interesting in this sense: Raman spectra acquired on Fe-GA complexes prepared in iron-excess conditions seem to have a better resolution and in general a higher quality. The reason of this fact is however not well understood and therefore further discussions about the pH-related trend of the main peaks are barely speculative. Bearing in mind the considerations mentioned in the "Aim of the thesis and definition of the methodological approach" chapter about Raman intrinsic constrains in fact, it is evident that these differences could be associated to many different factors such as the difference in the scattering properties of the bulk material, different residual humidity, homogenization of the powders etc. The only thing that could be said is that, in any case, the main differences in terms of relative intensities of the peaks can be observed in the spectral range 1700-1410cm^{-1} and in particular the peak whose relative intensity varies the most is the one around 1470-1480cm^{-1} which is considered one of the characteristic peaks of IGI and is commonly associated with aromatic C=C stretching. However, in order to obtain meaningful (and statistically relevant) results about the variables influencing the intensity and the profile of the peaks in this spectral range, a massive amount of spectra are needed and a proper experimental design which takes into account all the possible variable should be constructed.

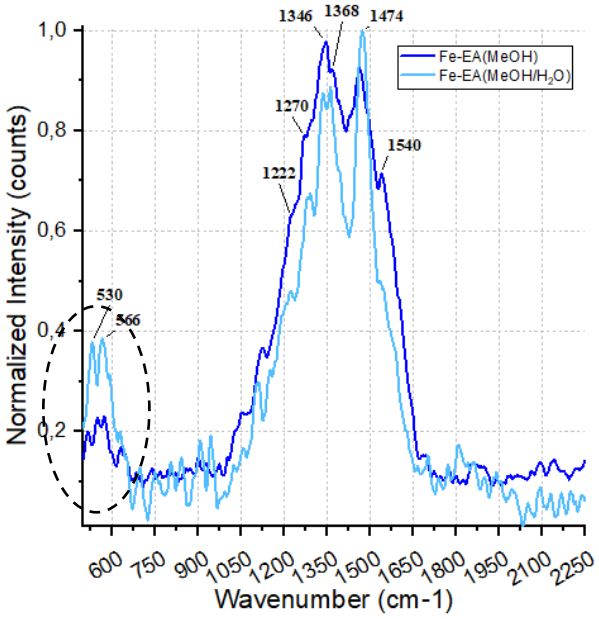

Fig. 44 Raman spectra of Fe-EA complexes prepared using EA methanol solution (MeOH) and EA fine dispersion in methanol/water mixture (MeOH/H_2O).

The spectra acquired on Fe-EA complexes are not dissimilar from the ones already discussed, having all the main peaks already described in Tab.6 for Fe-GA complexes (Fig. 44). In this case however, the influence of external variables in the overall spectra quality, already underlined for Fe-GA, appears even more dramatic: small changes in the laser power have influenced significantly the overall quality of the spectra (see Fig. 1 Appendix C)[JJ]. The variation between the spectra acquired on different areas of the powder sample and the ones related to different laser powers again mostly influence the spectral range 1700-1410cm^{-1}. These elements do not allow any further discussions about Fe-EA complexes themselves and eventual comparisons with the Fe-GA complexes to determine differences and similarities.

Also regarding the Raman spectra acquired on the iron complexes prepared using the oak galls extracts, the main signals related to iron-polyphenolic complexes have been observed and no important differences have been highlighted (Fig. 45). As can be noticed from the spectra reported in Fig. 45, and as expected, these spectra appear noisier even after an important post-manipulation (manual baseline correction and smoothing). Also in the case of Fe-Ex the intrinsic Raman constraints in the in-depth characterization of these complexes already mentioned before, are evident and do not allow further relevant considerations (see also Fig.2 Appendix C).

[JJ] This issue cannot be solved just using a fixed laser power for all the samples: the heterogeneity of the samples imposes to change the laser power for every sample in order to optimize the signal.

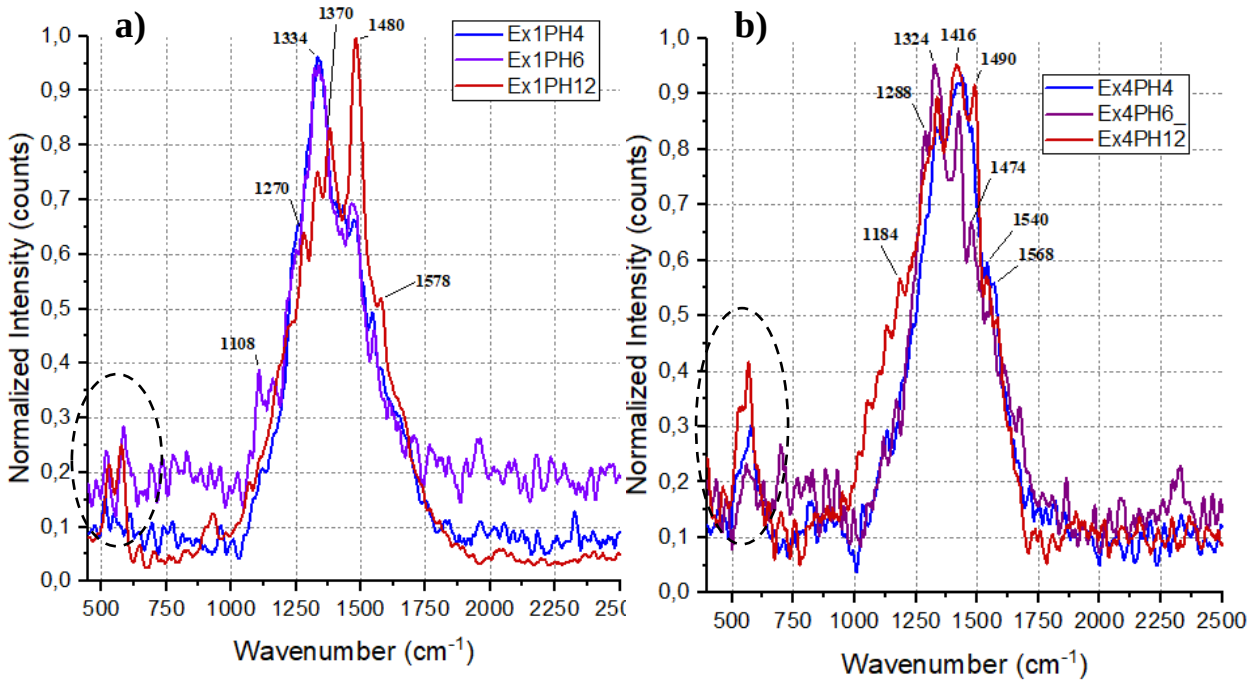

Fig. 45 Raman Spectra acquired on solid Fe-Ex complexes prepared started from a) Ex1 (Aleppo gallnuts extract) and b) Ex4 (Italian gallnut extract).

In all the Raman spectra here reported, other peaks have been observed. The most frequently observed are the ones in the spectral range 500-600cm^{-1}, generally observed in IGI spectra and sometimes attributed to out of plane vibrations of C-O bonds,[107] but still not properly identified (circled with dotted lines in the reported spectra). The signals around 2330cm^{-1} are difficult to interpret: their S/N ratio is in most of the cases borderline and it can be a classical example of an post-elaboration artifact. Checking the raw data (see Fig. 3 Appendix C) what can be said is that for some spectra (for example the ones related to Fe-GA complexes) those peaks can be defined as proper Raman signals but in some other spectra, such as for Fe-Ex complexes spectra, this is no longer the case. In any case these signals can be considered not important for the aim of the current investigation.

In all the reported spectra, the spectral region of major interest (1750-1000cm^{-1}) is actually crowded by a series of secondary signals difficult to interpret, even consulting the literature data. Moreover, please notice that the common assignments available in the scientific literature are not always in accordance: this makes the interpretation of the spectra and the extraction of structural information even more difficult.

To conclude this brief paragraph related to Raman spectroscopy results, the scheme in Fig. 46 summarizes the limitations and the prospective of Raman in the characterization of IGI emerged in this study.

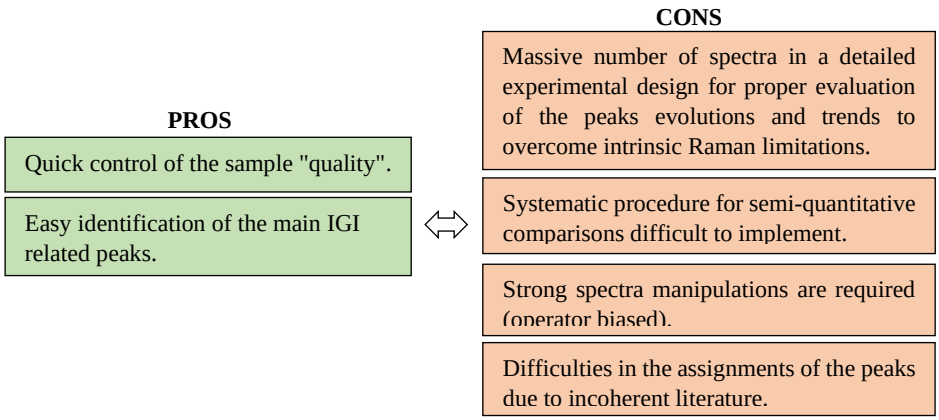

Fig. 46 Schematic summary of the advantages and disadvantages in the Raman characterization of IGI

Experimental section

1) Preparation of galls aqueous extracts

As previously mentioned in the chapter dedicated to the general description of the methodological approach, the procedure for the aqueous extracts preparation has been based on an historical IGI recipe, denominated as *Montpellier*.[5,28] The original recipe, contained in the manuscript H490 of the Medical Faculty of Montpellier[12], can be considered as one of the most classic recipe for medieval IGI preparation[KK]. The polyphenols-rich extracts used to be resulting from the maceration of crushed gallnuts in water (about 35mL of water for each gram of crushed galls) at RT for three days. After the maceration period the system used to be boiled up to reduction of the total volume to 1/4 and finally it was filtrated. However, considering the aim of the current study, it has been necessary to simplify and systematise the extraction procedure.
Polyphenols-rich aqueous extracts have been prepared starting from five different typologies of oak galls kindly provided by Dr. Cappa. In order to optimize the extraction, for each gall sample an initial grinding processing has been operated roughly crushing the galls and then using a proper grinder machine. Just for the gall sample 1 (Aleppo oak galls) a ball-milling powdering step has been attempted. The loss of mass in each step has been recorded in order to optimize this preliminary step. Considering the material loss and the time constrains, the ball-milling powdering step has been considered not necessary and therefore it has not been performed for the samples 2 to 5. A brief description of the galls samples and the data related to the mass loss during the grinding process is reported in Tab.7.

Tab. 7 Galls samples synthetic description and loss of material during the grinding process. The initial mass value is refered to the one measured after the rough crushing operation.

	Galls description				
Sample	**Provenance**	**Botanical specie**	**Initial mass (g)**	**Mass after grinding (g)**	**Material loss (%)**
1	Aleppo, Turkey (distributed by Kramer Pigmente)	*Quercus Infectoria*	17.23	15.09 14.39*	12.42 16.48*
2	Zavattarello (PV), Italy	*Quercus Robus*	17.33	14.95	13.73
3	Menconico (PV), Italy	*Quercus Robus*	16.70	14.94	10.54
4	Ticino Valley Natural Park (NO), Italy	*Quercus Robus*	21.70	18.55	14.52
5		*Quercus Robus*	13.56	11.34	16.37

* mass measured after the ball-milling powdering step

Milli-Q water has been added to around half of the grinded galls in the ratio 35mL for each gram of sample (the rest of the grinded sample has been stored as stock material). The so-prepared systems have been kept under moderate stirring at room temperature for three days. The best methodology for the separation of the insoluble part, necessary at the end of the extraction, after some tests turned out to be a preliminary gross Buckner filtration (white band filter paper) followed by a centrifugation cycle of 10mins at 9'000rpm. For sample number 1, due to the smaller dimension of the insoluble particles due to the ball-milling powdering step, two centrifugation cycles have been performed. The volumes of the resulting clear solutions have been significantly reduced with a rotavapor cycle and the extraction solvent has been finally completely removed through freeze-drying. The complete removal of water from the systems is a necessary step for the following

[KK] Original recipe: *"Para tinta. R. 1 libra de azeche et 1 libra et mediam gallarum et 1 libra gumi. Frange gallas et pone ad remoliendum in tres quartilos aque per 3 dies. Post coque et minuatur quasi 3 partes aque et si feruens cola eam. Ea sic colata micte intus 1 uncia gumi et uolue usque liqueffiat totum gumi. Postea in dicta aqua frigida micte 1 uncia predictam azeche et volve et sit sic per vnam diem. Post cola et micte in ampolla et caetera."*

extracts characterization via NMR techniques. In Fig. 47, a scheme for the extraction preparation is reported while in the following table (Tab.8) the data referred to the extraction procedure are summarized.

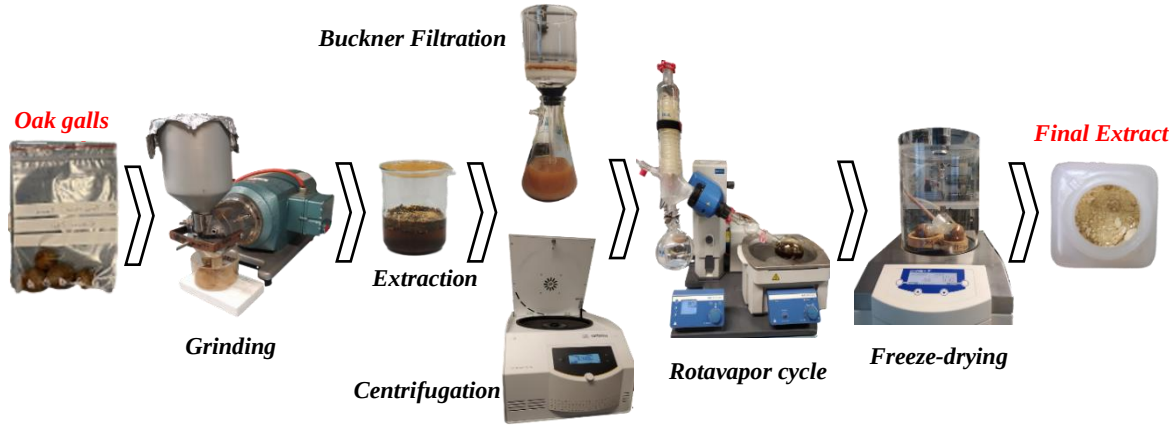

Fig. 47 Oak galls water extract preparation procedure

Tab. 8 Preparation of the oak galls water extracts

Sample	Mass of the extraction matrix (g)	Milli-Q water (mL)	Freeze-dried extract mass (g)	Extraction yield (%)*
1	7.19	252	5.2336	72.7
2	7.50	263	1.5745	20.9
3	7.46	261	0.9540	12.7
4	8.69	304	1.7575	20.3
5	5.62	197	1.0268	18.3

* yield calculated considering just three significant figures of the freeze-dried extract mass

2) Characterization of oak galls extracts via NMR techniques

As illustrated in the previous chapters, two NMR techniques have been used for the characterization of the gallnuts extracts: HSQC and ^{31}PNMR.

Concerning the characterization via HSQC, a small amount of the freeze-dried extracts (about 80-100mg) has been dissolved in 600µL of deuterated dimethyl sulfoxide (DMSO-d_6) in small vials. To facilitate the complete dissolution, magnetic stirring was used. Once completely dissolved, the solutions have been placed in NMR tubes and analysed with a suitable method.

Samples pre-treatment of the for the ^{31}P NMR analyses instead, includes different steps.

Following the protocols optimized for the lignin study[47,57], a little amount of the freeze-dried extracts (about 30mg) has been placed in small vials and 100µL of the internal standard (cholesterol and chromium acetyl acetonate[LL] in pyridine and deuterated chloroform 1.6:1) have been then added. A pyridine/deuterated chloroform 1.6 : 1 mixture, acting as proper solvent, has been added to the vials. Magnetic stirring was used also in this case to facilitate the complete sample dissolution. Once obtained homogeneous solutions, 50 to 150µL of the phosphorous reagent (2-chloro-4,4,5,5-tetramethyl-1,3-2-dioxaphospholane – TMDP) have been added according to the expected concentration of hydroxylated species in the sample. The addition of 3 drops of dimethylformamide (DMF) turned out to be necessary to completely dissolve and homogenize the samples[MM]. The so-prepared solutions have been then placed in NMR tubes and analysed with a suitable method.

All the data regarding the sample pre-treatment are summarized in Tab.9.

[LL] Chromium (III) acetylacetonate is usually introduced into the solvent system as a relaxation agent to shorten the spin-lattice relaxation time of the phosphorus nuclei.

[MM] The addition of DMF to facilitate the solubilization is in accordance with the protocols used as reference.[47,57]

Tab. 9 Sample pre-treatment for NMR analyses. IS mass is always refered to 100μL of solution.

	HSQC analyses		^{31}PNMR analyses			
Sample	**Sample mass (mg)**	**DMSO(μL)**	**Sample mass (mg)**	**IS mass (mg)**	**Pyridine/chloroform (μL)**	**TMDP (μL)**
1	105.6	500	35.1	127.7	750	50
2	83.1	500	29.9	125.8	750	100
3	90.5	500	28.5	123.6	750	100
4	90.2	500	31.7	127.5	500	100
5	43.3[#]	500	31.5	127.4	500	150

The smaller amount of sample in this case is due to difficulties in the freeze-drying of the extract.

Both HSQC and ^{31}P NMR analyses have been performed using a Bruker Magnet System spectrometer Ascend™ 400. The instrumental parameters used for the NMR experiments are listed in the table below (Tab. 10).

Tab. 10 Instrumental parameter for the ^{31}P NMR and HSQC experiments

Instrumental parameter	**^{31}P NMR**	**HSQC**
Size of field	25860	2048
Spectral width (f1)	99.7776ppm	200ppm
Spectral width (f2)		9.9967ppm
Number of scans	128	32
Pulse	8μs	10 μs
Transmitter frequency offset	140.000ppm	5.000ppm
Frequency offset of 2nd nucleus	4.000ppm	100.000ppm

3) Preparation of iron-polyphenolic complexes

The preparation and the isolation of iron-polyphenolic complexes in pH-controlled conditions has required a special effort due to the very poor scientific literature about these protocols. The optimization of the procedure therefore turned out to be a time-consuming but fundamental step for the successive iron-polyphenolic complexes characterization

3.1) Iron complexes with simple polyphenolic ligands: gallic acid and ellagic acid

The preparation and isolation of iron complexes with simple polyphenolic ligands has been the first step addressed. The selected compounds used as ligands have been Gallic Acid(97.5-102.5% pure) and Ellagic acid (>95% pure), both purchased by Sigma Aldrich®. As previously mentioned, the formation of Fe(II)-polyphenols coordination compounds is a strongly pH-dependent process (see paragraph 2.1 in the "Introduction" chapter). In both cases therefore, preliminary bibliographic research upon the protonation/deprotonation states was necessary to establish the pH conditions at which the ligands are completely protonated, partially deprotonated and almost completely deprotonated.[73,74,79,126,127]

Comparing and critically reviewing the available data upon the topic[NN], three pH conditions have been withheld suitable for the current study: pH 4 for the complete protonation states, pH6 for the partial protonation states and pH 12 for the strong deprotonation states of both EA and GA (Fig. 48). According to scientific literature, different iron to ligand ratios of the complexes prepared at these three pH conditions are expected. [70,78] These data have been used as starting point for the construction of the preparation procedure of the complexes in pH-controlled conditions. In particular, for the successive calculations it has been assumed that the 1:1 iron to ligand ratio is the predominant stoichiometry at pH 4, while 1:2.5 is

[NN] The available data upon protonation equilibria of organic compounds are strongly dependent to the analytical methodology used for the determination of the molar ratio of the different species in solution. The results can be therefore significantly divergent, and some evaluations and assumptions should be done.

the iron to ligand ratio at pH 6 (virtual value used to take in consideration both the 1:2 and 1:3 stoichiometric ratios) and 1:3 the one at pH 12.

For the preparation of the Fe-GA complexes at pH 4 and pH 6, an exact amount of GA has been initially dissolved in 10mL of CH_3COOH/CH_3COONa buffers prepared using concentrated acetic acid (96%, purchased by Sigma-Aldrich®) and sodium hydroxide pearls (>97%, purchased by Merk KGaA®). The complete dissolution of GA required the use of a quick sonication bath (about 5-10mins). The final pH of the GA solutions has been checked using short pH range litmus paper (pH colour-fixed indicator strips – Macherey-Nagel™). The preparation of Fe-GA complexes at pH 12 instead, required a special effort and a slightly different procedure due to the strong acidic pH of GA solution. An exact amount of GA has been directly dissolved in 10mL of NaOH 1M[OO]. In this case the final pH has been checked with a proper pH-meter (Horiba LAQUAtwin) due to the un-readability of litmus papers caused by the darker colour of the resulting GA solutions. The pH has been adjusted until pH 12 with little additions of solid NaOH.

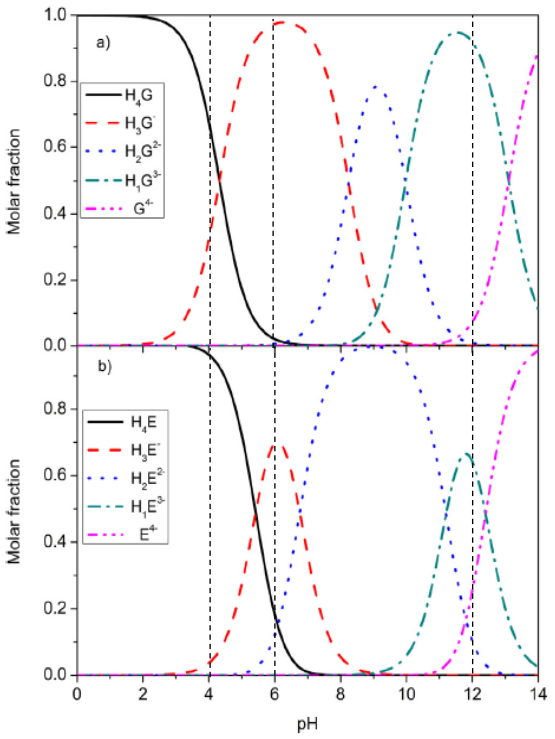

Fig. 48 Molar fractions of different gallic (top) and ellagic (bottom) acid ionisation recently calculated with a spectrophotometric approach by Hostnik et al.

However, due to the poor solubility of ellagic acid (0.82mg/mL), it has not been possible to prepare Fe-EA complexes in pH-controlled conditions. For this reason, Fe-EA complexes have been prepared starting from EA methanol solutions (Methanol pure for analysis, purchased by Merk KGaA®) and EA fine dispersions in 1:1 $MeOH/H_2O$ solutions (a sonication bath of about 10mins has been performed in both cases, in order to check if significant structural changes in the complexes can be noticed and therefore to probe the possibility to simply work with EA $MeOH/H_2O$ dispersions in future studies.

Starting from the hypothesized iron to ligand ratio, a freshly prepared 350g/L $FeSO_4 \cdot 7H_2O$ solution (Fe(II)-sulphate, purchased by Kremer Pigmente®, 85% pure,) has been added to the organic ligands solutions and dispersions using P100 and P1000 micropipettes (PipetmanNeo® - Gilson®) . To better interpret the data resulting from the successive EPR characterization, the Fe(II) solution was added as to obtain "pseudo stoichiometric" complexes[PP]. Moreover, as mentioned previously, the role of the Fe excess in the successive EPR characterization has been addressed preparing complexes at pH 6 both in "pseudo stoichiometric" and in "iron excess" conditions (around twice the stoichiometric requested quantity).

The addition of the Fe(II) solution immediately results in the formation of the dark iron complexes. Since no significant literature about the iron-polyphenolic complexes isolation is present, it has been established,

[OO] The choice of the use of NaOH 1M solution was dictated by several technical difficulties in the preparation of a suitable buffer and in any case followed a series of tests including the pH adjustment with concentrated and diluted ammonia, diluted NaOH etc. Due to these difficulties, during the preparation procedure optimization, **complexes at intermediate alkaline pH have been prepared (pH 7.5 and pH 10.3).**

[PP] A precise Fe(II) stoichiometric addition is difficult to calculate considering the assumptions already mentioned about the iron to ligand ratios. The term "pseudo-stoichiometric" should be therefore interpret as "as close as possible to the theoretical stoichiometric ratio".

after a series of trials, but still arbitrary, an oxidizing and thickening period of 5 days. During this period, the closed 15mL Falcon tubes in which the complexes have been prepared have been stored in a dark place. After five days the solid Fe(III)-polyphenolic complexes have been separated from the solution by centrifugation. At least 3 centrifugation-washing cycles turned out to be necessary (centrifugation: 14'500rpm, 15mins). This step of the isolation procedure turned out to be the most critical one: due to the small dimensions of the insoluble Fe(III)-polyphenolic complexes, high G values in the centrifugation are required. Generally, these conditions can be achieved with centrifuges working with low volumes. Therefore, it has been necessary to split the fine dispersion volume into multiple and suitable centrifugation tubes. This operation has inevitably affected the apparent reaction yield[QQ].

The supernatants resulting from this process have been collected and stored in clean Falcon tubes in a dark environment, while the solid part instead has been dried in oven (24h, 50°C, 10% ventilation) and then weighted. This weight can be used to calculate "Reaction and Oxidation rough yields" (ROry) as: $\frac{Fe(III)-polyph\ ob.\ mass}{Fe(III)-polyph\ exp.\ mass} * 100$; where the numerator is the obtained mass of the iron-complex and the denominator is the expected mass calculated starting from the pseudo-stoichiometric assumptions and the added reagents quantities.
Being the thickening and oxidation time set arbitrary, this value, which is obviously related to the proper reaction yield, is depending also on the oxidation rate. Considering the technical constraints related to the centrifugation process mentioned above, the reason of the use of the "rough" adjective appears more evident. In any case ROry is an important practical indication useful also for future studies.
In the following tables (Tab.11-12) the data referred to the preparation of the complexes are reported.

Tab. 11 Fe-GA preparation description. The calculations have been made as to obtain a final product of about 200mg. The reaction yield has been calculated for a second trail (as mentioned in the Results and Discussion chapter).

Pseudo stoichiometric Fe-GA		**pH 4 H_4GA-Fe**	**pH 6 $(H_3GA^-)_{2.5}$-Fe**	**pH 12 $(HGA^{3-})_3$-Fe**
GA (Sigma Aldrich™)	Mass (mg)	151.11	177.71	187.26
	Pure (mmol)	0.870	1.024	1.079
FeSO4•7H_2O 350g/L	Volume (mL)	0.38	0.18	0.16
Fe excess Fe-GA		/	**pH 6 $(H_3GA^-)_{2.5}$-Fe**	/
GA (Sigma Aldrich®)	Mass (mg)	/	163.30	/
	Pure (mmol)	/	0.941	/
FeSO4•7H_2O 350g/L	Volume (mL)	/	1	/
	Pure (mmol)	/	1.958	/
	Excess*(%mmol)	/	108*	/

* The iron excess has been calculated based on the stoichiometric assumptions explained above. Therefore, this value should be interpreted just as "around twice the theoretical stoichiometric quantity".

[QQ] Considering these practical constraints, it is now more evident the reason why it was not possible to work with EA water solutions.

Tab. 12 Fe-EA preparation description. The calculations have been made considering the 1:1 iron to ligand ratio as the predominant one in this case.

Pseudo stoichiometric Fe-EA		**MeOH H_4EA-Fe**	**MeOH/H_2O (1:1) H_4EA-Fe**
EA (Sigma Aldrich®)?	Mass (mg)	19.83	18.18
	Pure (mmol)	0.0630	0.0578
FeSO4•7H_2O 350g/L	Volume (μL)	32.2	29.6
Fe(III)-EA complex	Mass (mg)	4.91	/
	ROry(% mg/mg)	21.8%	/

* The ROry for the MeOH/H_2O has not been reported due to the fact that is dramatically influenced by the weight of the insoluble unreacted EA.

3.2) Iron complexes with oak galls aqueous extracts

The optimized preparation and isolation procedure described above has been applied also for the preparation of iron complexes using some of the oak galls extracts. For this preliminary study, two of the prepared freeze-dried extracts have been selected which, accordingly to the characterization techniques performed, turned out to be significantly different: Extract 1 and Extract 4.

An exact amount of the freeze-dried extracts has been dissolved in 10mL of buffer or strongly alkaline solutions as described for the preparation of Fe-GA complexes. However, even using the same assumptions in terms of relation between complexes stoichiometry and pH, in this case it has not been possible to prepare "pseudo stoichiometric" complexes due to the complexity of the extracts. To avoid any Fe(II) deficiency and ligand excess, the addition of Fe(II) has been calculated considering the weight of freeze-dried extract as pure GA and doubling the resulting Fe(II) "pseudo-stoichiometric" millimoles value. Due to the fact that these complexes are characterized by a strong initial iron excess, in this case it has not been possible to extrapolate ROry values.

In the following table (Tab. 13), the data related to the preparation of Fe-Extracts complexes are reported.

Tab. 13 Preparation procedure for Fe-Extract complexes

			pH 4	**pH 6**	**pH 12**
Ex 1	Extract 1 (Aleppo oak galls)	Mass (mg)	105.2	98.43	99.83
		GA mmol	0.618	0.579	0.587
	FeSO4•7H_2O 350g/L	Volume (μL)	800	300	254
	Fe-Extract 1 complex	Mass (mg)	110.66	172.69*	10.04*
Ex 4	Extract 4 (Ticino Park oak galls)	Mass (mg)	79.87	78.54	72.99
		GA mmol	0.469	0.462	0.429
	FeSO4•7H_2O 350g/L	Volume(μL)	608	240	186
	Fe-Extract 4 complex	Mass (mg)	88.58	169.57*	24.71

* These values are strongly influenced by the humidity content and by the isolation process.

To conclude the complexes preparation description, in Fig.49 a scheme of the preparation and isolation procedure for Fe-Extracts complexes is reported.

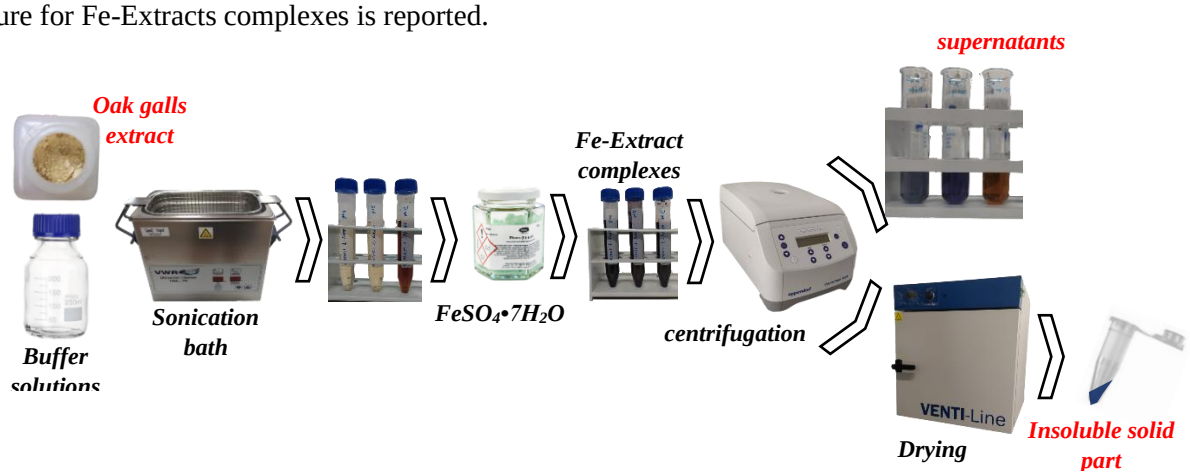

Fig. 49 General scheme for the Fe-Extracts complexes preparation and isolation

4) Iron-polyphenolic complexes characterization Preparation of iron-polyphenolic complexes

4.1) Raman spectroscopy as simple auxiliary technique

As previously mentioned, Raman spectroscopy has been used as auxiliary technique in the characterization of the complexes. Raman spectra have been acquired on the dried solid samples using a ProRaman-L-Dual-G analyzer of Enwave Optronics® which is a fully integrated and portable Raman spectrometer. For the current study it has been used a 785nm laser (maximum laser power of about 350mW, with a narrow linewidth of 2.0cm^{-1}) with variable laser powers ranging from 2 to 3mW. The Raman spectrometer is equipped with an integrated microscope operating with a 50x long working distance objective lens connected with a 1.3 Megapixel camera with in-line LED illumination. The number of scans, the laser power and the pulse time have been varied as to optimize the signal quality.
Three to six spectra have been acquired for each solid sample. In the following scheme (Fig. 50) a summary of the measurements performed is reported.

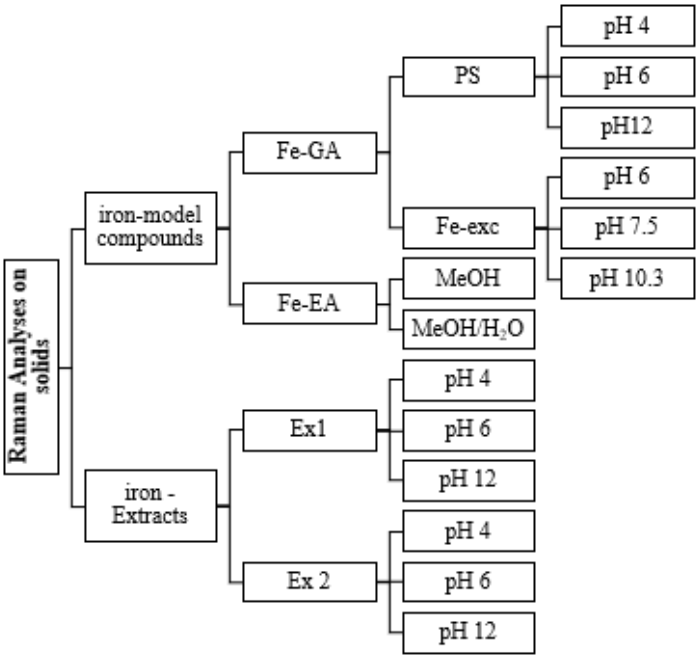

Fig. 50 Summary of the Raman spectra acquired. PS=pseudo stoichiometric preparation, Fe-exc= iron excess preparation. Some of the extra sample mentioned in the paragraph 4.1 note D have been analysed too(Fe-GA complexes at pH 7.5 and 10.3).

4.2) Characterization of iron-polyphenolic complexes via CW-EPR

The CW-EPR characterization of the complexes represents the core of the second part of the experimental part of this study. The study has involved two main blocks of measurements. In the first block both the dried solid samples and the supernatants resulting from the centrifugation (called just "liquid" for brevity) have been analysed at RT and at 100K in order to have a first monitoring and a general overview. A first rough interpretation of the spectra resulting from this first block of measurements, has enabled the selection of a small set of samples upon which a second block of measurements have been performed. This second block of measurements involved the acquisition of spectra at 140, 160 and 180K as to create a temperature gradient. Just one liquid sample, and in particular the liquid sample Fe-GA prepared in pseudo-stoichiometric conditions at pH 6, instead has been selected to perform a time monitoring: the spectra have been acquired after 2, 8, and 10 days both on the same capillary and on new capillaries prepared using the same original liquid sample. In Fig. 51 a summary of the measurements performed is schematically reported.

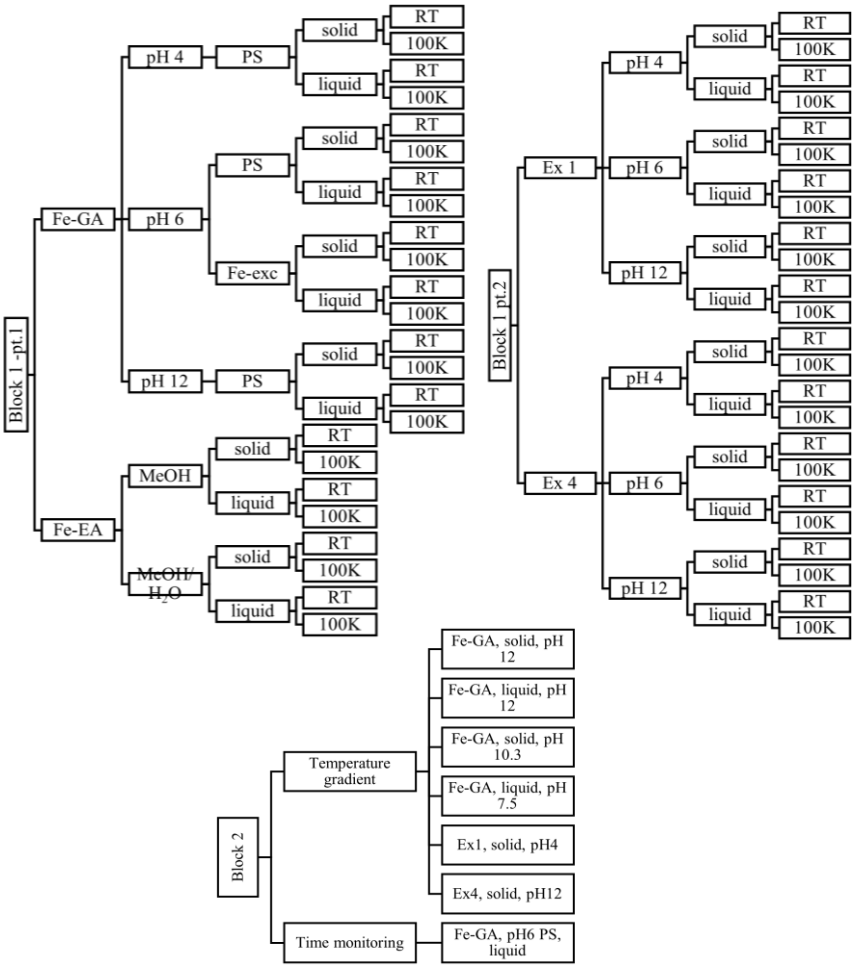

Fig. 51 Summary of the EPR measurements performed. PS=pseudo stoichiometric preparation, Fe-exc= iron excess preparation. In the second block of measurements some of the extra sample mentioned in the paragraph 4.1 note D have been analysed (Fe-GA complexes at pH 7.5 and 10.3)

Both for liquid and solid samples did not undergo any pre-treatment. Concerning the solid samples, a minim amount of the powdery dried complex (in the order of few milligrams) have been placed in small capillaries (1.15±0.5mm diameter micro haematocrit tubes by BRAND™) properly sealed with Critoseal©. The exact amount of sample to be analysed has been varied as accordingly to the quality of

the resulting EPR spectrum. The capillaries have then been placed into clean the NMR quartz tubes (generally used also in EPR) to be analysed. The use of capillaries has been implied also for the analysis of the liquid samples (Fig. 52).

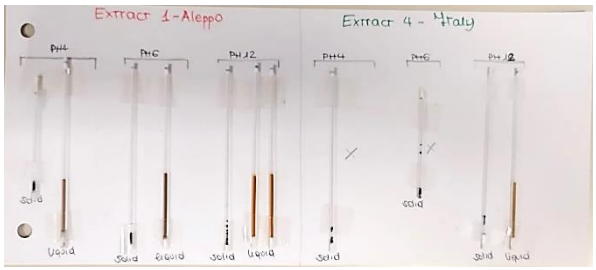

Fig. 52 Capillaries of Extract 1 and Extract 4 complexes prepared for the CW-EPR measurements.

All the spectra have been acquired with the Elexsys E 500 instrument by Bruker™. The instrument is designed for measurements in the X-band (frequency of the radiation of 9.75GHz). The sample is placed in a microwave cavity attached to a waveguide that has been eventually connected to a N_2 tank equipped with a thermocouple to acquire the EPR spectra at low temperature (second block of measurement). The instrumental parameters adjustment for the tuning is automatically performed by the instrument. According to the quality of the resulting spectra, the number of scans and the acquisition time have been varied (respectively between 5 and 10scans and 60-120s) while the attenuation has been set at 10dB for all the acquisitions[RR].

5) Data elaboration

The data resulting from the NMR analyses have been treated and elaborated using the MestReNova© software. Pre-treatments operations performed on the spectra included: automatic baseline and phase correction, reference position adjustment, apodization (Exponential mode) and in some cases also denoising and/or smoothing. Concerning the quantitative ^{31}P NMR procedure, the final results presented have been extrapolated starting from the values of the areas in the selected regions of the spectra, directly calculated with the MestReNova© software, and comparing them with the area of the internal standard peak, whose concentration in the sample is known.
All the other data instead have been instead treated and elaborated using Origin2021©. Pre-treatments operations performed on Raman spectra included: manual base-line correction, soft smoothing and normalization. EPR spectra did not undergone any treatments except from intensities normalization.

6) Practical constraints and criticism in the operative workflow

In order to better evaluate the results proposed in the previous chapter, it is important to bear in mind that, being a preliminary study and considering time and technical constraints, the methodological approach implemented in the current thesis project presents several criticism that should be improved in future studies. Some of the most critical aspects are listed below:

- *Lack of suitable statistics*

Unfortunately, due to time constraints, it has not been possible to work as to obtain statistically robust results in all the characterization analyses involved in the study. This would have required the acquisition and the processing of a huge amount of data. A suitable experimental design model could help in reducing significantly the number of analyses to perform, but also the generation of this type of models can result in a time-consuming operation.
The lack of a suitable statistics legitimates doubts related to the reproducibility and repeatability of the results obtained. In future studies this aspect should be more properly and carefully addressed.

- *Practical difficulties in the isolation of iron-polyphenolic complexes*

As previously mentioned, the isolation of the solid Fe(III)-polyphenolic complexes turned out to be the most challenging practical aspect of the second part of the study. The isolation methodology still presents some

[RR] These instrumental parameters have been set starting from previous studies performed by Dr. Cappa F.

criticisms. Concerning the centrifugation-washing cycles, the differences in the ROry resulted in significantly different washing volumes needed and consequently the final volume splitting required for the centrifugation. This part should be addressed in future studies more meticulously evaluating the impact of these operation on the global characterization process.

Due to time constraints the drying process has not been carried out using the classical oven-and- weighing cycles until constant weight. This is another element strongly affecting the ROry and should be more properly addressed in future studies.

- *Stability of the formed iron-polyphenolic complexes*

The stability of the solid complexes against possible pH changes during the drying process should be better addressed in future studies and eventually a milder drying process should be considered. The stability in time of the liquid complexes should be better addressed as well, also in this case considering the impact on the final characterization process.

Conclusion

Considering the results of the two sections of the experimental procedure involved in this thesis project, it is now necessary to underline some important aspects which seem to emerge merging all the data.

1) New evidences emerged from the current thesis project

1.1) Elucidation of oak galls composition

The current thesis project has demonstrated, using a different and innovative approach, that the general chemical composition of oak galls extracts is significantly different from the one reported in most of the main recent papers about IGI chemistry elucidation. Consequentially the studies conducted using GA as reference polyphenolic compound for iron complexes preparation should be revisited and rediscussed.

In particular, the characterization of galls extracts via HSQC and ^{31}P NMR, first of all suggested an important qualitative difference in the composition of the extract prepared starting form Aleppo oak galls and the other extracts prepared using Italian oak galls. Aleppo gallnuts aqueous extract seems to be very rich in HT, as expected, but with an important amount of TA. This last aspect is particularly important to underline considering that most of the studies about IGI are performed considering just GA and low molecular weight GT as main components of the extracts.[5,28,89] Recent studies about IGI for instance suggest the predominance of tannins such as tetra- and penta- galloyl glucose.[28] The difference in between the results obtained in these studies and the ones proposed here, can be related to two types of reasoning. The first hypothesis could be that, for some reason, not easy to define due to the large amount of un-controlled variables involved, the tannins present in the extracts analysed in those studies undergone an important hydrolysis. This option is hard to believe since generally this type of GT experiences a very mild hydrolysis in neutral and acidic environments, however, it cannot be excluded that the evidence the authors support is derived from a temperature-driven hydrolysis or thermal degradation. However, it is much more probable that the reason why no tannic acid has been revealed is simply because it could not be detected with the analytical techniques the authors decided to use (for instance ESI-MS).[28] In the results illustrated in the previous chapter, the occurrence of internal and terminal gallate units is evident in both ^{31}P NMR and HSQC but, in any case is strongly suggested in future studies to use a further techniques to confirm this evidence. The most suitable analytical method to do so would be MALDI-TOF and eventually also a chromatographic technique. In any case, it would be important to use an analytical technique which is actually able to detect large molecules without fragmenting them (very soft ionization techniques in the case of mass spectrometry). The characterization of the Italian oak galls samples instead seems to suggest an important presence of a small amount of proanthocyanidins and a not well-defined content of ET. It has not been possible just using NMR techniques to quantify their content and to elucidate their structure.

1.2) New insight upon iron-polyphenolic complexes in IGI

The characterization of EPR highlighted then at least two important aspects. First of all, no stable organic radicals have been detected, which in other terms means that the formation of radicals due to reduction of Fe^{3+} and the formation of ROSs species is not immediate. *However the main and unexpected results in this investigation is that complexes in IGI seem to have a different structure from the one proposed by Ponce et al.[89] or Feller-Cheetham[90] exactly due to the fact that polyphenols present in gallnuts extracts commonly used for IGI preparation are not so rich in free gallic acid bearing free carboxylic group able to cooperate in the formation of the solid structures proposed in those studies. In fact apart from the excess of iron, which is in an octahedral coordination site geometry as expected, complexes resulting from interaction between GT and iron seem to be in a tetrahedral coordination site geometry.*

In particular, it has been demonstrated that in Fe-GA complexes, not only colour can change accordingly with the pH conditions used in their preparation, but also the coordination sites geometry which is clearly predominantly octahedral in the case of the complexes prepared in strong acidic pH, mainly tetrahedral in slightly acidic and alkaline pH where, in this latter case, also distorted octahedral sites with an internal axial symmetry is observed too. But the very important point is that these differences have not been observed for complexes prepared starting with oak galls extracts, in which iron seems to exhibit a tetrahedral coordination site independently from the pH conditions in which the complexes have been prepared. So, this point is interesting because should be merged with what previously said about the composition of oak galls extracts, meaning the predominance of medium-to-high molecular weight tannins with very few free carboxylic groups.

It is important to underline that, even if the methodological procedure presented some criticism, this innovative approach enabled to obtain new evidences regarding the IGI chemistry which have never clearly highlighted and stated before (Fig. 53).

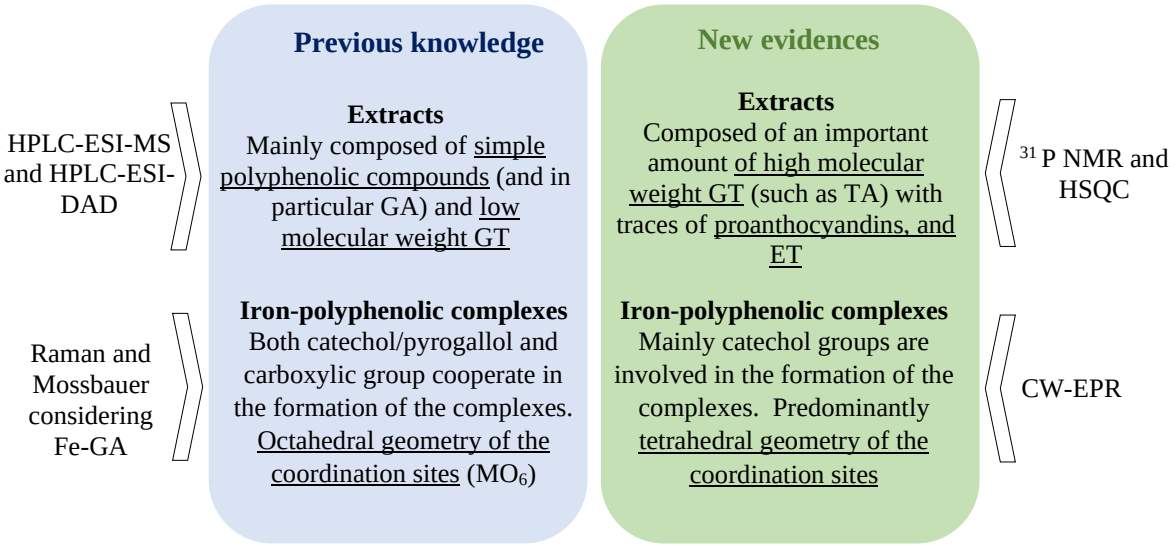

*Fig. 53 Summary of the most important results emerged from the current thesis project on the IGI chemistry. The box "previous knowledge" is mainly referred to three of the most recent and mentioned study upon IGI chemistry: Ponce et al. **2016**, Diaz et al. **2018** and Teixeira et al. **2021**.*

2) Methodological approach potentialities

What about the methodological approach itself? Being a preliminary study, the current project was focused on probing the potentialities of the approach more than having the best possible results. Nevertheless, this thesis project demonstrates that a more accurate approach, in which a stricter control of the variables involved in the processes studied, can actually brough to the light new evidences which can be important for future studies regarding IGI. The in-depth characterization of oak gallnuts extracts has been fundamental in this project. In many parts of the thesis, including the very previous paragraph, the suggestion of coupling these methods with a mass spectrometry technique is reported. However, it has been also reported that the choice of the ionization method should be done very accurately, preferring those soft methods which enable to detect also high molecular weight ions, as MALDI-TOF (see paragraph 1.1.3 in the introduction chapter). What can be said instead about the second part of the study, the one focused on the preparation and characterization of iron-polyphenolic complexes? In the previous chapter several aspects have been already mentioned, especially regarding the preparation of complexes, and therefore will not be reported here again. Considering more in general the approach used, EPR turned out to be an interesting and innovative investigation tool not only to identify the presence of organic radicals but also to have more detailed information about the structure of the

iron complexes. What can be done in future studies to improve this part of the procedure, is to use EPR not only qualitatively but also (semi)quantitatively, using suitable standards, as, for instance, to determine the ratios between octahedral and tetrahedral or octahedral and distorted coordination sites geometries. Moreover, the use of proper simulation programs and computational methods (for instance the popular DFT-based ones) can be useful to extract even more information, especially if an ageing of the sample would be involved in such studies. Experiments performed using other EPR methods such as impulse methods and higher frequencies (for instance ENDOR, Q-band or multi-frequency settings) should be included too as to better study the spin state systems in the iron-polyphenolic complexes and to avoid iron oxides particles interferences.

The use of Raman spectroscopy, as mentioned in the "Results and discussion" chapter, turned out to be a valid tool just as "control technique" to detect quickly problems in the preparation of the samples (presence of un-desired substances, degradation of the complexes etc). Scientists interested in continuing study these types of inks should evaluate then if it would be appropriate to spend some effort in try to correlate data from EPR (or other analytical techniques able to provide detailed structural information) with the ones of Raman spectroscopy. This would require for sure a massive amount of spectra to acquire and the construction of a suitable model (statistically robust). Eventually the use of Raman-derived spectroscopic techniques, generally based on the formation of localized plasmons of resonances, such as Tip Enhanced Raman scattering, can be considered in such evaluations.[107]
To conclude, the following scheme briefly summarize the improvements of the methodological approach suggested above (Fig. 54).

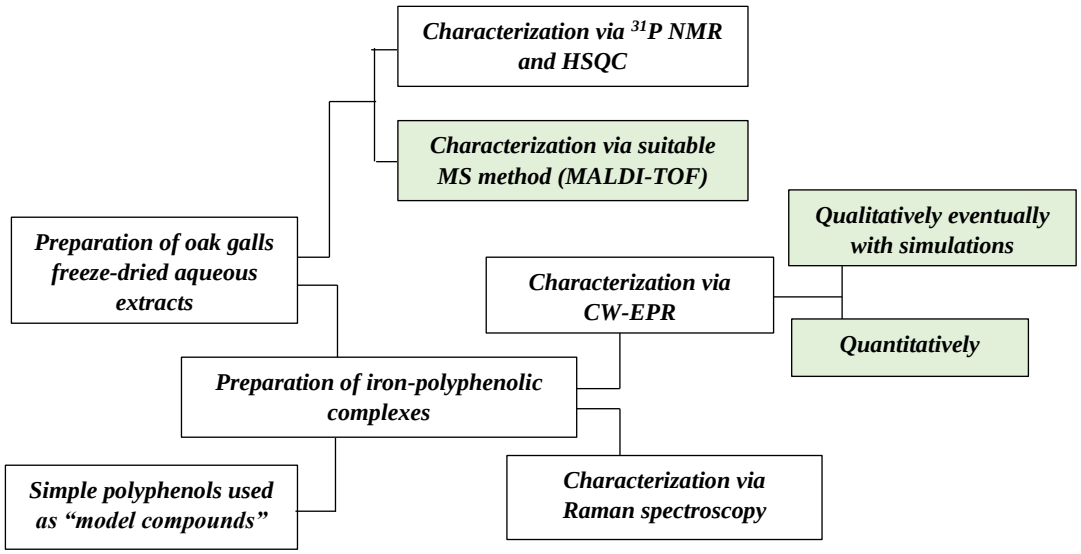

Fig. 54 Methodological approach suggestions for improvements (green boxes).

3) Future perspectives

Regarding the oak galls extracts in-depth characterization, there are at least two groups of elements, that are in somehow related one another, which should push scientists involved in this field to going further. The first is related to the in depth understanding of degradation mechanisms related to IGI, especially those involving the formation of organic radicals within the ink itself. In other words, it would be important to see how the oxidative stress experienced by manuscripts along decades or centuries resulted in different degradation patterns according to tannins with different molecular weights (and therefore capabilities in stabilize organic radicals). The second group of reasons regards instead the resulting iron-polyphenolic complexes. If tannic acid and other GT are predominant in oak galls extracts and very few carboxylic groups are available to cooperate in the formation of the complexes, how do these complexes are structured though? Are the internal gallates bearing free catechol groups capable of interact with iron or are they excluded from the formation of coordinative bonding due to steric constraints? Is the 3D structure of the final solid

particles still similar to the ones proposed in the famous studies mentioned in the first chapter[89–91] or the hypothetical models should be revisited completely? How much the final properties (in terms of photo-stability, electrochemical potential properties etc) of iron complexes of tannic acid and other high molecular weight tannins diverge from those observed and studied for iron-gallic acid coordination compounds?

The presence of both proanthocyadinins and ET in Italian oak galls then, opens a series of new questions about iron-polyphenolic complexes in IGI. Are the final properties of iron complexes resulting from the interaction of iron with this type of polyphenols still similar to those studied for iron-gallic acid and iron-gallotannins complexes? And if not, in which extent they diverge? Are the capabilities in stabilize organic radicals of ET and proanthocyadinis similar to those of GT. Is it possible to see significant differences in degradation patterns of inks containing also these polyphenols to those mainly containing GT? If yes, do they undergo a faster degradation or a slower one? And also, about the iron-polyphenolic complexes, in case of this type of ligands how exactly are they structured? How the 3D structure in solid particles is formed? The reader might not have missed that, since these polyphenols have not been here quantified the first point to reply to these questions is their precise quantification, as to reformulate the questions considering their actual content in the oak galls extract. For instance, is indeed the content of proanthocyanidins and ellagitannins enough to eventually induce significant differences in degradation patterns of inks?

Concerning instead the structural elucidation of iron-polyphenolic complexes in IGI, it is evident the reason why the coordination site geometry of iron in complexes with tannins (and not simple low molecular weight polyphenols) is not so sensitive to pH: the carboxylic groups are mainly engaged in depside bonds and therefore not available while presumably the acidic constants of phenolic hydroxyl groups are more dispersed, which make the construction of molar fraction curves of protonation states of GT difficult to construct. This evidence obviously should encourages all the experts in this field to continue study the actual structure of complexes in IGI. For instance, which are the most frequently occurring structures of iron-polyphenolic complexes in IGI? Is their stability in terms of formation/instability constants similar to those of iron-gallic acid complexes?

Lastly, preparation of oak-galls extracts starting with different vegetal matrices weight to water volume ratios, different extract solvents (wine, vinegar etc), considering the presence of additives or other vegetal matrices could be important trials to understand the actual variability of polyphenolic substances present in these kinds of extracts (and therefore the variability of iron-polyphenolic complexes), while a proper and detailed study, performed also but not only with EPR and in any case involving a proper controlled accelerated ageing step, could give more detailed information the stability and the degradation patterns of this series of iron complexes.

Concluding, this thesis project has been important both to obtain new evidences and information about the structure of iron-polyphenolic complexes in IGI as well as to define an innovative methodological approach, to be improved in further studies, for their in-depth characterization. Considering this thesis project as a preliminary study, it can be stated that the results obtained are satisfactory enough to encourage scientists involved in this field to going further in the study of this attractive and fascinating field of study.

References

(1) Magdalena, P.-S. Cultural Heritage in EU Policies, 2018.

(2) Levey, M. The Manufacture of Inks, Līqs, Erasure Fluids, and Glues-A Preliminary Survey in Arabic Chemical Technology. *Chymia* **1961**, *7*, 57–72. https://doi.org/10.2307/27757205.

(3) Ghigo, T.; Albarrán Martínez, M. J. The Practice of Writing inside an Egyptian Monastic Settlement: Preliminary Material Characterisation of the Inks Used on Coptic Manuscripts from the Monastery of Apa Apollo at Bawit. *Herit Sci* **2021**, *9* (1), 62. https://doi.org/10.1186/s40494-021-00541-0.

(4) Carvalho David Nunes. *Forty Centuries of Ink Or, A Chronological Narrative Concerning Ink and Its Backgrounds, Introducing Incidental Observations and Deductions, Parallels of Time and Color Phenomena, Bibliography, Chemistry, Poetical Effusions, Citations, Anecdotes and Curiosa Together with Some Evidence Respecting the Evanescent Character of Most Inks of to-Day and an Epitome of Chemico-Legal Ink.*, First edition.; The bank law publishing Co.: New York, 1998.

(5) Díaz Hidalgo, R. J.; Córdoba, R.; Nabais, P.; Silva, V.; Melo, M. J.; Pina, F.; Teixeira, N.; Freitas, V. New Insights into Iron-Gall Inks through the Use of Historically Accurate Reconstructions. *Herit Sci* **2018**, *6* (1), 63. https://doi.org/10.1186/s40494-018-0228-8.

(6) Fagan, M. M. The Uses of Insect Galls. *The American Naturalist* **1918**, *52* (614), 155–176. https://doi.org/10.1086/279661.

(7) Hartley, S. E. The Chemical Composition of Plant Galls: Are Levels of Nutrients and Secondary Compounds Controlled by the Gall-Former? *Oecologia* **1998**, *113* (4), 492–501. https://doi.org/10.1007/s004420050401.

(8) Kot, I.; Jakubczyk, A.; Karaś, M.; Złotek, U. Biochemical Responses Induced in Galls of Three Cynipidae Species in Oak Trees. *Bull. Entomol. Res.* **2018**, *108* (4), 494–500. https://doi.org/10.1017/S0007485317001055.

(9) Chen, H.; Liu, J.; Cui, K.; Lu, Q.; Wang, C.; Wu, H.; Yang, Z.; Ding, W.; Shao, S.; Wang, H.; Ling, X.; King-Jones, K.; Chen, X. Molecular Mechanisms of Tannin Accumulation in Rhus Galls and Genes Involved in Plant-Insect Interactions. *Sci Rep* **2018**, *8* (1), 9841. https://doi.org/10.1038/s41598-018-28153-y.

(10) Azmaz, M.; Kilinçarslan Aksoy, Ö.; Katilmiş, Y.; Mammadov, R. Investigation of the Antioxidant Activity and Phenolic Compounds of Andricus Quercustozae Gall and Host Plant (Quercus Infectoria). *International Journal of Secondary Metabolite* **2020**, 77–87. https://doi.org/10.21448/ijsm.674930.

(11) Costa, A.; Fonseca, N.; Carvalho, S.; Santos, F.; Barki, L.; Freitas, D.; Herbst, M.; Lutterbach, M. Archaeometric Investigations on Naturally and Thermally-Aged Iron-Gall Inks Using Different Tannin Sources. *Open Chemistry* **2013**, *11* (11), 1729–1739. https://doi.org/10.2478/s11532-013-0303-7.

(12) Ricardo Cordoba de la Llave. Un Recetario Técnico Castellano Del Siglo XV:El Manuscrito H490 de LaFacultad de Medicina de Montpellier. *En la Espana Medieval* **2005**, No. 28, 7–48.

(13) Reverendo Alessio Piemontese. *De' Secreti del reverendo Donno Alessio Piemontese*; Antonio degli Antoni: Venezia, 1610; Vol. Prima parte-Quinto Libro.

(14) Preparation of Black Ink. *Harper's Bazar*. February 21, 1880, pp 113–114.

(15) William B. Dick. Inks. In *Practical Recipes and Processing*; Dick & Fitzgerald: New York, 1870; p 607.

(16) Serrano, J.; Puupponen-Pimiä, R.; Dauer, A.; Aura, A.-M.; Saura-Calixto, F. Tannins: Current Knowledge of Food Sources, Intake, Bioavailability and Biological Effects. *Mol. Nutr. Food Res.* **2009**, *53* (S2), S310–S329. https://doi.org/10.1002/mnfr.200900039.

(17) Bravo, L. Polyphenols: Chemistry, Dietary Sources, Metabolism, and Nutritional Significance. *Nutrition Reviews 56* (11), 17.

(18) Karamali, K.; Teunis, van R. Tannins: Classification and Definition. *Nat. Prod. Rep.* **2001**, *18* (6), 641–649. https://doi.org/10.1039/b101061l.
(19) Wall-Medrano, A. TANINOS HIDROLIZABLES; BIOQUÍMICA, ASPECTOS NUTRICIONALES Y ANALÍTICOS Y. *NUTRICION HOSPITALARIA* **2015**, No. 1, 55–66. https://doi.org/10.3305/nh.2015.31.1.7699.
(20) Brglez Mojzer, E.; Knez Hrnčič, M.; Škerget, M.; Knez, Ž.; Bren, U. Polyphenols: Extraction Methods, Antioxidative Action, Bioavailability and Anticarcinogenic Effects. *Molecules* **2016**, *21* (7), 901. https://doi.org/10.3390/molecules21070901.
(21) Lopes, G.; Sousa, C.; Silva, L. R.; Pinto, E.; Andrade, P. B.; Bernardo, J.; Mouga, T.; Valentão, P. Can Phlorotannins Purified Extracts Constitute a Novel Pharmacological Alternative for Microbial Infections with Associated Inflammatory Conditions? *PLoS ONE* **2012**, *7* (2), e31145. https://doi.org/10.1371/journal.pone.0031145.
(22) Le Bourvellec, C.; Renard, C. M. G. C. Interactions Between Polyphenols and Macromolecules: Effect of Tannin Structure. In *Encyclopedia of Food Chemistry*; Elsevier, 2019; pp 515–521. https://doi.org/10.1016/B978-0-08-100596-5.21486-8.
(23) Renard, C. M. G. C.; Watrelot, A. A.; Le Bourvellec, C. Interactions between Polyphenols and Polysaccharides: Mechanisms and Consequences in Food Processing and Digestion. *Trends in Food Science & Technology* **2017**, *60*, 43–51. https://doi.org/10.1016/j.tifs.2016.10.022.
(24) Watrelot, A. A.; Le Guernevé, C.; Hallé, H.; Meudec, E.; Véran, F.; Williams, P.; Robillard, B.; Garcia, F.; Poncet-Legrand, C.; Cheynier, V. Multimethod Approach for Extensive Characterization of Gallnut Tannin Extracts. *J. Agric. Food Chem.* **2020**, *68* (47), 13426–13438. https://doi.org/10.1021/acs.jafc.9b08221.
(25) Zahida T.Maqsood; S. Arif Kazmi, S. A. K. Determination of Stability Constant, Enthalpy and Entropy of Formation of Iron(III) Complexes of Gallic Acid and Methyl Ester of Gallic Acid. *Journal of the Chemical Society of Pakistan* **1993**, *15* (1).
(26) Oudane, B. Isolation, Characterization, Antioxidant Activity, and Protein-Precipitating Capacity of the Hydrolyzable Tannin Punicalagin from Pomegranate Yellow Peel (Punica Granatum). *Journal of Molecular Structure* 7.
(27) Saad, H.; Charrier-El Bouhtoury, F.; Pizzi, A.; Rode, K.; Charrier, B.; Ayed, N. Characterization of Pomegranate Peels Tannin Extractives. *Industrial Crops and Products* **2012**, *40*, 239–246. https://doi.org/10.1016/j.indcrop.2012.02.038.
(28) Teixeira, N.; Nabais, P.; de Freitas, V.; Lopes, J. A.; Melo, M. J. In-Depth Phenolic Characterization of Iron Gall Inks by Deconstructing Representative Iberian Recipes. *Sci Rep* **2021**, *11* (1), 8811. https://doi.org/10.1038/s41598-021-87969-3.
(29) Rasines-Perea; Jacquet; Jourdes; Quideau; Teissedre. Ellagitannins and Flavano-Ellagitannins: Red Wines Tendency in Different Areas, Barrel Origin and Ageing Time in Barrel and Bottle. *Biomolecules* **2019**, *9* (8), 316. https://doi.org/10.3390/biom9080316.
(30) Vanholme, R.; Demedts, B.; Morreel, K.; Ralph, J.; Boerjan, W. Lignin Biosynthesis and Structure. *Plant Physiology* **2010**, *153* (3), 895–905. https://doi.org/10.1104/pp.110.155119.
(31) Haslam, E.; Cai, Y. Plant Polyphenols (Vegetable Tannins): Gallic Acid Metabolism. *Nat. Prod. Rep.* **1994**, *11*, 41. https://doi.org/10.1039/np9941100041.
(32) Serna, D.; Martínez, J. Phenolics and Polyphenolics from Melastomataceae Species. *Molecules* **2015**, *20* (10), 17818–17847. https://doi.org/10.3390/molecules201017818.
(33) Takako Yamashita; Yosuke Matsuo, Y. M.; Yoshinori Saito, Y. S.; Takashi Tanaka, T. T. Formation of Dehydrohexahydroxydiphenoyl Esters by Oxidative Coupling of Galloyl Esters in an Aqueous Medium Involved in Ellagitannin Biosynthesis. *Nat. Prod. Rep.* **2001**, *18* (6), 641–649. https://doi.org/10.1039/b101061l.
(34) Nonaka, G. Isolation and Structure Elucidation of Tannins. *Pure and Applied Chemistry* **1989**, *61* (3), 357–360. https://doi.org/10.1351/pac198961030357.

(35) Melone, F.; Saladino, R.; Lange, H.; Crestini, C. Tannin Structural Elucidation and Quantitative ^{31} P NMR Analysis. 2. Hydrolyzable Tannins and Proanthocyanidins. *J. Agric. Food Chem.* **2013**, *61* (39), 9316–9324. https://doi.org/10.1021/jf401664a.
(36) Melone, F.; Saladino, R.; Lange, H.; Crestini, C. Tannin Structural Elucidation and Quantitative ^{31} P NMR Analysis. 1. Model Compounds. *J. Agric. Food Chem.* **2013**, *61* (39), 9307–9315. https://doi.org/10.1021/jf401477c.
(37) Okuda, T.; Yoshida, T.; Hatano, T. Classification of Oligomeric Hydrolysable Tannins and Specificity of Their Occurrence in Plants. *Phytochemistry* **1993**, *32* (3), 507–521. https://doi.org/10.1016/S0031-9422(00)95129-X.
(38) Zhen, L.; Lange, H.; Zongo, L.; Crestini, C. Chemical Derivatization of Commercially Available Condensed and Hydrolyzable Tannins. *ACS Sustainable Chem. Eng.* **2021**, *9* (30), 10154–10166. https://doi.org/10.1021/acssuschemeng.1c02114.
(39) Li, C.; Leverence, R.; Trombley, J. D.; Xu, S.; Yang, J.; Tian, Y.; Reed, J. D.; Hagerman, A. E. High Molecular Weight Persimmon (Diospyros Kaki L.) Proanthocyanidin: A Highly Galloylated, A-Linked Tannin with an Unusual Flavonol Terminal Unit, Myricetin. *J. Agric. Food Chem.* **2010**, *58* (16), 9033–9042. https://doi.org/10.1021/jf102552b.
(40) Xie, D.-Y.; Dixon, R. A. Proanthocyanidin Biosynthesis – Still More Questions than Answers? *Phytochemistry* **2005**, *66* (18), 2127–2144. https://doi.org/10.1016/j.phytochem.2005.01.008.
(41) Jonker, A.; Yu, P. The Occurrence, Biosynthesis, and Molecular Structure of Proanthocyanidins and Their Effects on Legume Forage Protein Precipitation, Digestion and Absorption in the Ruminant Digestive Tract. *IJMS* **2017**, *18* (5), 1105. https://doi.org/10.3390/ijms18051105.
(42) Crestini, C.; Lange, H.; Bianchetti, G. Detailed Chemical Composition of Condensed Tannins via Quantitative ^{31} P NMR and HSQC Analyses: *Acacia Catechu* , *Schinopsis Balansae* , and *Acacia Mearnsii*. *J. Nat. Prod.* **2016**, *79* (9), 2287–2295. https://doi.org/10.1021/acs.jnatprod.6b00380.
(43) Ferreira, D.; Bekker, R. Oligomeric Proanthocyanidins: Naturally Occurring O-Heterocycles. *NATURAL PRODUCT REPORTS* **1996**, 23.
(44) Restivo, A.; Degano, I.; Ribechini, E.; Colombini, M. P. Development and Optimisation of an HPLC-DAD-ESI-Q-ToF Method for the Determination of Phenolic Acids and Derivatives. *PLoS ONE* **2014**, *9* (2), e88762. https://doi.org/10.1371/journal.pone.0088762.
(45) Kelly-Hunt, A. E.; Mehan, A.; Brooks, S.; Leanca, M. A.; McKay, J. E. D.; Mahamed, N.; Lambert, D.; Dempster, N. M.; Allen, R. J.; Evans, A. R.; Sarker, S. D.; Nahar, L.; Sharples, G. P.; Drew, M. G. B.; Fielding, A. J.; Ismail, F. M. D. Synthesis and Analytical Characterization of Purpurogallin: A Pharmacologically Active Constituent of Oak Galls. *J. Chem. Educ.* **2022**, *99* (2), 983–993. https://doi.org/10.1021/acs.jchemed.1c00699.
(46) Beasley, T. H.; Ziegler, H. W.; Bell, A. D. Determination and Characterization of Gallotannin by High Performance Liquid Chromatography. *Anal. Chem.* **1977**, *49* (2), 238–243. https://doi.org/10.1021/ac50010a016.
(47) Argyropoulos, D. S.; Pajer, N.; Crestini, C. Quantitative ^{31}P NMR Analysis of Lignins and Tannins. *JoVE* **2021**, No. 174, 62696. https://doi.org/10.3791/62696.
(48) Sukor, N. F.; Jusoh, R.; Kamarudin, N. S.; Abdul Halim, N. A.; Sulaiman, A. Z.; Abdullah, S. B. Synergistic Effect of Probe Sonication and Ionic Liquid for Extraction of Phenolic Acids from Oak Galls. *Ultrasonics Sonochemistry* **2020**, *62*, 104876. https://doi.org/10.1016/j.ultsonch.2019.104876.
(49) Fraga-Corral, M.; García-Oliveira, P.; Pereira, A. G.; Lourenço-Lopes, C.; Jimenez-Lopez, C.; Prieto, M. A.; Simal-Gandara, J. Technological Application of Tannin-Based Extracts. *Molecules* **2020**, *25* (3), 614. https://doi.org/10.3390/molecules25030614.
(50) Ignat, I.; Volf, I.; Popa, V. I. A Critical Review of Methods for Characterisation of Polyphenolic Compounds in Fruits and Vegetables. *Food Chemistry* **2011**, *126* (4), 1821–1835. https://doi.org/10.1016/j.foodchem.2010.12.026.

(51) Ajila, C. M.; Brar, S. K.; Verma, M.; Tyagi, R. D.; Godbout, S.; Valéro, J. R. Extraction and Analysis of Polyphenols: Recent Trends. *Critical Reviews in Biotechnology* **2011**, *31* (3), 227–249. https://doi.org/10.3109/07388551.2010.513677.

(52) Sanches Silva, A.; Reboredo-Rodríguez, P.; Sanchez-Machado, D. I.; López-Cervantes, J.; Barreca, D.; Pittala, V.; Samec, D.; Orhan, I. E.; Gulcan, H. O.; Forbes-Hernandez, T. Y.; Battino, M.; Nabavi, S. F.; Devi, K. P.; Nabavi, S. M. Evaluation of the *Status Quo* of Polyphenols Analysis: Part II—Analysis Methods and Food Processing Effects. *Comprehensive Reviews in Food Science and Food Safety* **2020**, *19* (6), 3219–3240. https://doi.org/10.1111/1541-4337.12626.

(53) Zhao, J.; Wang, M.; Saroja, S. G.; Khan, I. A. NMR Technique and Methodology in Botanical Health Product Analysis and Quality Control. *Journal of Pharmaceutical and Biomedical Analysis* **2022**, *207*, 114376. https://doi.org/10.1016/j.jpba.2021.114376.

(54) Eisenreich, W.; Bacher, A. Advances of High-Resolution NMR Techniques in the Structural and Metabolic Analysis of Plant Biochemistry. *Phytochemistry* **2007**, *68* (22–24), 2799–2815. https://doi.org/10.1016/j.phytochem.2007.09.028.

(55) Sette, M.; Lange, H.; Crestini, C. QUANTITATIVE HSQC ANALYSES OF LIGNIN: A PRACTICAL COMPARISON. *Computational and Structural Biotechnology Journal* **2013**, *6* (7), e201303016. https://doi.org/10.5936/csbj.201303016.

(56) Zhen, L.; Lange, H.; Crestini, C. An Analytical Toolbox for Fast and Straightforward Structural Characterisation of Commercially Available Tannins. *Molecules* **2021**, *26* (9), 2532. https://doi.org/10.3390/molecules26092532.

(57) Meng, X.; Crestini, C.; Ben, H.; Hao, N.; Pu, Y.; Ragauskas, A. J.; Argyropoulos, D. S. Determination of Hydroxyl Groups in Biorefinery Resources via Quantitative 31P NMR Spectroscopy. *Nature Protocols* **2019**, *14* (9), 2627–2647. https://doi.org/10.1038/s41596-019-0191-1.

(58) Kachlicki, P.; Piasecka, A.; Stobiecki, M.; Marczak, Ł. Structural Characterization of Flavonoid Glycoconjugates and Their Derivatives with Mass Spectrometric Techniques. *Molecules* **2016**, *21* (11), 1494. https://doi.org/10.3390/molecules21111494.

(59) Motilva, M.-J.; Serra, A.; Macià, A. Analysis of Food Polyphenols by Ultra High-Performance Liquid Chromatography Coupled to Mass Spectrometry: An Overview. *Journal of Chromatography A* **2013**, *1292*, 66–82. https://doi.org/10.1016/j.chroma.2013.01.012.

(60) Alvarez-Rivera, G.; Ballesteros-Vivas, D.; Parada-Alfonso, F.; Ibañez, E.; Cifuentes, A. Recent Applications of High Resolution Mass Spectrometry for the Characterization of Plant Natural Products. *TrAC Trends in Analytical Chemistry* **2019**, *112*, 87–101. https://doi.org/10.1016/j.trac.2019.01.002.

(61) Lozada-Ramírez, J. D.; Ortega-Regules, A. E.; Hernández, L. R.; Anaya de Parrodi, C. Spectroscopic and Spectrometric Applications for the Identification of Bioactive Compounds from Vegetal Extracts. *Applied Sciences* **2021**, *11* (7), 3039. https://doi.org/10.3390/app11073039.

(62) Giovando, S.; Pizzi, A.; Pasch, H.; Pretorius, N. Structure and Oligomers Distribution of Commercial Tara (Caesalpina Spinosa) Hydrolysable Tannin. **2013**, *9*, 11.

(63) Navarrete, P.; Pizzi, A.; Pasch, H.; Rode, K.; Delmotte, L. MALDI-TOF and 13C NMR Characterization of Maritime Pine Industrial Tannin Extract. *Industrial Crops and Products* **2010**, *32* (2), 105–110. https://doi.org/10.1016/j.indcrop.2010.03.010.

(64) Pasch, H.; Pizzi, A.; Rode, K. MALDI±TOF Mass Spectrometry of Poly¯avonoid Tannins. **2001**, 9.

(65) Radebe, N.; Rode, K.; Pizzi, A.; Giovando, S.; Pasch, H. MALDI-TOF-CID for the Microstructure Elucidation of Polymeric Hydrolysable Tannins. *J. Appl. Polym. Sci.* **2013**, *128* (1), 97–107. https://doi.org/10.1002/app.38156.

(66) Zubarev, R. A.; Makarov, A. Orbitrap Mass Spectrometry. *Anal. Chem.* **2013**, 9.

(67) Zamorano, G. M. C. The Presence of Iron in Inks Used in Valencian Manuscripts from the 13th to 17th Century. *Microchemical Journal* **2018**, *143*, 484–492. https://doi.org/10.1016/j.microc.2018.07.043.
(68) Jančovičová, V.; Čeppan, M.; Havlínová, B.; Reháková, M.; Jakubíková, Z. Interactions in Iron Gall Inks. *Chemical Papers* **2007**, *61* (5). https://doi.org/10.2478/s11696-007-0053-0.
(69) Nkhili, E.; Loonis, M.; Mihai, S.; El Hajji, H.; Dangles, O. Reactivity of Food Phenols with Iron and Copper Ions: Binding, Dioxygen Activation and Oxidation Mechanisms. *Food Funct.* **2014**, *5* (6), 1186–1202. https://doi.org/10.1039/C4FO00007B.
(70) Perron, N. R.; Brumaghim, J. L. A Review of the Antioxidant Mechanisms of Polyphenol Compounds Related to Iron Binding. *Cell Biochem Biophys* **2009**, *53* (2), 75–100. https://doi.org/10.1007/s12013-009-9043-x.
(71) Matin, M. A.; Islam, M. M.; Bredow, T.; Aziz, M. A. The Effects of Oxidation States, Spin States and Solvents on Molecular Structure, Stability and Spectroscopic Properties of Fe-Catechol Complexes: A Theoretical Study. 17.
(72) Ozkorucuklu, S. P.; Beltrán, J. L.; Fonrodona, G.; Barrón, D.; Alsancak, G.; Barbosa, J. Determination of Dissociation Constants of Some Hydroxylated Benzoic and Cinnamic Acids in Water from Mobility and Spectroscopic Data Obtained by CE-DAD. *J. Chem. Eng. Data* **2009**, *54* (3), 807–811. https://doi.org/10.1021/je800595x.
(73) Tam, K. Y.; Takács-Novák, K. Multi-Wavelength Spectrophotometric Determination of Acid Dissociation Constants: A Validation Study. *Analytica Chimica Acta* **2001**, *434* (1), 157–167. https://doi.org/10.1016/S0003-2670(01)00810-8.
(74) Jabbari, M. Solvent Dependence of Protonation Equilibria for Gallic Acid in Water and Different Acetonitrile–Water Cosolvent Systems. *Journal of Molecular Liquids* **2015**, *208*, 5–10. https://doi.org/10.1016/j.molliq.2015.03.055.
(75) Kim, J.; Lee, K.; Nam, Y. S. Metal-Polyphenol Complexes as Versatile Building Blocks for Functional Biomaterials. *Biotechnol Bioproc E* **2021**, *26* (5), 689–707. https://doi.org/10.1007/s12257-021-0022-4.
(76) Berto, S.; Alladio, E. Application of Chemometrics Tools to the Study of the Fe(III)–Tannic Acid Interaction. *Front. Chem.* **2020**, *8*, 614171. https://doi.org/10.3389/fchem.2020.614171.
(77) Li, Y.; Wen, J.; Qin, M.; Cao, Y.; Ma, H.; Wang, W. Single-Molecule Mechanics of Catechol-Iron Coordination Bonds. **2017**, 11.
(78) Frešer, F.; Hostnik, G.; Tošović, J.; Bren, U. Dependence of the Fe(II)-Gallic Acid Coordination Compound Formation Constant on the PH. *Foods* **2021**, *10* (11), 2689. https://doi.org/10.3390/foods10112689.
(79) Galano, A.; Francisco Marquez, M.; Pérez-González, A. Ellagic Acid: An Unusually Versatile Protector against Oxidative Stress. *Chem. Res. Toxicol.* **2014**, *27* (5), 904–918. https://doi.org/10.1021/tx500065y.
(80) Malacaria, L.; Corrente, G. A.; Beneduci, A.; Furia, E.; Marino, T.; Mazzone, G. A Review on Coordination Properties of Al(III) and Fe(III) toward Natural Antioxidant Molecules: Experimental and Theoretical Insights. *Molecules* **2021**, *26* (9), 2603. https://doi.org/10.3390/molecules26092603.
(81) Hynes, M. J.; Ó Coinceanainn, M. The Kinetics and Mechanisms of the Reaction of Iron(III) with Gallic Acid, Gallic Acid Methyl Ester and Catechin. *Journal of Inorganic Biochemistry* **2001**, *85* (2–3), 131–142. https://doi.org/10.1016/S0162-0134(01)00205-7.
(82) Bijlsma, J.; de Bruijn, W. J. C.; Hageman, J. A.; Goos, P.; Velikov, K. P.; Vincken, J.-P. Revealing the Main Factors and Two-Way Interactions Contributing to Food Discolouration Caused by Iron-Catechol Complexation. *Sci Rep* **2020**, *10* (1), 8288. https://doi.org/10.1038/s41598-020-65171-1.
(83) Ejima, H.; Richardson, J. J.; Liang, K.; Best, J. P.; van Koeverden, M. P.; Such, G. K.; Cui, J.; Caruso, F. One-Step Assembly of Coordination Complexes for Versatile Film and Particle Engineering. *Science* **2013**, *341* (6142), 154–157. https://doi.org/10.1126/science.1237265.

(84) Boyatzis, S. C.; Velivasaki, G.; Malea, E. A Study of the Deterioration of Aged Parchment Marked with Laboratory Iron Gall Inks Using FTIR-ATR Spectroscopy and Micro Hot Table. *Herit Sci* **2016**, *4* (1), 13. https://doi.org/10.1186/s40494-016-0083-4.
(85) Völkel, L.; Prohaska, T.; Potthast, A. Combining Phytate Treatment and Nanocellulose Stabilization for Mitigating Iron Gall Ink Damage in Historic Papers. *Herit Sci* **2020**, *8* (1), 86. https://doi.org/10.1186/s40494-020-00428-6.
(86) Ryan, P.; Hynes, M. J. The Kinetics and Mechanisms of the Complex Formation and Antioxidant Behaviour of the Polyphenols EGCg and ECG with Iron(III). *Journal of Inorganic Biochemistry* **2007**, *101* (4), 585–593. https://doi.org/10.1016/j.jinorgbio.2006.12.001.
(87) Perron, N. R.; Wang, H. C.; DeGuire, S. N.; Jenkins, M.; Lawson, M.; Brumaghim, J. L. Kinetics of Iron Oxidation upon Polyphenol Binding. *Dalton Trans.* **2010**, *39* (41), 9982. https://doi.org/10.1039/c0dt00752h.
(88) Lu, L.; Li, Y.; Lu, X. Kinetic Study of the Complexation of Gallic Acid with Fe(II). *Spectrochimica Acta Part A: Molecular and Biomolecular Spectroscopy* **2009**, *74* (3), 829–834. https://doi.org/10.1016/j.saa.2009.08.025.
(89) Ponce, A.; Brostoff, L. B.; Gibbons, S. K.; Zavalij, P.; Viragh, C.; Hooper, J.; Alnemrat, S.; Gaskell, K. J.; Eichhorn, B. Elucidation of the Fe(III) Gallate Structure in Historical Iron Gall Ink. *Anal. Chem.* **2016**, *88* (10), 5152–5158. https://doi.org/10.1021/acs.analchem.6b00088.
(90) Feller, R. K.; Cheetham, A. K. Fe(III), Mn(II), Co(II), and Ni(II) 3,4,5-Trihydroxybenzoate (Gallate) Dihydrates; a New Family of Hybrid Framework Materials. *Solid State Sciences* **2006**, *8* (9), 1121–1125. https://doi.org/10.1016/j.solidstatesciences.2006.04.013.
(91) Russell Kenneth Feller. Dense Organic-Inorganic Framework Materials Containing Transition Metal Ions, UNIVERSITY OF CALIFORNIA Santa Barbara, 2008.
(92) Rizvi, M. A.; Mane, M.; Khuroo, M. A.; Peerzada, G. M. Computational Survey of Ligand Properties on Iron(III)–Iron(II) Redox Potential: Exploring Natural Attenuation of Nitroaromatic Compounds. *Monatsh Chem* **2017**, *148* (4), 655–668. https://doi.org/10.1007/s00706-016-1813-8.
(93) Chvátalová, K.; Slaninová, I.; Březinová, L.; Slanina, J. Influence of Dietary Phenolic Acids on Redox Status of Iron: Ferrous Iron Autoxidation and Ferric Iron Reduction. *Food Chemistry* **2008**, *106* (2), 650–660. https://doi.org/10.1016/j.foodchem.2007.06.028.
(94) Bardon, T.; May, R. K.; Taday, P. F.; Strlič, M. Systematic Study of Terahertz Time-Domain Spectra of Historically Informed Black Inks. *Analyst* **2013**, *138* (17), 4859. https://doi.org/10.1039/c3an00331k.
(95) Corregidor, V.; Viegas, R.; Ferreira, L. M.; Alves, L. C. Study of Iron Gall Inks, Ingredients and Paper Composition Using Non-Destructive Techniques. *Heritage* **2019**, *2* (4), 2691–2703. https://doi.org/10.3390/heritage2040166.
(96) Codre, H.; Radepont, M.; Echard, J.; Belhadj, O.; Vaiedelich, S.; Rouchon, V. The Use of XRF Imaging for the Chemical Discrimination of Iron-gall Ink Inscriptions: A Case Study in Stradivari's Workshop. *X-Ray Spectrom* **2021**, *50* (4), 244–252. https://doi.org/10.1002/xrs.3160.
(97) Duh, J.; Krstić, D.; Desnica, V.; Fazinić, S. Non-Destructive Study of Iron Gall Inks in Manuscripts. *Nuclear Instruments and Methods in Physics Research Section B: Beam Interactions with Materials and Atoms* **2018**, *417*, 96–99. https://doi.org/10.1016/j.nimb.2017.08.033.
(98) Chiavari, G.; Montalbani, S.; Prati, S.; Keheyan, Y.; Baroni, S. Application of Analytical Pyrolysis for the Characterisation of Old Inks. *Journal of Analytical and Applied Pyrolysis* **2007**, *80* (2), 400–405. https://doi.org/10.1016/j.jaap.2007.04.011.
(99) Wagner, B.; Bulska, E.; Stahl, B.; Heck, M.; Ortner, H. M. Analysis of Fe Valence States in Iron-Gall Inks from XVIth Century Manuscripts by 57Fe Mössbauer Spectroscopy. *Analytica Chimica Acta* **2004**, *527* (2), 195–202. https://doi.org/10.1016/j.aca.2004.04.011.

(100) Burgaud, C.; Rouchon, V.; Wattiaux, A.; Bleton, J.; Sabot, R.; Refait, P. Determination of the Fe(II)/Fe(III) Ratio in Iron Gall Inks by Potentiometry: A Preliminary Study. *Journal of Electroanalytical Chemistry* **2010**, *650* (1), 16–23. https://doi.org/10.1016/j.jelechem.2010.09.015.
(101) Gimat, A.; Kasneryk, V.; Dupont, A.-L.; Paris, S.; Averseng, F.; Fournier, J.; Massiani, P.; Rouchon, V. Investigating the DMPO-Formate Spin Trapping Method for the Study of Paper Iron Gall Ink Corrosion. *New J. Chem.* **2016**, *40* (11), 9098–9110. https://doi.org/10.1039/C6NJ01480A.
(102) Kanngießer, B.; Hahn, O.; Wilke, M.; Nekat, B.; Malzer, W.; Erko, A. Investigation of Oxidation and Migration Processes of Inorganic Compounds in Ink-Corroded Manuscripts. *Spectrochimica Acta Part B: Atomic Spectroscopy* **2004**, *59* (10–11), 1511–1516. https://doi.org/10.1016/j.sab.2004.07.013.
(103) Goltz, D. M. A Review of Instrumental Approaches for Studying Historical Inks. *Analytical Letters* **2012**, *45* (4), 314–329. https://doi.org/10.1080/00032719.2011.644712.
(104) Vetter, W.; Frühmann, B.; Cappa, F.; Schreiner, M. Materials and Techniques Used for the "Vienna Moamin": Multianalytical Investigation of a Book about Hunting with Falcons from the Thirteenth Century. *Herit Sci* **2021**, *9* (1), 87. https://doi.org/10.1186/s40494-021-00553-w.
(105) Wei, D.; Chen, S.; Liu, Q. Review of Fluorescence Suppression Techniques in Raman Spectroscopy. *Applied Spectroscopy Reviews* **2015**, *50* (5), 387–406. https://doi.org/10.1080/05704928.2014.999936.
(106) Espina, A.; Sanchez-Cortes, S.; Jurašeková, Z. Vibrational Study (Raman, SERS, and IR) of Plant Gallnut Polyphenols Related to the Fabrication of Iron Gall Inks. *Molecules* **2022**, *27* (1), 279. https://doi.org/10.3390/molecules27010279.
(107) Kurouski, D.; Zaleski, S.; Casadio, F.; Van Duyne, R. P.; Shah, N. C. Tip-Enhanced Raman Spectroscopy (TERS) for *in Situ* Identification of Indigo and Iron Gall Ink on Paper. *J. Am. Chem. Soc.* **2014**, *136* (24), 8677–8684. https://doi.org/10.1021/ja5027612.
(108) Çakar, S.; Güy, N.; Özacar, M.; Fındık, F. Investigation of Vegetable Tannins and Their Iron Complex Dyes for Dye Sensitized Solar Cell Applications. *Electrochimica Acta* **2016**, *209*, 407–422. https://doi.org/10.1016/j.electacta.2016.05.024.
(109) Jablonsky, M.; Šima, J. Oxidative Degradation of Paper – A Minireview. *Journal of Cultural Heritage* **2021**, *48*, 269–276. https://doi.org/10.1016/j.culher.2021.01.014.
(110) Larsen, R. The Chemical Degradation of Leather. *Chimia* **2008**, *62* (11), 899. https://doi.org/10.2533/chimia.2008.899.
(111) Dong, H.; Sans, C.; Li, W.; Qiang, Z. Promoted Discoloration of Methyl Orange in H2O2/Fe(III) Fenton System: Effects of Gallic Acid on Iron Cycling. *Separation and Purification Technology* **2016**, *171*, 144–150. https://doi.org/10.1016/j.seppur.2016.07.033.
(112) Chen, R.; Pignatello, J. J. Role of Quinone Intermediates as Electron Shuttles in Fenton and Photoassisted Fenton Oxidations of Aromatic Compounds. *Environ. Sci. Technol.* **1997**, *31* (8), 2399–2406. https://doi.org/10.1021/es9610646.
(113) Duesterberg, C. K.; Waite, T. D. Kinetic Modeling of the Oxidation of P-Hydroxybenzoic Acid by Fenton's Reagent: Implications of the Role of Quinones in the Redox Cycling of Iron. *Environmental Science & Technology* **2007**, *41* (11), 4103–4110. https://doi.org/10.1021/es0628699.
(114) Vyskočilová, G.; Ebersbach, M.; Kopecká, R.; Prokeš, L.; Příhoda, J. Model Study of the Leather Degradation by Oxidation and Hydrolysis. *Herit Sci* **2019**, *7* (1), 26. https://doi.org/10.1186/s40494-019-0269-7.
(115) Shin, M.; Park, E.; Lee, H. Plant-Inspired Pyrogallol-Containing Functional Materials. *Adv. Funct. Mater.* **2019**, *29* (43), 1903022. https://doi.org/10.1002/adfm.201903022.

(116) Cherepanov, P. V.; Rahim, A.; Bertleff-Zieschang, N.; Sayeed, A.; O'Mullane, A. P.; Moulton, S. E.; Caruso, F. Electrochemical Behavior and Redox-Dependent Disassembly of Gallic Acid/FeIII Metal–Phenolic Networks. *ACS Appl. Mater. Interfaces* **2018**, 7.
(117) Rahim, A.; Ejima, H.; Cho, K. L.; Kempe, K.; Mu, M.; Best, J. P.; Caruso, F. Coordination-Driven Multistep Assembly of Metal−Polyphenol Films and Capsules. *Chem. Mater.* **2014**, 9.
(118) Pucci, C.; Martinelli, C.; Pasquale, D. D.; Battaglini, M. Tannic Acid–Iron Complex-Based Nanoparticles as a Novel Tool against Oxidative Stress. *ACS Appl. Mater. Interfaces* **2022**, 15.
(119) Lee, H.; Nguyen, D. T.; Kim, N.; Han, S. Y.; Hong, Y. J.; Yun, G.; Kim, B. J.; Choi, I. S. Enzyme-Mediated Kinetic Control of Fe^{3+} –Tannic Acid Complexation for Interface Engineering. *ACS Appl. Mater. Interfaces* **2021**, *13* (44), 52385–52394. https://doi.org/10.1021/acsami.1c15503.
(120) Han, N.; Xu, Z.; Cui, C.; Li, Y.; Zhang, D.; Xiao, M.; Fan, C.; Wu, T.; Yang, J.; Liu, W. A Fe3+-Crosslinked Pyrogallol-Tethered Gelatin Adhesive Hydrogel with Antibacterial Activity for Wound Healing. *Biomaterials Science* **2020**, 9.
(121) Włodarczyk-Biegun, M.; Julieta I Paez; Maria Villiou; Jun Feng; Aranzazu del Campo. Printability Study of Metal Ion Crosslinked PEGcatechol Based Inks. *Biofabrication* **2020**, *12*. https://doi.org/10.1088/1758-5090/ab673a.
(122) Rathnayake, H.; Dawood, S.; Pathiraja, G.; Adrah, K.; Ayodele, O. Green Synthesis of De Novo Bioinspired Porous Iron-Tannate Microstructures with Amphoteric Surface Properties. *Sustainable Chemistry* **2022**, *3* (2), 192–204. https://doi.org/10.3390/suschem3020013.
(123) Korpany, K. V.; Majewski, D. D.; Chiu, C. T.; Cross, S. N.; Blum, A. S. Iron Oxide Surface Chemistry: Effect of Chemical Structure on Binding in Benzoic Acid and Catechol Derivatives. *Langmuir* **2017**, *33* (12), 3000–3013. https://doi.org/10.1021/acs.langmuir.6b03491.
(124) Daniel, P.; Shylin, S. I.; Lu, H.; Tahir, M. N.; Panthöfer, M.; Weidner, T.; Möller, A.; Ksenofontov, V.; Tremel, W. The Surface Chemistry of Iron Oxide Nanocrystals: Surface Reduction of γ-Fe_2O_3 to Fe_3O_4 by Redox-Active Catechol Surface Ligands. *J. Mater. Chem. C* **2018**, *6* (2), 326–333. https://doi.org/10.1039/C7TC04795A.
(125) Yuen, A. K. L.; Hutton, G. A.; Masters, A. F.; Maschmeyer, T. The Interplay of Catechol Ligands with Nanoparticulate Iron Oxides. *Dalton Trans.* **2012**, *41* (9), 2545. https://doi.org/10.1039/c2dt11864e.
(126) Hostnik, G.; Tošović, J.; Štumpf, S.; Petek, A.; Bren, U. The Influence of PH on UV/Vis Spectra of Gallic and Ellagic Acid: A Combined Experimental and Computational Study. *Spectrochimica Acta Part A: Molecular and Biomolecular Spectroscopy* **2022**, *267*, 120472. https://doi.org/10.1016/j.saa.2021.120472.
(127) Simić, A. Z.; Verbić, T. Ž.; Sentić, M. N.; Vojić, M. P.; Juranić, I. O.; Manojlović, D. D. Study of Ellagic Acid Electro-Oxidation Mechanism. *Monatsh Chem* **2013**, *144* (2), 121–128. https://doi.org/10.1007/s00706-012-0856-8.
(128) Anders Lund; Masaru Shiotani; Shigetaka Shimada. *Principles and Applications of ESR Spectroscopy*, 1st ed.; Springer Dordrecht: UK, 2011.
(129) Cutsail, G. E.; Telser, J.; Hoffman, B. M. Advanced Paramagnetic Resonance Spectroscopies of Iron–Sulfur Proteins: Electron Nuclear Double Resonance (ENDOR) and Electron Spin Echo Envelope Modulation (ESEEM). *Biochimica et Biophysica Acta (BBA) - Molecular Cell Research* **2015**, *1853* (6), 1370–1394. https://doi.org/10.1016/j.bbamcr.2015.01.025.
(130) Regulla, D. F. ESR Spectrometry: A Future-Oriented Tool for Dosimetry and Dating. *Applied Radiation and Isotopes* **2005**, *62* (2), 117–127. https://doi.org/10.1016/j.apradiso.2004.08.030.
(131) Yu, L. L.; Cheng, Z. Application of Electron Spin Resonance (ESR) Spectrometry in Nutraceutical and Food Research. *Mol. Nutr. Food Res.* **2008**, *52* (1), 62–78. https://doi.org/10.1002/mnfr.200700395.
(132) A. Abragam; B. Bleaney. *Electron Paramagnetic Resonance of Transition Ions*; Oxford university press: London, 1970.

(133) J.W. Orton. *ELECTRON PARMAGNETIC RESONANCE - An Introduction to Transition Group Ions In Crystals*; ILIFFE BOOKS LTD: London, 1968.
(134) Lavoie, S.; Ouellet, M.; Fleury, P.-Y.; Gauthier, C.; Legault, J.; Pichette, A. Complete ^{1}H and ^{13}C NMR Assignments of a Series of Pergalloylated Tannins: ^{1}H and ^{13}C NMR of Pergalloylated Tannins. *Magn. Reson. Chem.* **2016**, *54* (2), 168–174. https://doi.org/10.1002/mrc.4328.
(135) Huang, Q.; Hu, T.; Xu, Z.; Jin, L.; McAllister, T. A.; Acharya, S.; Zeller, W. E.; Mueller-Harvey, I.; Wang, Y. Composition and Protein Precipitation Capacity of Condensed Tannins in Purple Prairie Clover (Dalea Purpurea Vent.). *Front. Plant Sci.* **2021**, *12*, 715282. https://doi.org/10.3389/fpls.2021.715282.
(136) Schendel, R. R.; Bunzel, M. 2D-HSQC-NMR-Based Screening of Feruloylated Side-Chains of Cereal Grain Arabinoxylans. *Front. Plant Sci.* **2022**, *13*, 951705. https://doi.org/10.3389/fpls.2022.951705.
(137) Fecka, I.; Włodarczyk, M.; Starzec, A. Isolation and Structure Elucidation of Cistusin: A New Ellagitannin from Cistus × Incanus L. Leaves. *Industrial Crops and Products* **2020**, *158*, 112971. https://doi.org/10.1016/j.indcrop.2020.112971.
(138) Pfundstein, B.; El Desouky, S. K.; Hull, W. E.; Haubner, R.; Erben, G.; Owen, R. W. Polyphenolic Compounds in the Fruits of Egyptian Medicinal Plants (Terminalia Bellerica, Terminalia Chebula and Terminalia Horrida): Characterization, Quantitation and Determination of Antioxidant Capacities. *Phytochemistry* **2010**, *71* (10), 1132–1148. https://doi.org/10.1016/j.phytochem.2010.03.018.
(139) Lancefield, C. S.; Wienk, H. L. J.; Boelens, R.; Weckhuysen, B. M.; Bruijnincx, P. C. A. Identification of a Diagnostic Structural Motif Reveals a New Reaction Intermediate and Condensation Pathway in Kraft Lignin Formation. *Chem. Sci.* **2018**, *9* (30), 6348–6360. https://doi.org/10.1039/C8SC02000K.
(140) Sette, M.; Wechselberger, R.; Crestini, C. Elucidation of Lignin Structure by Quantitative 2D NMR. *Chem. Eur. J.* **2011**, *17* (34), 9529–9535. https://doi.org/10.1002/chem.201003045.
(141) Wawer, I.; Zielinska, A. 13C CP/MAS NMR Studies of Flavonoids. *Magn. Reson. Chem.* **2001**, *39* (7), 374–380. https://doi.org/10.1002/mrc.871.
(142) Ryan, P.; Hynes, M. J. The Kinetics and Mechanisms of the Complex Formation and Antioxidant Behaviour of the Polyphenols EGCg and ECG with Iron(III). *Journal of Inorganic Biochemistry* **2007**, *101* (4), 585–593. https://doi.org/10.1016/j.jinorgbio.2006.12.001.
(143) Zoleo, A.; Confortin, D.; Dal Mina, N.; Brustolon, M. The Role of Metal Ions in the Study of Ancient Paper by Electron Paramagnetic Resonance. *Appl Magn Reson* **2010**, *39* (3), 215–223. https://doi.org/10.1007/s00723-010-0149-5.
(144) Zoleo, A.; Vecchia, F.; Brustolon, M. Characterization of Ancient and Modern Papers by CW-EPR Spectroscopy. *Appl Magn Reson* **2009**, *35* (2), 213–220. https://doi.org/10.1007/s00723-008-0155-z.
(145) Bronzato, M.; Zoleo, A.; Biondi, B.; Centeno, S. A. An Insight into the Metal Coordination and Spectroscopic Properties of Artistic Fe and Fe/Cu Logwood Inks. *Spectrochimica Acta Part A: Molecular and Biomolecular Spectroscopy* **2016**, *153*, 522–529. https://doi.org/10.1016/j.saa.2015.08.042.
(146) Turci, F.; Tomatis, M.; Lesci, I. G.; Roveri, N.; Fubini, B. The Iron-Related Molecular Toxicity Mechanism of Synthetic Asbestos Nanofibres: A Model Study for High-Aspect-Ratio Nanoparticles. *Chem. Eur. J.* **2011**, *17* (1), 350–358. https://doi.org/10.1002/chem.201001893.
(147) Cnockaert, V.; Maes, K.; Bellemans, I.; Crivits, T.; Vrielinck, H.; Blanpain, B.; Verbeken, K. Quantification of the Fe3+ Concentration in Lead Silicate Glasses Using X-Band CW-EPR. *Journal of Non-Crystalline Solids* **2020**, *536*, 120002. https://doi.org/10.1016/j.jnoncrysol.2020.120002.
(148) Dunaeva, E. S.; Uspenskaya, I. A.; Pokholok, K. V.; Minin, V. V.; Efimov, N. N.; Ugolkova, E. A.; Brunet, E. Coordination and RedOx Ratio of Iron in Sodium-silicate Glasses. *Journal of*

Non-Crystalline Solids **2012**, *358* (23), 3089–3095. https://doi.org/10.1016/j.jnoncrysol.2012.08.004.
(149) Kliava, J.; Berger, R. Size and Shape Distribution of Magnetic Nanoparticles in Disordered Systems: Computer Simulations of Superparamagnetic Resonance Spectra. *Journal of Magnetism and Magnetic Materials* **1999**, *205* (2–3), 328–342. https://doi.org/10.1016/S0304-8853(99)00510-7.
(150) Berger, R.; Bissey, J.-C.; Kliava, J.; Daubric, H.; Estournès, C. Temperature Dependence of Superparamagnetic Resonance of Iron Oxide Nanoparticles. *Journal of Magnetism and Magnetic Materials* **2001**, *234* (3), 535–544. https://doi.org/10.1016/S0304-8853(01)00347-X.
(151) Bicchieri, M.; Monti, M.; Piantanida, G.; Sodo, A. Non-Destructive Spectroscopic Investigation on Historic Yemenite Scriptorial Fragments: Evidence of Different Degradation and Recipes for Iron Tannic Inks. *Anal Bioanal Chem* **2013**, *405* (8), 2713–2721. https://doi.org/10.1007/s00216-012-6681-4.
(152) Piantanida, G.; Menart, E.; Bicchieri, M.; Strlič, M. Classification of Iron-Based Inks by Means of Micro-Raman Spectroscopy and Multivariate Data Analysis: Classification of Iron-Based Inks by Means of Micro-Raman Spectroscopy and Multivariate Data Analysis. *J. Raman Spectrosc.* **2013**, *44* (9), 1299–1305. https://doi.org/10.1002/jrs.4351.
(153) Lee, A. S.; Mahon, P. J.; Creagh, D. C. Raman Analysis of Iron Gall Inks on Parchment. *Vibrational Spectroscopy* **2006**, *41* (2), 170–175. https://doi.org/10.1016/j.vibspec.2005.11.006.
(154) Lee, A. S.; Otieno-Alego, V.; Creagh, D. C. Identification of Iron-Gall Inks with near-Infrared Raman Microspectroscopy. *J. Raman Spectrosc.* **2008**, *39* (8), 1079–1084. https://doi.org/10.1002/jrs.1989.

Appendix A

Oak galls extract characterization results

Fig.1 ^{31}P NMR spectrum of Ex3

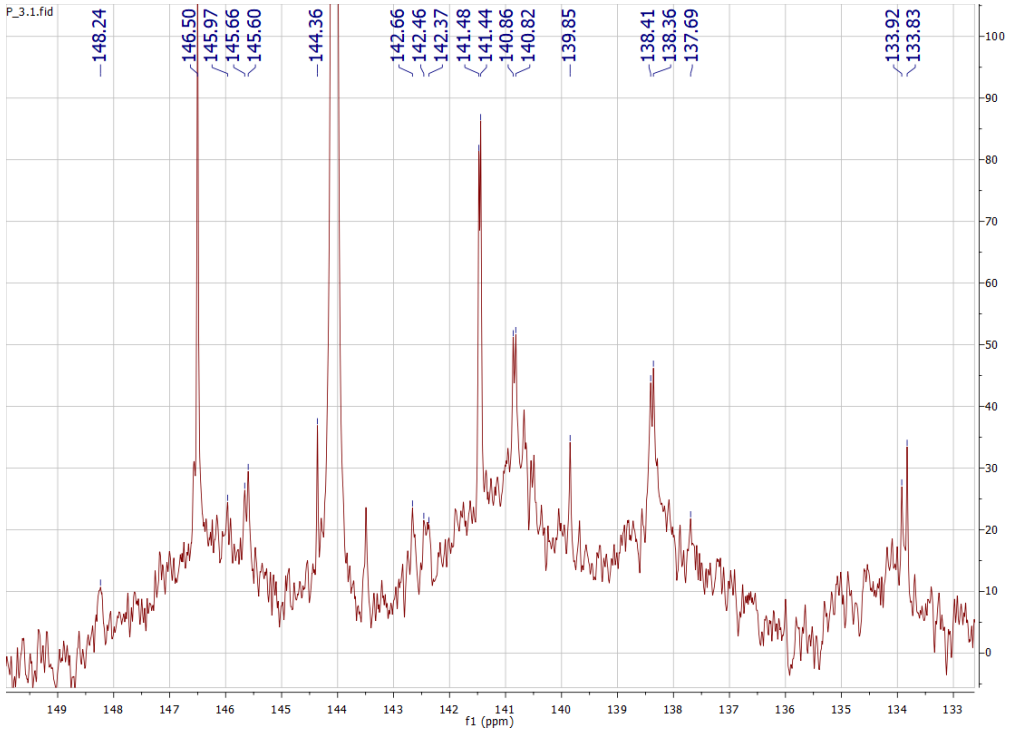

Fig. 2 ^{31}P NMR spectrum of Ex4

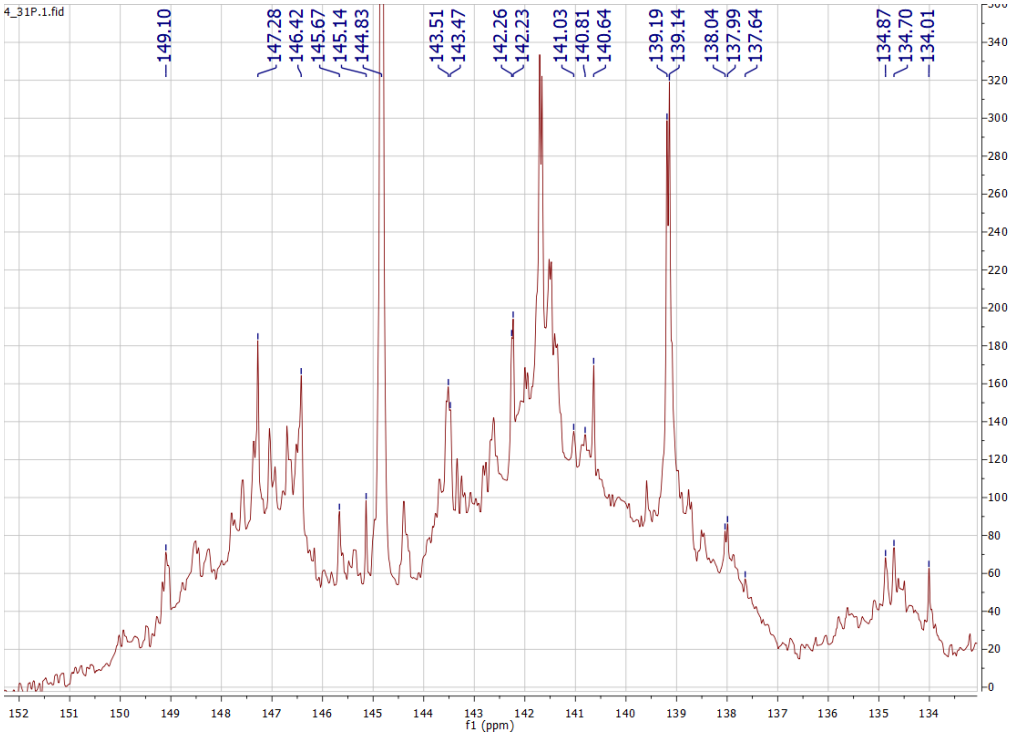

Fig. 3 ^{31}P NMR spectrum of Ex5

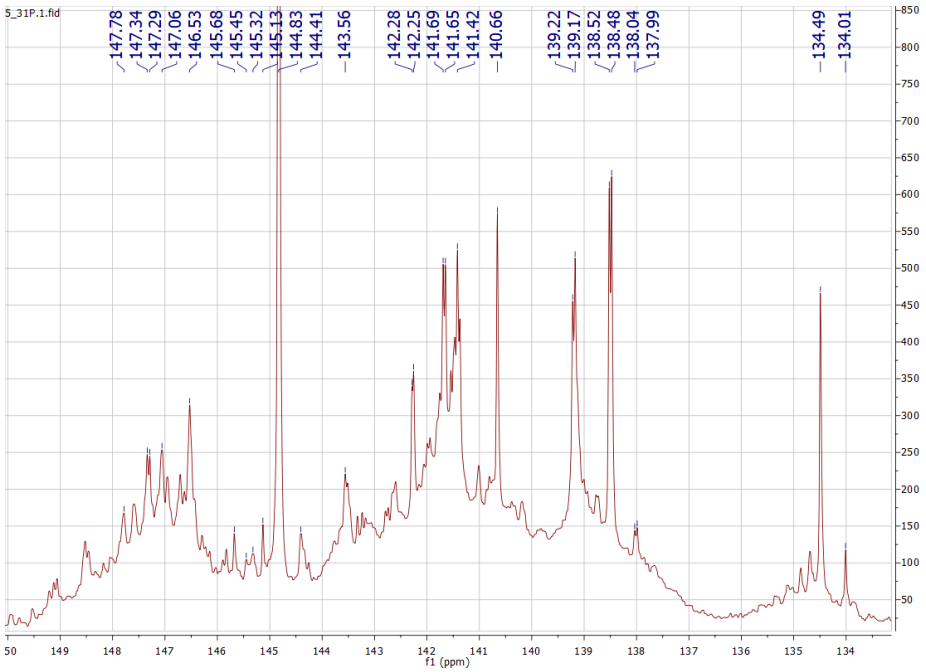

Tab.1 Quantitative ^{31}P NMR results of Ex2

			Area MestreNova	Concentration (mmol/g)
Aliphatic OH	Carbohydrates (149.5-146ppm)		1.10	0.38
	C-ring proanthocyanidins (145.25-146ppm)		0.22	0.08
	Total aliphatic (149.5-145.15ppm)		1.32	0.45
Phenolic OH	**ortho-disubstituted**	Syringil like moieties (143.5-142.5ppm)	/	/
		B-ring proanthocyanidins (142.5-141.9ppm)	0.25	0.09
		Gallate units (142.0-141.1ppm)	0.55	0.19
	ortho-substituted	(140.6-137.6ppm)	1.31	0.45
	Total phenolic (143.5-137.6ppm)		3.05	1.05
Carboxylic OH	Carboxylic acids (136.0-133.0ppm)		0.68	0.23

Tab.2 Quantitative ^{31}P NMR results of Ex3

			Area MestreNova	Concentration (mmol/g)
Aliphatic OH	Carbohydrates (149.5-146ppm)		0.46	0.16
	C-ring proanthocyanidins (145.25-146ppm)		0.09	0.03
	Total aliphatic (149.5-145.15ppm)		0.55	0.19
Phenolic OH	**ortho-disubstituted**	Syringil like moieties (143.5-142.5ppm)	/	/
		B-ring proanthocyanidins (142.5-141.9ppm)	0.15	0.05

		Gallate units (142.0-141.1ppm)	0.30	0.11
	ortho-substituted	(140.6-137.6ppm)	0.51	0.18
	Total phenolic (143.5-137.6ppm)		1.28	0.45
Carboxylic OH	Carboxylic acids (136.0-133.0ppm)		0.68	0.08

Tab.3 Quantitative ^{31}P NMR results of Ex4

			Area MestreNova	**Concentration (mmol/g)**
Aliphatic OH	Carbohydrates (149.5-146ppm)		1.78	0.59
	C-ring proanthocyanidins (145.25-146ppm)		0.29	0.10
	Total aliphatic (149.5-145.15ppm)		2.07	0.68
Phenolic OH	**ortho-disubstituted**	Syringil like moieties (143.5-142.5ppm)	1.01	0.33
		B-ring proanthocyanidins (142.5-141.9ppm)	0.27	0.09
		Gallate units (142.0-141.1ppm)	1.03	0.34
	ortho-substituted	(140.6-137.6ppm)	1.99	0.65
	Total phenolic (143.5-137.6ppm)		5.08	1.67
Carboxylic OH	Carboxylic acids (136.0-133.0ppm)		0.60	0.20

Tab.4 Quantitative ^{31}P NMR results of Ex5

			Area MestreNova	**Concentration (mmol/g)**
Aliphatic OH	Carbohydrates (149.5-146ppm)		2.59	0.86
	C-ring proanthocyanidins (145.25-146ppm)		0.42	0.14
	Total aliphatic (149.5-145.15ppm)		3.01	0.99
Phenolic OH	**ortho-disubstituted**	Syringil like moieties (143.5-142.5ppm)	1.31	0.43
		B-ring proanthocyanidins (142.5-141.9ppm)	0.51	0.17
		Gallate units (142.0-141.1ppm)	1.68	0.56
	ortho-substituted	(140.6-137.6ppm)	3.47	1.15
	Total phenolic (143.5-137.6ppm)		7.74	2.56
Carboxylic OH	Carboxylic acids (136.0-133.0ppm)		0.83	0.27

Fig. 4 HSQC spectrum of Ex2

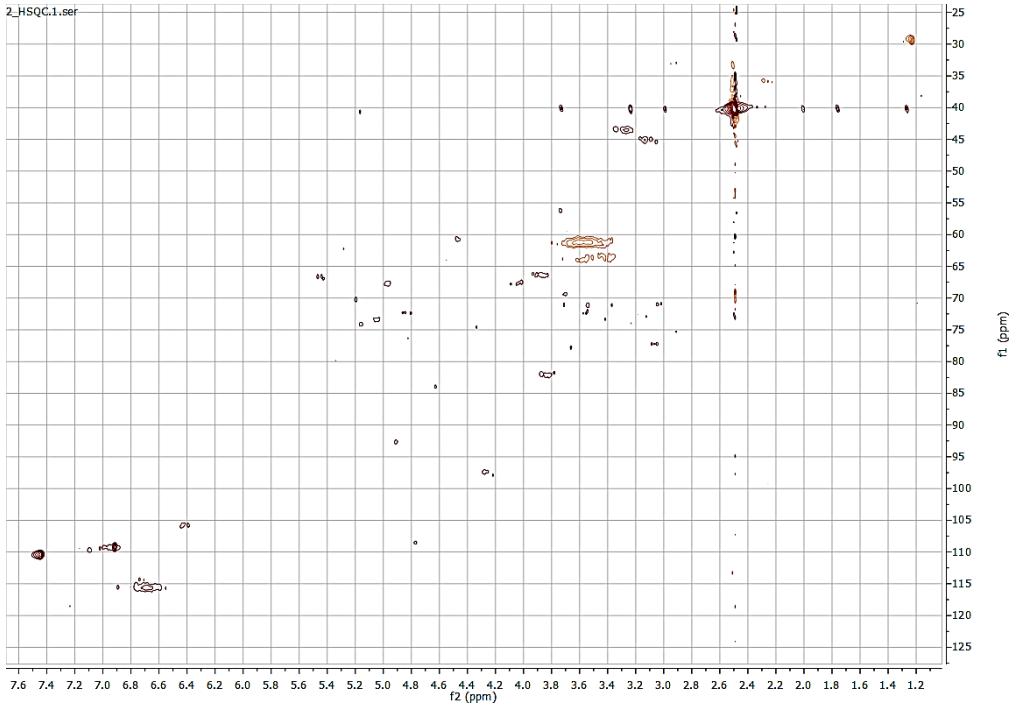

Fig. 5 HSQC spectrum of Ex3

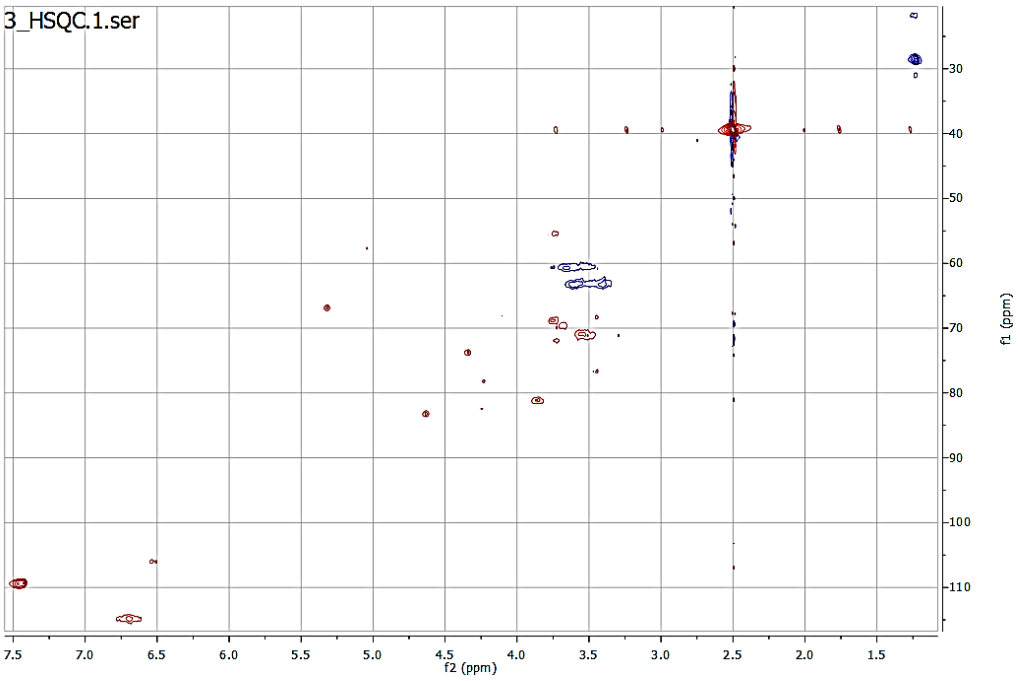

Fig. 6 HSQC spectrum of Ex5

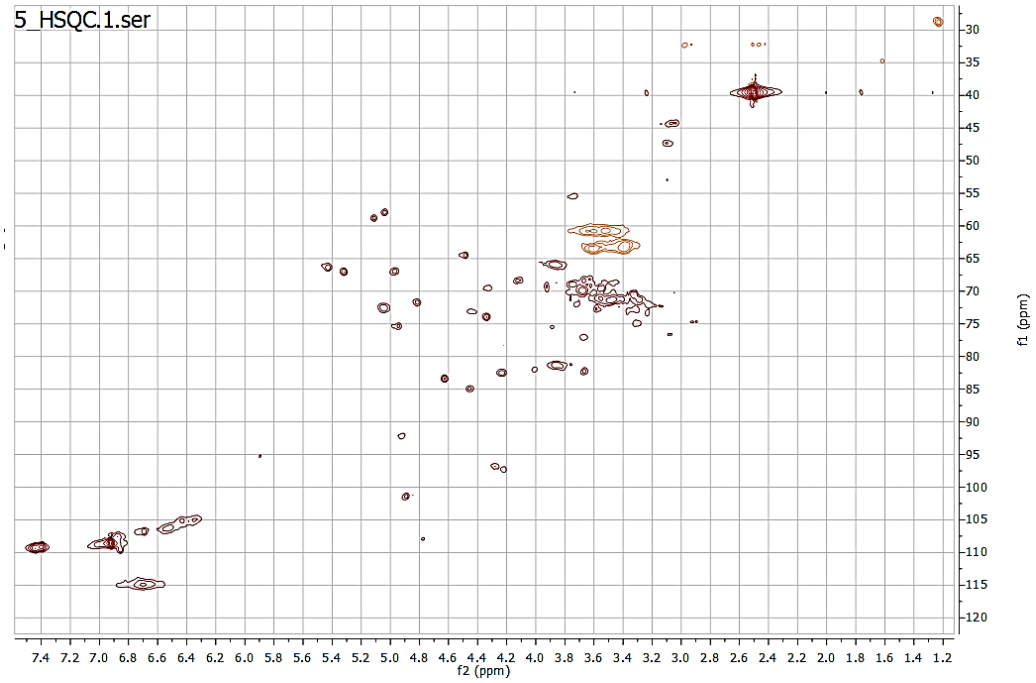

Appendix B

CW-EPR Characterization results

Fig. 1 EPR spectra of solid Fe-GA complexes prepared at intermediate pH in iron excess conditions acquired at RT

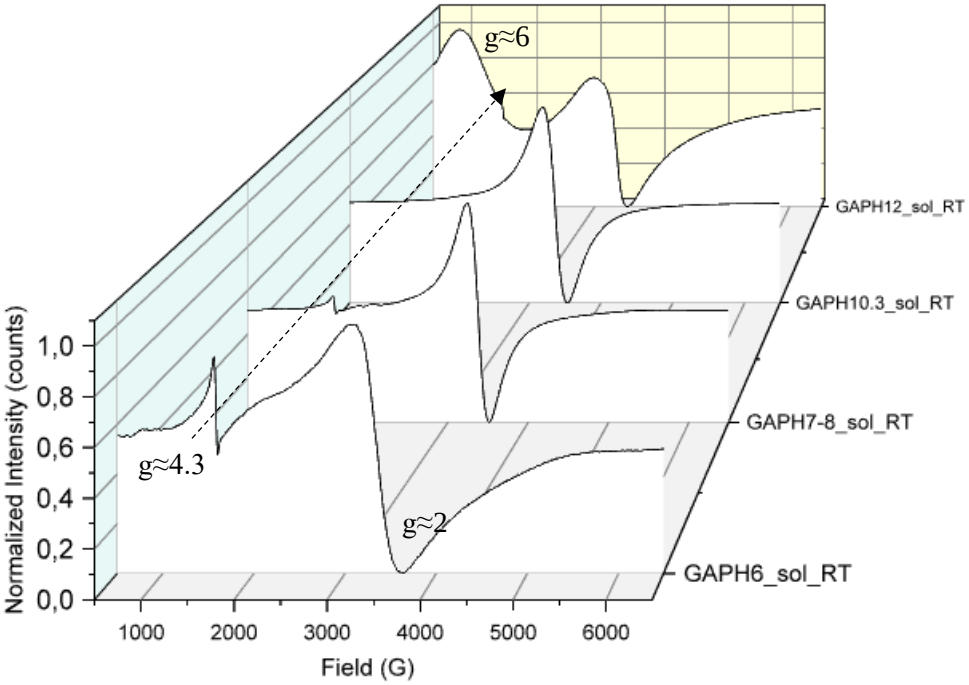

Fig. 2 EPR spectrum of $FeSO_4 \cdot 7H_2O$ used for the complexes preparation (acquired in solid phase at RT)

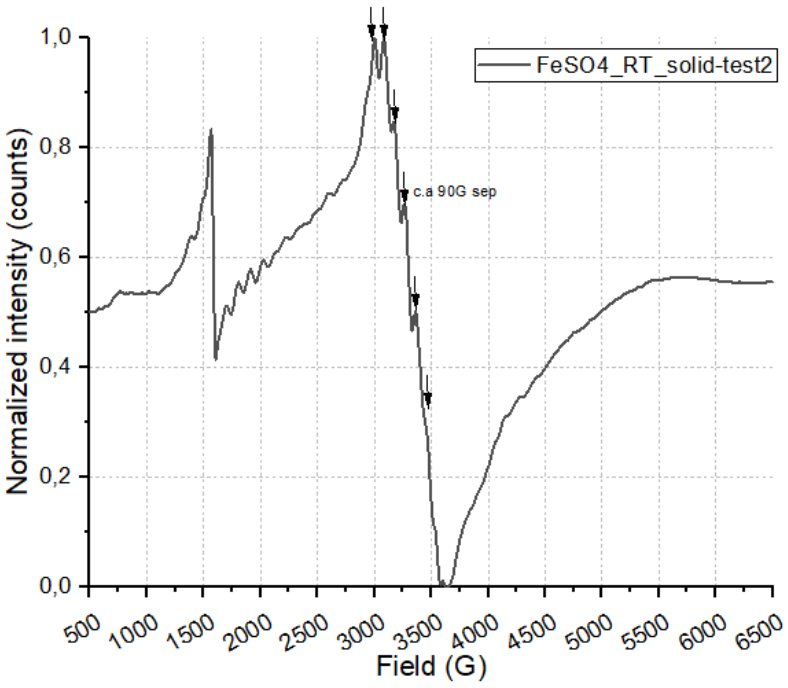

Fig. 3 Comparison between EPR spectra of solid Fe-GA complexes prepared at intermediate pH in iron excess conditions acquired at RT and 100K

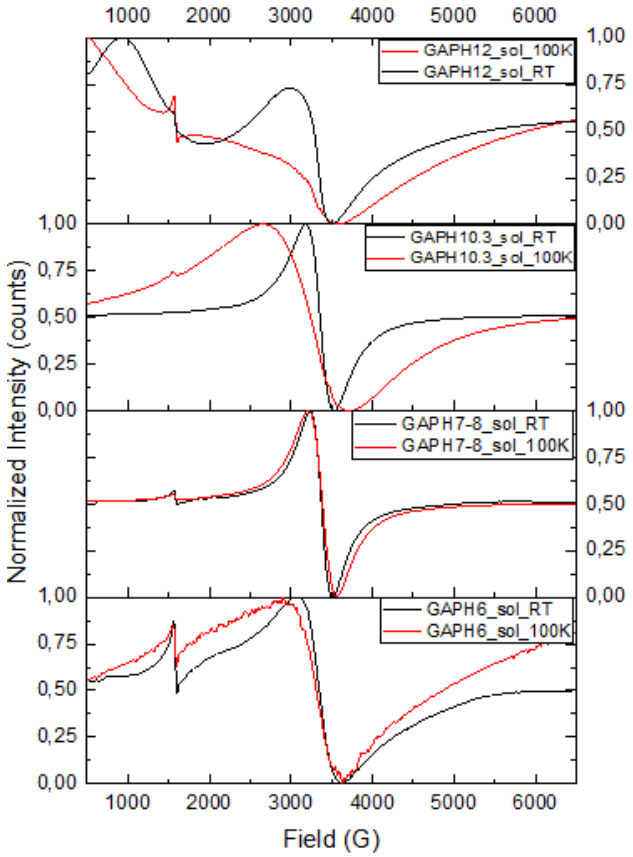

Fig. 4 Time-monitoring experiment on the Fe-GA complexes in the supernatant (liquid) prepared at pH 6 in pseudo-stoichiometric conditions. a) time monitoring on freshly separated supernatant b) time monitoring on the same of capillaries of "a" at different times.

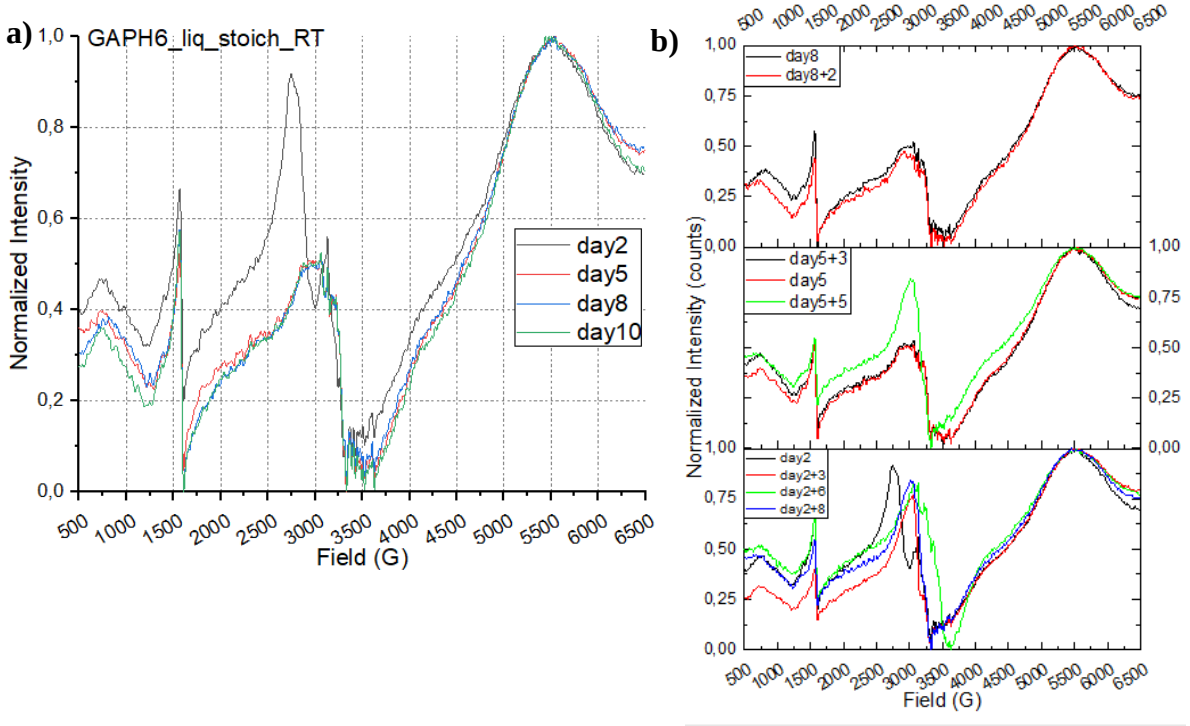

Fig. 5 Temperature gradient experiment on the solid Fe-Ex1 sample prepared at pH 4

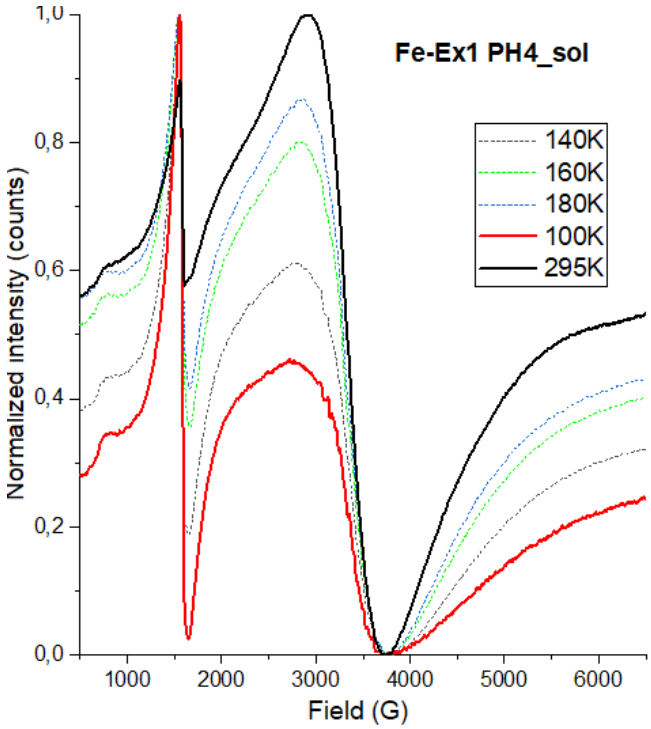

Fig. 6 Temperature gradient experiment on the solid Fe-Ex4 sample prepared at pH 12

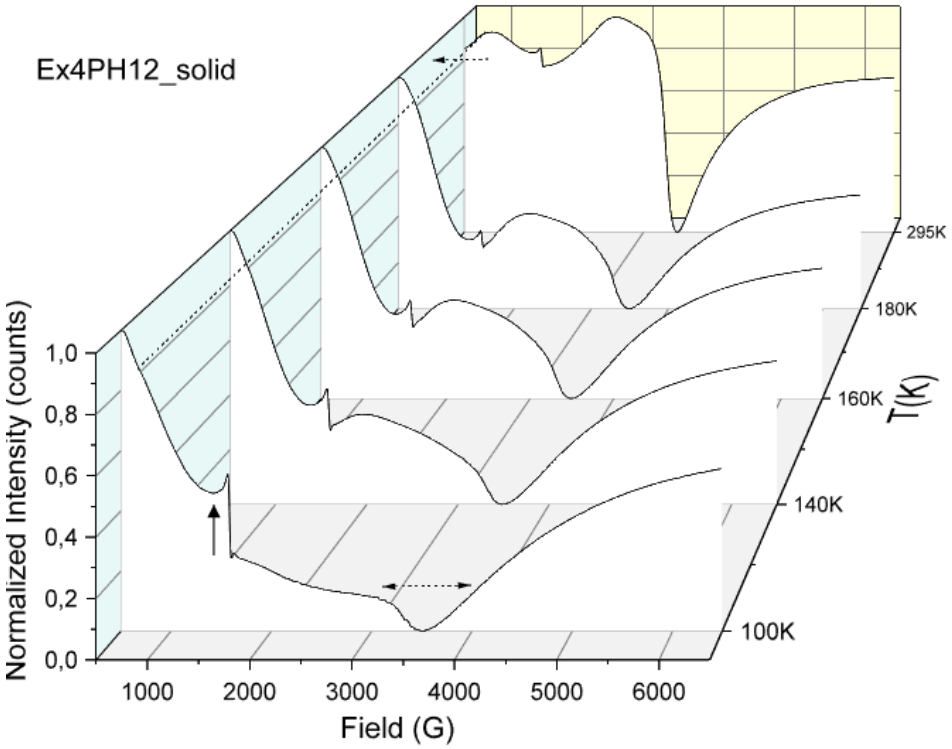

Fig. 7 EPR spectra of liquid Fe-Ex samples acquired both at RT and 100K

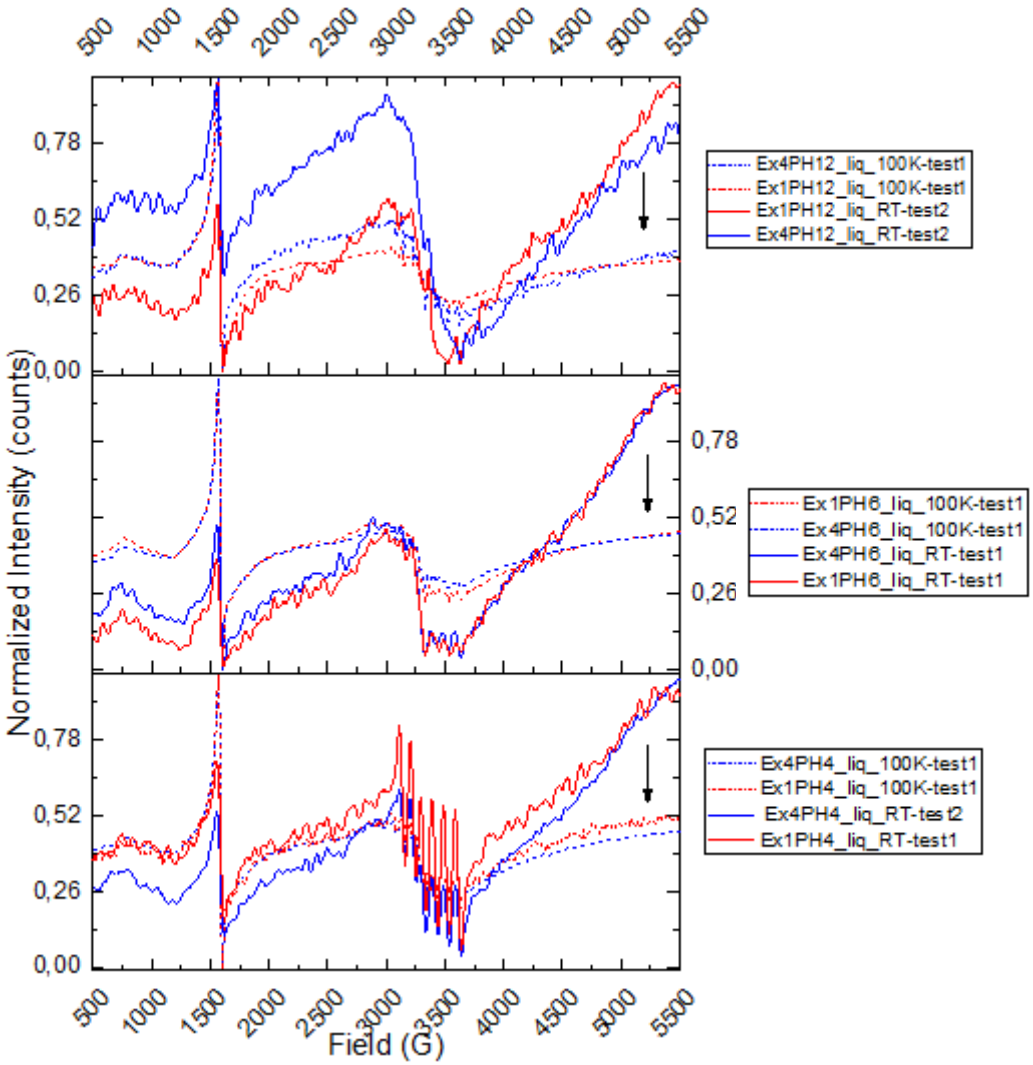

Appendix C

Raman analyses results

Fig. 1 Raman spectra of iron complexes prepared in a) MeOH EA solution and b) MeOH/H_2O (1:1) EA fine dispersion, acquired with different instrumental parameters (two slightly different laser powers for "a" and different accumulations series for "b").

a)

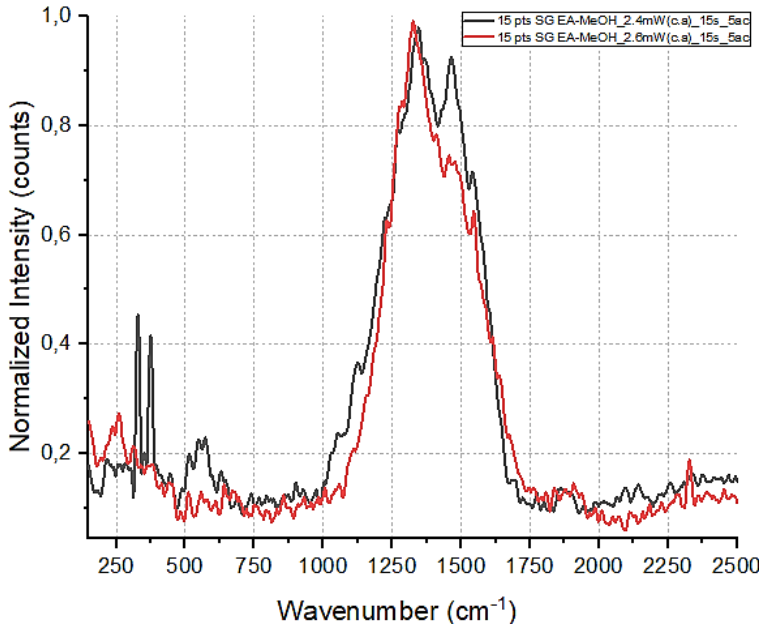

b)

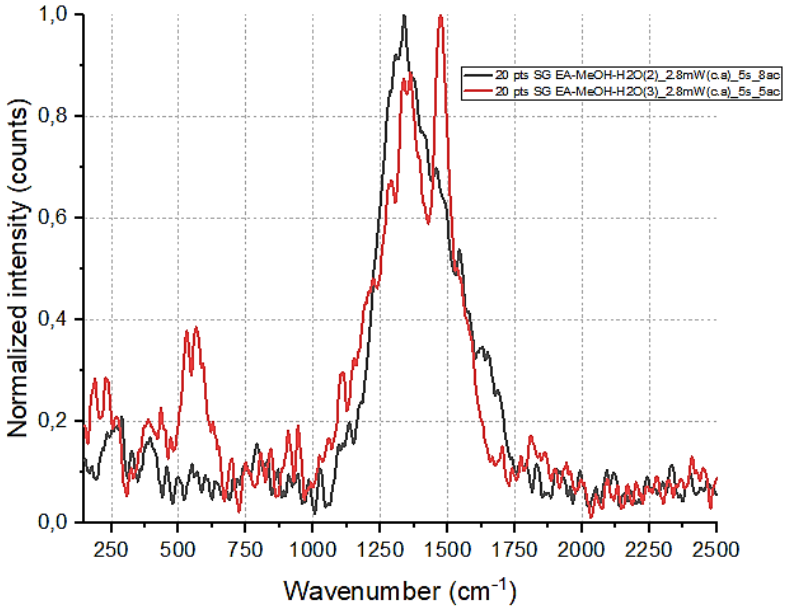

Fig.2 Raw Raman spectra of Fe-Ex4 complexes acquired with similar instrumental parameters.

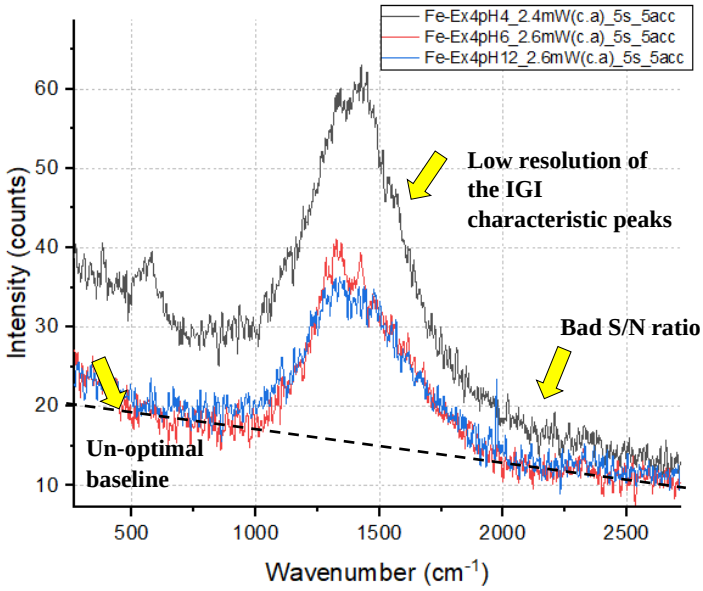

Fig. 3 Raw Raman spectra of a) Fe-GA pseudo stoichiometric complexes and b) Fe-Ex4 complexes acquired with slightly different instrumental parameters.